1972

# Physical and chemical changes related to epigenetic dolomitization

David Eugene Simon
*Iowa State University*

# Physical and chemical changes related to epigenetic dolomitization

by

David Eugene Simon

A Dissertation Submitted to the
Graduate Faculty in Partial Fulfillment of
The Requirements for the Degree of
DOCTOR OF PHILOSOPHY

Department: Earth Science
Major: Geology

Approved:

Signature was redacted for privacy.

In Charge of Major Work

Signature was redacted for privacy.

For the Major Department

Signature was redacted for privacy.

For the Graduate College

Iowa State University
Ames, Iowa

1972

TABLE OF CONTENTS

# INTRODUCTION

The major purpose of this study is to account for, by chemical and physical methods, the changes which occur in geological materials; specifically changes related to alteration or replacement processes. Geologic alteration or replacement generally results from reactions of minerals with components of a fluid phase flowing through the rock. Because changes in mass and pore volumes usually accompany the replacements, study of associated composition and volume changes is necessary to explain how the replacement operates. This type of study requires measurement of physical and chemical changes occurring in a gradational sequence of rocks undergoing replacement; in this study epigenetic dolomitization of limestone. A majority of past studies on dolomitization have described the nature and direction of the process, but not the actual mass and volume changes which occurred. This study will utilize a model of replacement by which related mass and volume changes can be determined. Such knowledge will provide a better insight into some aspects of epigenetic dolomitization.

It is generally agreed that the majority of dolomites owe their origin to replacement of pre-existing calcium carbonate material. However, the exact method by which this replacement occurs and the related composition-volume relationships are still unknown. Epigenetic dolomitization is here defined as the post-lithification replacement of limestone, which probably includes the late-diagenetic classification of some investigators (Fairbridge, 1957; Friedman and Sanders, 1967). Epigenetic dolomites commonly exhibit a cross-cutting relationship across bedding planes of the

host limestones. This parent-daughter relationship allows study of gains and losses of component oxides, phases and volume changes for the system, evaluation of the method by which the process operates, and to what extent local controls, if any, influence the process. Investigations by numerous people (Landes, 1946; Hewett, 1928; Lovering, 1949; Murray, 1960; Weyl, 1960) have shown that dolomitization porosity changes range from large increases in some instances to none in others and to actual decreases in still others. Usually two methods, mole-for-mole and volume-for-volume, are used to describe the dolomitization process but they do not adequately explain the mass and void volume changes actually observed. However, through use of parent-daughter sample sets considered representative of epigenetic dolomitization, measurement of related mass and pore volume changes, chemical changes and petrographic study will yield interrelated data concerning the changes associated with dolomitization. Such an approach is undertaken in this study and makes it possible to explain how these changes occurred.

The following sections will review composition-volume relationships, epigenetic dolomitization and the proposed model of alteration or replacement processes. Following these reviews the systems selected for study, experimental methods, data obtained, and interpretations will be presented.

## EPIGENETIC DOLOMITES

Recent comprehensive reviews of modern and ancient dolomites indicate most modern workers in carbonate petrology believe that most dolomites originate by replacement of pre-existing calcium carbonate material by hypersaline brines (Friedman and Sanders, 1967; Zenger, 1972; Bathurst, 1971). For detailed discussions of various aspects of the dolomitization, the reader is referred to the above references. In general, three types of dolomites are recognized:

(1) Syngenetic dolomite-formed essentially penecontemporaneously with deposition, generally considered to be a marine evaporite basin.

(2) Diagenetic dolomite-formed by replacement of calcium carbonate sediments during the period when the sediments are being consolidated.

(3) Epigenetic dolomite-formed by replacement of limestone along faults, joints, bedding planes and other primary and secondary structural elements long after the sediment is lithified.

Epigenetic dolomites are of primary concern in this study because they usually show a cross-cutting relationship of the dolomitized zones across the original limestone bedding. These zones generally have gradational to sharp contacts between the limestone and dolomite which allow parent-daughter sample sequences to be obtained laterally within the same bed and serve as a basis to study the alteration process.

Friedman and Sanders (1967) have discussed several unsolved problems regarding the replacement of calcium carbonate by dolomite. They point out that it is not understood if the dolomite replacement occurs by the simultaneous solution of the host calcium carbonate and deposition of

dolomite, or diffusion and ion exchange of Mg for Ca in the crystal or the amount and how the Mg ions are introduced. Current thinking regarding the mechanics of dolomitization indicates it may occur by one of two methods; molecule-for-molecule in which the simple end-member equation of Van Hise (1904) is representative, or volume-for-volume in which no simple or single chemical equation can be applied. A 12.3% mass volume shrinkage accompanies the molecule-for-molecule process and was termed "dolomitization porosity" by Van Tuyl (1916), in his classic study of Iowa dolomites. Some geologists believe that volume-for-volume replacement is a more common form of dolomitization because of the lack of apparent porosity increases in some dolomites with respect to the host limestones (Hewett, 1928; Twenhofel, 1932; Steidlmann, 1917; Lovering, 1949).

Landes (1946) in a study of oil bearing dolomites from Indiana, postulated that if the framework of the carbonate rock was maintained, the increased porosity in certain dolomites must be due to differences in the rates of calcite solution and dolomite deposition. Thus dolomites with high porosity result from a greater leaching of the host limestone and a lesser deposition of dolomite in order to yield a net increase in porosity. When the rates of leaching and deposition are the same, volume-for-volume replacement is assumed.

Fairbridge (1957) felt that the amount of late diagenetic dolomite produced was a function of the availability of Mg ions to the system and not the end member stoichiometry commonly used to explain the process. If a semi-rigid framework is maintained and contains some initial porosity, early dolomitization may further increase the porosity, but continued dolomitization may fill the remaining pore space to yield a tight low

porosity dolomite.

Hewett's (1928) descriptive paper on hydrothermal dolomites, which is still a classic in this area, noted that adjacent to ore deposits there was a zone of dolomitization. Commonly a narrow transition zone occurred between the limestones and dolomites with fossils and other primary features of the limestone destroyed, and an increase of grain size and color changes. Generally the dolomite contains more iron and occasionally some additional manganese relative to the limestone. The porosity of the original limestone and that of the secondary dolomite show little differences, unless subsequent leaching has occurred. Also, addition of iron and manganese to the system demonstrates that the process is not simple, and other reactions occur simultaneously with dolomitization. Hewett also noted that the bodies of dolomitized limestone did not show evidence of volume changes or a disruption of the limestone bedding.

Friedman and Sanders (1967) reported on a study of fault-related epigenetic dolomites in Oklahoma showing that no lateral indication or gradational increase of dolomite was apparent as the replacement front was approached. Generally the dolomitization obliterated the textures characteristic of the host limestone. Also, there was a consistent increase of manganese and magnesium, but an inconsistent trend for iron.

Hanshaw et al. (1971), in a study of the Florida aquifer system, concluded that extensive dolomite replacement of calcium carbonate occurs in the zone of mixing between fresh water and subsurface saline waters. Mixing of the saline waters with the potable waters (both in equilibrium with calcite and dolomite) can result in undersaturation of the brackish waters with respect to calcite. Thus dissolution of calcite can occur,

followed by deposition of dolomite and may account for the extensive dolomitization observed in the brackish water zone. They also consider that supply of the $Mg^{2+}$ is due to circulating saline pore waters through the rock and not to a static pore fluid.

Through use of schematic salt phase diagrams Usdowski (1968) postulated that pre-existing calcium carbonate reacts with pore solutions to form dolomite. Generally the reaction proceeds as follows: Metastable $CaCO_3$ which initially forms instead of the stable dolomite in sea water is changed into dolomite by diagenetic pore solutions that contain abundant $Mg^{2+}$ ions. Different amounts of dolomite are formed depending on the anion species present in the pore solutions. If $CO_3^{2-}$ or $SO_4^{2-}$ are present there is an increase of mass and volume for the reaction, as Ca and Mg ions are readily carried by solutions containing these ions. Only in a solution containing $Cl^-$ is the reaction mole-for-mole. Usdowski proposed that dolomite can form when a limestone containing pore solutions of a given Ca/Mg ratio is heated to a higher temperature. At higher temperatures the pore fluids enter the dolomite stability field and conversion of limestone to dolomite occurs.

Lovering (1969) independently arrived at similar conclusions as did Usdowski (1968) for the formation of hydrothermal and diagenetic dolomites by the heating of pore fluids with a given Ca/Mg ratio in relation to temperature changes as a means of altering limestone to dolomite. In general Lovering felt that for a given Ca/Mg ratio there exists a minimum temperature of dolomite formation.

Beales (1965) summarized his studies of pelletal limestone diagenesis and showed that dolomitic varieties are common. The dolomitization of

pelletal limestones is markedly variable, but highly selective, usually replacing the sparry calcite matrix first, then progressively altering the entire rock. Complete dolomitization of a pelletal limestone usually obliterates all primary features of the former limestone. However, Beales did not pursue any further the mechanism of the selective replacement demonstrated by the dolomitization process.

In summary, epigenetic dolomite replacement of a limestone has not been adequately explained in terms of composition-volume relationships. The concensus of opinion is that saline waters are responsible, but the mechanism and exact interchange for the replacement is still unexplained. Is the magnesium exchanged for calcium via diffusion without breakdown of the pre-existing calcium carbonate structure or is it by solution of the calcium carbonate and deposition of the dolomite? Studies of epigenetic and hydrothermal dolomites indicate that although rock volumes of parent limestone and daughter dolomite have not been appreciably changed, the porosity has changed.

## COMPOSITION-VOLUME RELATIONSHIPS

One of the first geologists to address himself to compositional changes due to alteration was Van Hise (1904) in a study of metamorphic processes. He concluded that the chemical reactions representative of the processes occur on a molecule-for-molecule basis by which simple chemical equations could be written assuming that the end member minerals or rocks were the only participants. Also, from these equations the expected volume changes could be computed on the following basis: "The volume of the original compound is to the volume of the compound produced directly as their molecular weights and indirectly as their specific gravities".

In contrast to the views of Van Hise, Lindgren (1912, 1918), on the basis of numerous petrographic and field studies of ore deposits and the associated alterations, concluded that replacement is on a volume-for-volume basis and the simple end member equations postulated by Van Hise (1904) did not adequately explain the actual gains and losses associated with alteration. In his conclusions on replacement, Lindgren considered that the rock volumes of parent and daughter materials remained constant throughout the process and not the mass volume (that volume occupied by material). Thus any change occurring in mass volume would be reflected by an associated change in the void space of the rock. Also, because the replacement process is a combination of solution and deposition, the relative rates of solution and deposition may differ. Commonly, solution is considered to proceed faster than deposition resulting in a more porous structure (Lindgren, 1933).

Ridge (1949, 1961) demonstrated empirically the mass volume-for-volume

replacement by writing complex chemical equations that balance molecularly, volumetrically and electrically. His work showed it was possible to write theoretical equations that describe the replacement process and was accomplished by introducing additional components on both sides of the equation, which, while taking part in the replacement, leave no solid evidence behind. Because only solids are analyzed, there is no trace of the participation by some ions or molecules, as they are not a part of either guest or host, but are only required to balance the process on a stoichiometric basis. Also, Turner and Verhoogen (1960) used the mass volume-for-volume assumption in computation of material gains and losses due to metamorphic processes.

In recent years, experimental replacement studies by Michels (1966), Taylor (1965), Ames (1961), Garrels and Dreyer (1952) indicate that while the external shape of the host was generally preserved, the porosity of the guest may have increased. Thus it can be inferred that the mass volume had decreased. These investigators concluded that the replacement processes studied occurred by a complex stoichiometry and the laws of chemistry were not violated. However, the reactions were not characterized by the simple end-member reactions postulated by Van Hise (1904).

During study of natural alteration processes some investigators have recognized the limitations of weight percent data (representative of the relative distribution within a given sample) for making actual gain and loss comparisons between samples of a replacement system. Because of a common lack of the initial parent material, it is necessary in most replacement studies to make some assumptions regarding the nature of the initial parent material. Use of gradational sequences, relict features

and other assumptions to circumvent this difficulty of a lack of initial material has yielded various methods of recalculating data to obtain material gains and losses.

Barth (1948), assuming that rocks are basically an oxygen framework with cations in the holes due to the oxygen packing, recalculated his analyses on the basis of a constant number of oxygen atoms. He assumed that the rock volume remains constant during metasomatism, the number of oxygen atoms remains constant, and the rocks generally contain 100 cations for 160 oxygen atoms. His assumptions ignore the fact that a considerable portion of any material consists of empty space due to different atomic packing, grain boundaries and voids. Therefore, the proportion of empty space is likely to vary from one material to another and Barth's assumptions should be applied only to individual minerals.

Because the $SiO_4$ tetrahedron has a high energy barrier to destruction, Poldervaart(1953) assumed that the number of these structural units remains constant for a metasomatic process. He recomputed his data to a constant number of tetrahedra. Also he recognized the following distribution of partial volumes in a rock: (1) the atom volume, (2) the theoretical empty space resulting from the ideal packing of the atoms in minerals, (3) the empty space of disorder and vacancies, and (4) the pore space between the mineral grains. However, his computations ignore the latter two contributions to the volume.

Another commonly used technique of recomputation is the "Alumina Constant Magnitude" utilized by Goldich (1938), Garrels and Mackenzie (1971) and Krauskopf (1967). In this computation the aluminum content is assumed to remain constant throughout a process, based on observations that

aluminum is one of the least mobile ions in nature. However, this technique only gives direction and magnitude of change relative to any changes in the aluminum content.

Other investigators have utilized bulk density values as a basis of recomputations assuming that during alteration the rock volume remains constant (Boglepov, 1963; Lindgren, 1918; Lovering, 1949; Meyers and Hemley, 1967; Hemley and Jones, 1964; Lisitsyna, 1966; Simon et al., 1969). Because an exchange of mass may occur, this exchange could be accompanied by changes in porosity. Thus, use of bulk density accounts for changes in pore space (considered to be a mineral phase containing zero ions). Also, emphasis is made that petrographic study be undertaken to ascertain if any evidence of volume changes due to collapse or compaction is present.

Recently, Gresens (1967) developed a set of equations to estimate gains and losses in terms of chemical analyses and specific gravities of unaltered and altered rocks and minerals. The only restriction of these equations is if "N" different minerals are to be compared, "N-1" assumptions of volume or geochemical behavior must be made. Also, petrographic study of the rocks involved must be made to see if the alteration has been accompanied by deformation or volume changes.

Elwell et al. (1968), in an attempt to circumvent the necessity of assuming constant aluminia, outlined a procedure for evaluating gains and losses of material by use of oxide ratios obtained from before and after sample analyses. The ratios obtained show a range of values, with the extremes indicating large gains or losses, while a clustering of two or more ratios about a common value 'R' is then assumed to be indicative of minimal change for those oxides during the process. It is a technique by

which one seeks "Nature's Internal Standard" and results in a normalized extensive computation of gains and losses from a parent sample mass of 100 grams to (100 + 100 R) grams for various daughter samples.

A multitude of techniques exist by which recomputations have been made for estimating gains and losses of material during alteration. However, another aspect of alteration is how the observed gains and losses between parent and daughter samples occur. In other words the process by which alteration takes place is an important factor in study of alteration.

Lovering (1949), in his classic study of wall-rock alteration as an ore guide presented an outline of replacement as a combination of three basic chemical processes involving (1) atomic rearrangement, (2) chemical addition, and (3) chemical subtraction. He grouped these processes into the following combinations to explain observed changes in materials due to alteration processes:

(1) Atomic rearrangement alone. This phenomenon is illustrated by such changes as alpha to beta quartz and aragonite to calcite.

(2) Chemical addition alone. This is essentially precipitation of material in open spaces and is illustrated by cementation of sandstones.

(3) Chemical addition and atomic rearrangement only. This combination of two processes is most common where fluid phases react with a solid as in the hydration of a compound to a new hydrate in response to changes in humidity; for instance, anhydrite to gypsum.

(4) Chemical subtraction only. Removal of material with no other reaction is especially characteristic of solutions that depart far from equilibrium with their wall rock. It generally increases porosity

and permeability.

(5) Chemical subtraction and atomic rearrangement only. This type of change is characterized by the loss of volatiles with the attendant atomic rearrangement as in the change of gypsum to anhydrite. This type of reaction is primarily a readjustment to different physical conditions rather than to changes in the chemical environment.

(6) Chemical subtraction and addition only. This type of reaction is in two forms and is of major importance as to the timing of the removal and deposition of material.

(a) Simultaneous ion substitution that may involve removal of a particular ion from the crystal lattice and the addition of another one brought there by the solution.

(b) Sequential leaching and precipitation tending to produce initial cavities and to later fill them up is one of the major processes in replacement. Generally as long as the leaching exceeds precipitation, the replacement may go forward. When the reverse is true, the openings become filled and the solutions are diverted elsewhere.

(7) Subtraction, addition and atomic rearrangement. The combination of the three processes is usually operative in many alterations but insight can be gained by distinguishing which is dominant.

Lovering's grouping of the chemical processes focuses attention on the type of chemical changes, combinations thereof, and corresponding physical changes. Also, the timing aspect of gains and losses of material is an important feature to be aware of in any study of geologic alteration. Is alteration essentially a simultaneous removal and redeposition of material

in the rock or is it initial leaching and subsequent deposition within the leached pores (open space filling)? This aspect of timing for leaching and deposition broadens the scope of alteration process study by making it possible to consider the classical ideas of replacement as several particular methods in a general scheme by which materials may be altered.

In summation a multitude of assumptions have been used for computation of material gains and losses during the study of replacement processes. However, evaluation of the composition-volume relationships is necessary to ascertain changes occurring during replacement. Also, the need to describe the material changes as a series of chemical additions, subtractions and atomic rearrangements is important in the interpretation of how the process operates. Finally the timing aspect of material gains and losses as either simultaneous or sequential leaching and deposition is important in final evaluation of the replacement process.

## DEVELOPMENT OF A WORKING MODEL FOR STUDY OF REPLACEMENT PROCESSES

If a better understanding of an alteration process is to be obtained, a working model of the process must be formulated. Initially, let the system of study be defined as a total unit volume of space partitioned among the following: (1) atom space, (2) theoretical pore space due to the packing of the atoms, (3) disorder space of dislocations and vacancies, and (4) open pore space (Figure 1a). This total volume is considered a "Constant Container Volume" in which material may be removed or deposited. The unit container volume (Figure 1a) for experimental study may be represented by the following:

$$VOLUME_{total} = Volume_{mass} + Volume_{pores}$$

Once this initial system has been defined, alteration occurs such that material can enter or leave the volume during the process (Figure 1b). The total volume is considered to remain constant throughout the process with the understanding that the partial volumes, which sum to this total volume, may change during alteration. Thus the container initially contains 'X' amount of mass volume and 'Y' amount of pore volume where

$$VOLUME_{total}^{before} = Volume_{mass}^{before} + Volume_{pores}^{before}$$

and following alteration the amounts of mass and pore volume may have changed and is represented as

$$VOLUME_{total}^{after} = Volume_{mass}^{after} + Volume_{pores}^{after}$$

Figure 1a. Schematic diagram of partial volume distributions within unit container volume and the equivalent working model

Figure 1b. Three types of volume changes that can during alteration.

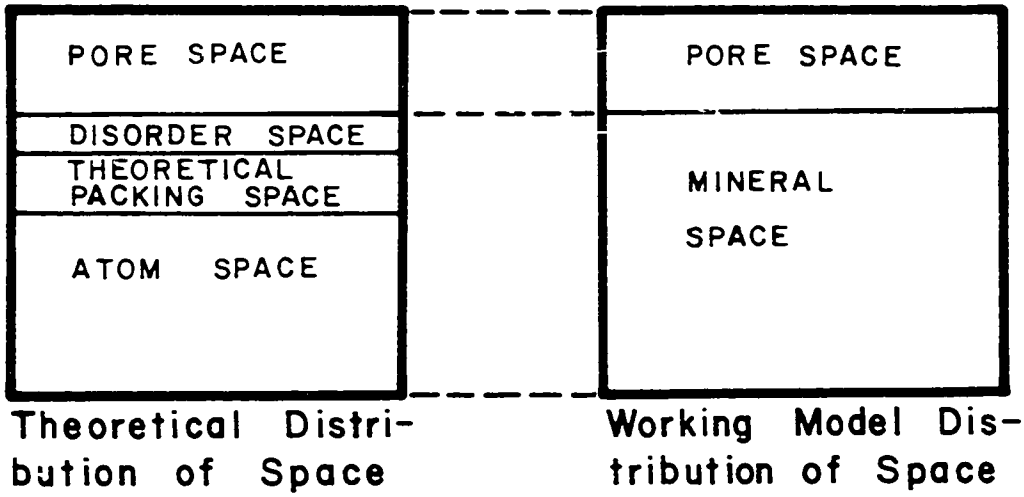
PORE SPACE
DISORDER SPACE
THEORETICAL PACKING SPACE
ATOM SPACE
PORE SPACE
MINERAL SPACE
Theoretical Distribution of Space
Working Model Distribution of Space

(A)

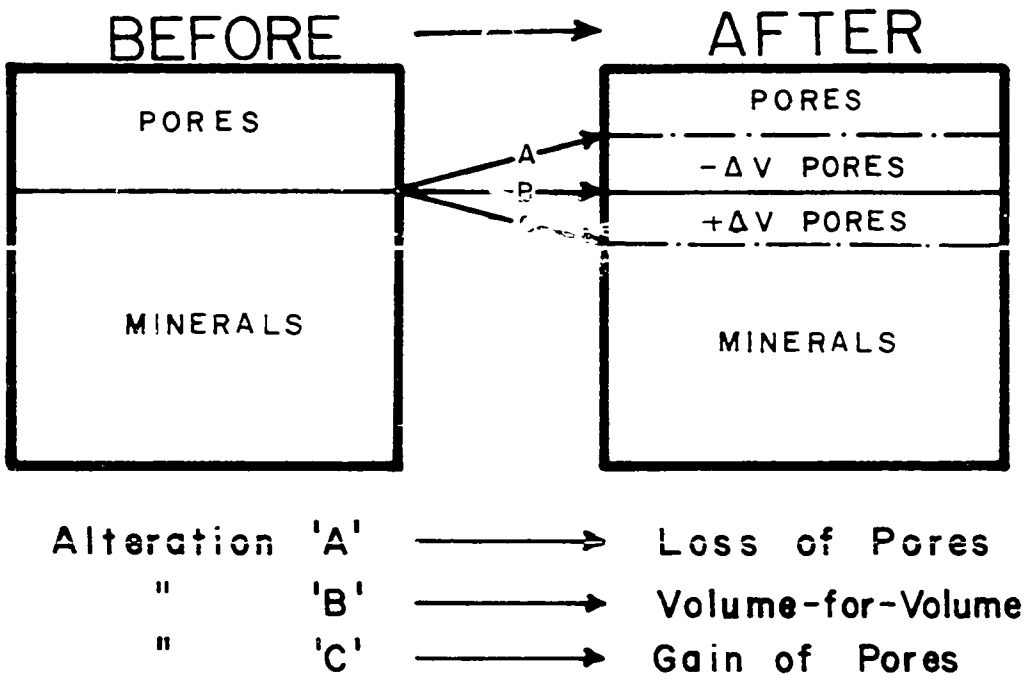
BEFORE
AFTER
PORES
MINERALS
A
B
PORES
-ΔV PORES
+ΔV PORES
MINERALS
Alteration 'A' → Loss of Pores
" 'B' → Volume-for-Volume
" 'C' → Gain of Pores

(B)

Generally, the mass and pore volumes of the before and after systems are different. However, the total volume is considered to remain constant. From this model of alteration, the entire spectrum of processes can be explained ranging from net pore filling (Alteration A, Figure 1b) to mass volume for volume exchange (Alteration B, Figure 1b) to net leaching (Alteration C, Figure 1b). Also, complete leaching could occur followed later by open space filling. However, use of before and after samples only gives the net changes for any number of processes which may have occurred.

Before this model can be applied, the petrographic and field evidence must support the Constant Container Volume assumption. Several criteria by which constancy of volume can be ascertained are:

(1) Presence of relict features, including pseudomorphs, ghost images and former grain outlines.

(2) Physical measurements and field evidence that the rock body from which the samples were obtained has not thickened or thinned at the outcrop.

(3) Gradational sequences of alteration zones showing sequential replacement, while a framework of the system has been maintained.

If these criteria can be validated, then the constant container volume model of alteration may be assumed valid, and used for making comparisons between sample sets to ascertain gains and losses of material. However, if evidence of volume changes is obtained, corrections for this change must be made prior to the computations.

# METHOD OF STUDY

Block samples were obtained from several quarries where a parent-daughter relationship of limestone to dolomite existed. The sample sequences obtained satisfied the following criteria for application of the model to study of dolomitization:

(1) Sequences were sampled which grade laterally and continuously within the same lithologic unit from parent limestone to daughter dolomite.

(2) The selected samples have a uniform texture; the blocky and irregular texture characteristic of mottled dolomites were avoided because of the lack of continuous change from limestone to dolomite.

(3) There is no apparent change in bed thickness at the sample localities.

Figure 2 is a flow chart of the various measurements obtained for each sample. In the laboratory cylindrical cores were extracted by diamond coring from the block samples for use in various phases of the study. The use of cores instead of chips or fragments provides better statistical accuracy for various measurements (Wallace, 1962). Also, thin and polished sections of cores and adjacent areas were made to determine the mineral paragenesis.

During preliminary studies it became apparent that for better control and internal consistency as many measurements as possible should be performed on each core. Therefore, the physical tests were performed on each core prior to chemical tests. Physical tests performed on the cores included bulk volume measured by mercury displacement (Tickell, 1965). Grain volume was determined by vacuum saturation with boiled deionized

Figure 2. Flow chart of various tests and measurements performed on each sample.

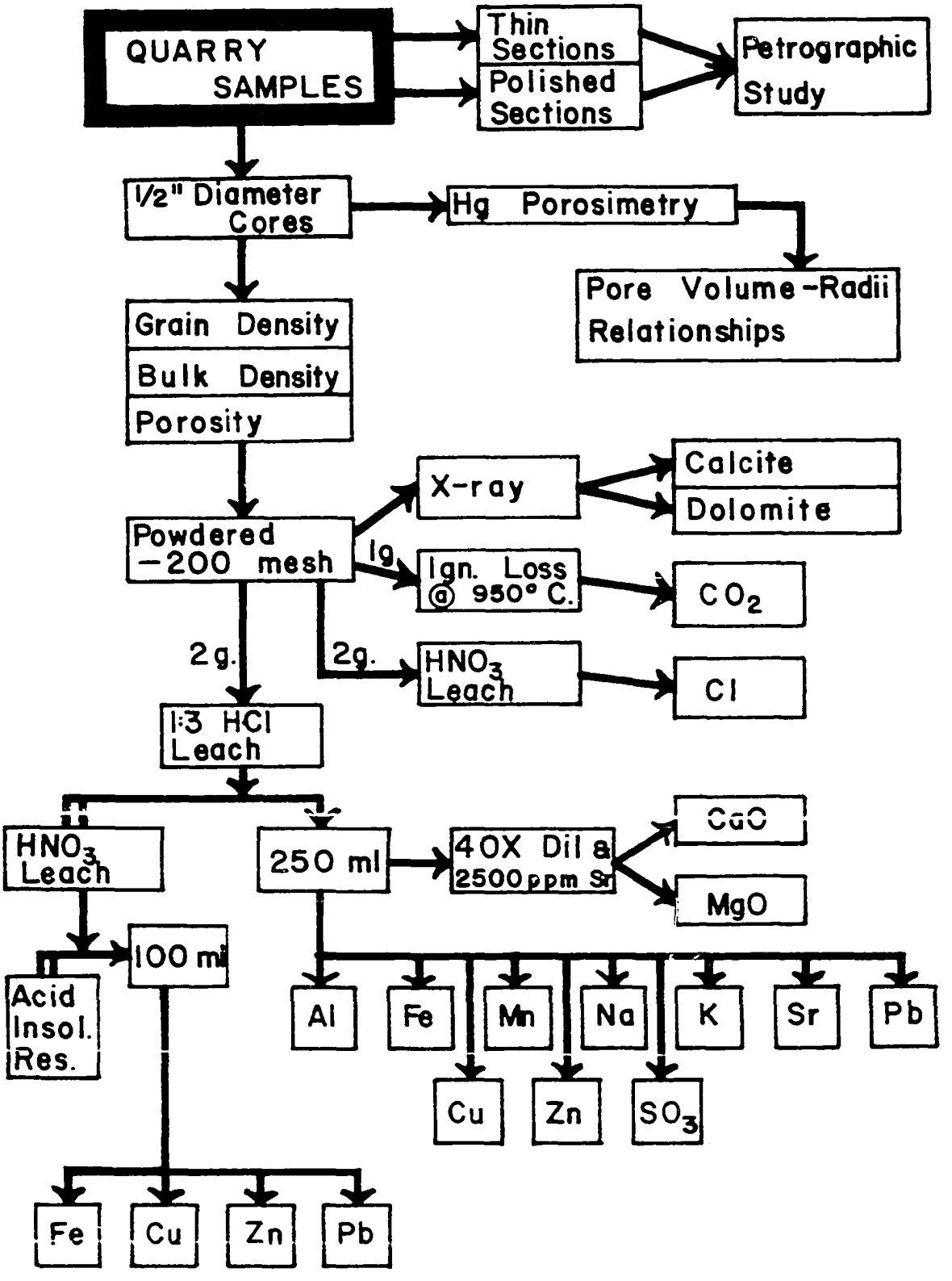
QUARRY SAMPLES
Thin Sections
Polished Sections
Petrographic Study
1/2" Diameter Cores
Hg Porosimetry
Pore Volume-Radii Relationships
Grain Density
Bulk Density
Porosity
X-ray
Calcite
Dolomite
Powdered −200 mesh
1g.
Ign. Loss @ 950° C.
$CO_2$
2g.
2g.
$HNO_3$ Leach
Cl
1:3 HCl Leach
$HNO_3$ Leach
250 ml
40X Dil a 2500 ppm Sr
CaO
MgO
100 ml
Acid Insol. Res.
Al
Fe
Mn
Na
K
Sr
Pb
Cu
Zn
$SO_3$
Fe
Cu
Zn
Pb

water and weighed while suspended in water (Hillebrand, 1919). The core is then dried at 110°C, cooled and a dry weight obtained. From these values the following volume and mass properties are computed:

(1) Bulk density = dry weight/bulk volume

(2) Grain density = dry weight/grain volume

(3) Porosity = [(Grain density - Bulk density)/Grain density] x 100.

The reproducibility on duplicate measurements is ± 0.003 g/cc for the densities and ± 0.08% for porosity. The measured grain densities were checked against a theoretical grain density obtained from summation of the analyzed Ca, Mg, Mn and Fe contents computed as carbonate phases, and pyrite and acid insoluble residue which was assumed to be quartz. The measured grain densities show agreement of better than ± 1% with respect to the theoretical grain densities.

Because of the destructive nature of mercury porosimetry a series cores considered representative of the limestones, dolomites and transition zones were selected. Mercury porosimetry involves measurement of mercury volumes pushed into the voids of a certain radii range at increasing pressure increments. The volume of injected mercury at each pressure increment is a measure of the void volume in the size range related to the pressure change. The instrument used in these tests allowed measurement of pore entry radii sizes from 21 to 0.05 microns. Thus only that portion of the total void volume within this size range is measured. Because these are interconnected pores an indication of the effective porosity is obtained (Hiltrop and Lemish, 1959; Wallace, 1962). The difference between the porosity measured by water saturation and mercury saturation is considered to be in the less than 0.05 micron size range. On the average

about 75% of the total porosity is measured by mercury porosimetry.

Following the above measurements the cores were powdered and mixed using an alcohol grinding medium in a mullite impact mixer mill. Chemical analyses of an HCl dissolution of weighed portion of the sample were performed by atomic absorption spectrometry (Appendix A). The elements analyzed included Ca, Mg, Mn, Fe, Al, Na, K, Sr, Cu, Pb, and Zn. A reproducibility check for calcium, magnesium and carbon dioxide content is listed in Table 1 for dolomite reference sample No. 400 from G. Frederick Smith and reagent grade calcium carbonate. The carbon dioxide content was estimated by loss on ignition at 950°C with corrections for oxidation of pyrite, as well as iron and manganeses solid solution in the carbonates (Galle and Runnells, 1960). The hydrochloric acid insoluble residue is further partitioned by a concentrated nitric acid leach to dissolve any sulfide minerals that may be present. The iron content of the nitric acid soluble portion is considered an estimate of the pyrite content. The remaining nitric acid insoluble residue is composed primarily of quartz with minor amounts of illite as identified by X-ray diffraction. The sulfate content was measured by the method of additions utilizing a spectrophotometric barium sulfate suspension test developed by Hach Chemical Company, Ames, Iowa.

Calcite and dolomite mineral contents were determined by a quantitative X-ray diffraction technique utilizing a step-wise integration of the principal $d_{10.4}$ peak of both minerals. The reproducibility of this technique is $\pm$ 1.1% at 95% confidence intervals (Simon, in preparation). The calcite and dolomite values are corrected for acid insoluble residue and pyrite contents. All chemical and physical data obtained for the samples are tabulated in Appendices B and C.

Table 1. Reproducibility of Ca and Mg by atomic absorption analysis and $CO_2$ ignition loss. Values given are mean and standard deviations for six replicate determinations

| | Dolomite #400 | | Ca $CO_3$ reagent grade | |
|---|---|---|---|---|
| | Obtained | Expected[a] | Obtained | Expected |
| CaO | 30.40 ± 0.10 | 30.47 ± 0.04 | 56.10 ± 0.15 | 56.03 |
| MgO | 21.26 ± 0.10 | 21.50 ± 0.04 | 0.00 | 0.00 |
| $CO_2$ | 47.18 ± 0.10 | 47.38 ± 0.08[b] | 43.95 ± 0.05 | 43.97 |

[a]Diehl (1964).

[b]Calculated from CaO and MgO contents.

# GEOLOGIC SETTING AND PETROLOGY

Two examples of epigenetic dolomitization were selected for study. One represents dolomitization of a peloid limestone obtained from the Ferguson Quarry and the other dolomitization of a lithographic limestone from the Randall Quarry. In both cases changes exist laterally along bedding from parent limestone to daughter dolomite. The term peloid is used in preference to the genetic terms pellet, oolite, surfical oolite, etc., because this term allows reference to grains composed of microcystalline calcite without the need to imply any mode of formation (Folk, 1959). The following sections will initially describe the general quarry section and then a petrographic description of the various carbonate rocks sampled. Following the petrographic descriptions will be a discussion of the carbonate phase compositions.

## Ferguson Quarry

The peloid limestone and its dolomitized equivalent are exposed in the Ferguson Quarry located in Marshall County, Iowa, Section 5, T82N, R17W. The essentially flat lying carbonate rocks of Mississippian Age are part of the Maynes Creek and Eagle City members of the Hampton formation of the Kinderhookian Series. The beds sampled in this study occur in the upper part of the quarry face, overlying a 40-50 foot sequence of dark gray to brown dolomitic limestone and calcitic dolomites containing abundant fossils and chert while retaining numerous primary depositional features (Schneider, 1954). See Figure 3 for generalized section of the quarry.

The peloid limestone beds form a distinctive massively bedded light

Figure 3. A generalized geologic section of carbonate rocks exposed at the Ferguson Quarry

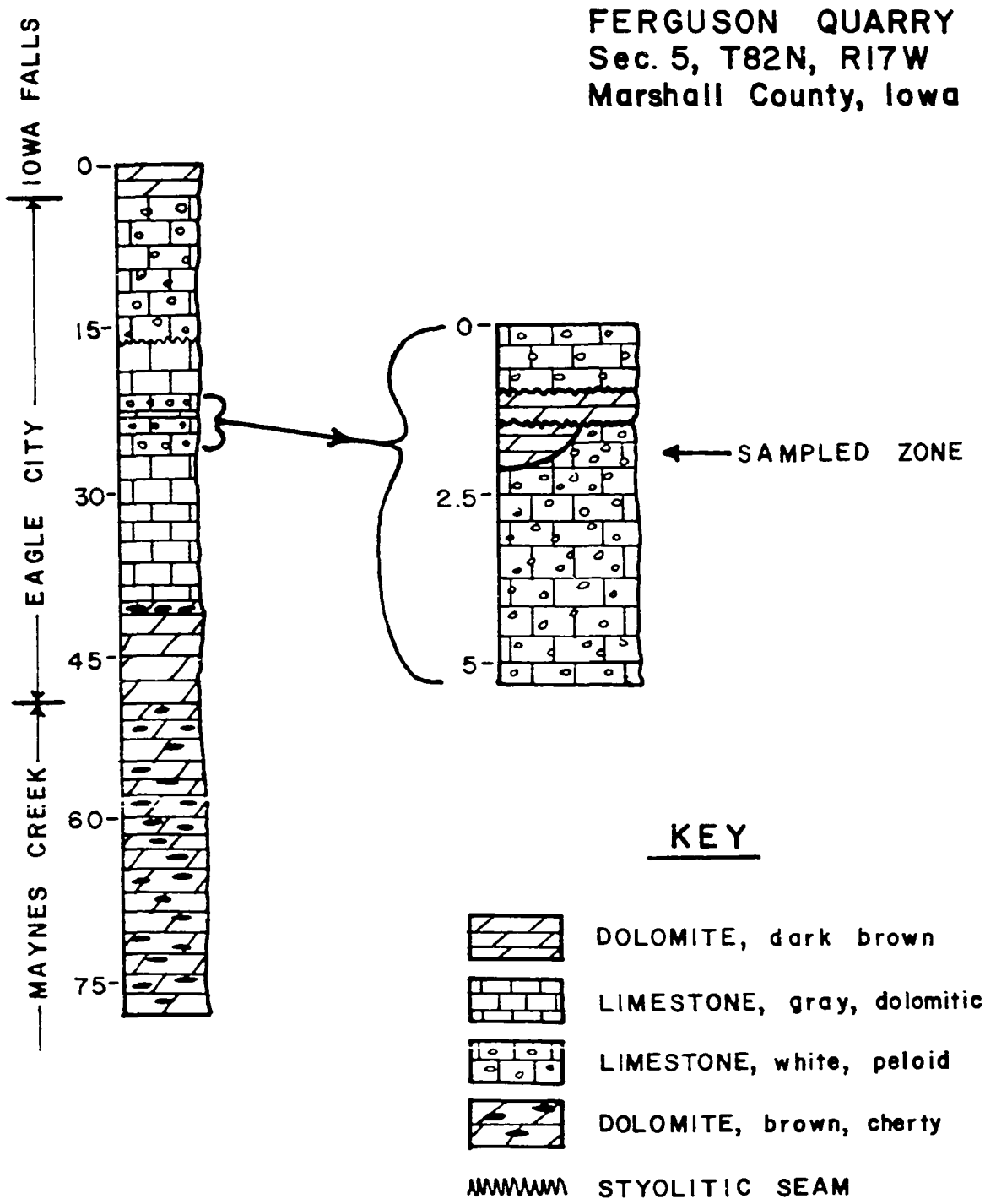
FERGUSON QUARRY
Sec. 5, T82N, R17W
Marshall County, Iowa
IOWA FALLS
EAGLE CITY
MAYNES CREEK
0
15
30
45
60
75
0
2.5
5
SAMPLED ZONE
KEY
DOLOMITE, dark brown
LIMESTONE, gray, dolomitic
LIMESTONE, white, peloid
DOLOMITE, brown, cherty
STYOLITIC SEAM

gray to creamy white unit 5-6 feet thick containing a prominent 6-15 inch thick layer of green to brown medium grained silicous dolomite. The peloid limestones show poorly developed primary features including localized cross-bedding, variation of peloid sizes and macerated fossil zones. The green to brown dolomite layer is bounded above and below by stylolitic seams. However, a crosscutting relationship of epigenetic dolomite and peloid limestone has developed below the lower stylolitic seam (Figure 3). Where the dolomitized zones are observed there is little or no evidence of the primary features associated with the limestone equivalent found. It is from this zone that samples were collected.

Peloid limestone

Macroscopic examination of the limestone shows it to consist of dense white ellipsoidal to spherical peloids in a matrix of clear sparry calcite. Weathering of the limestone preferentially removes the sparry calcite, freeing the peloids to form a peloid sand at the base of the outcrop. Microscopic study of thin and polished sections shows that the limestone is composed of silt to sand size components of poorly sorted, rounded to elliptical grains averaging about 0.4mm, usually devoid of any internal structure, and consisting of microcrystalline carbonate material in a sparry calcite matrix (Figure 4). Occasionally minor amounts of fossil debris can be observed. The sparry calcite framework about the peloids is of a variable grain size ranging from 0.05 to several mm. Relict features in the sparry calcite indicative of recrystallization include traces of former grains, fossils and floating grains. Also twinning of the sparry calcite was occasionally observed in the thin sections (Figure 5).

Figure 4. Microphotograph of the peloid limestone showing the general texture found. The dark areas are the peloids and the surrounding light areas are the sparry calcite matrix. Transmitted plane polarized light

Figure 5. Microphotograph of deformation twins occasionally observed in the sparry calcite matrix of the peloid limestone. Transmitted crossed polarized light

Figure 6. Microphotograph showing the early stages of epigenetic dolomitization. Note that the dolomite is selectively replacing the sparry calcite matrix. Transmitted plane polarized light

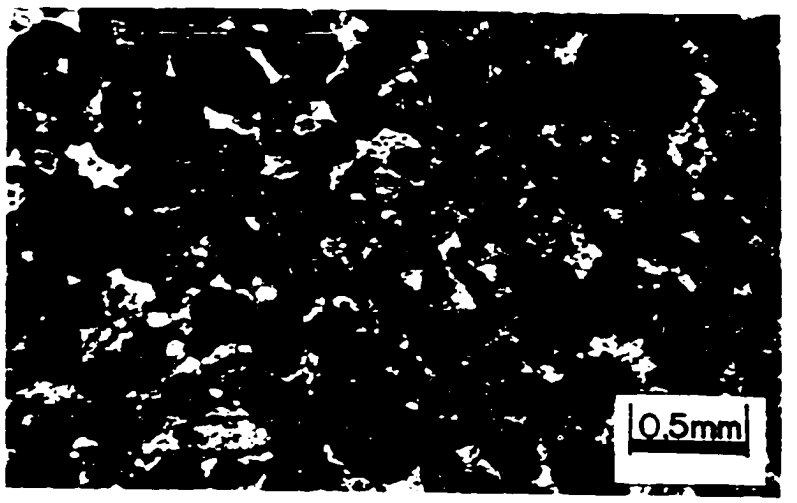
0.5mm


0.1mm

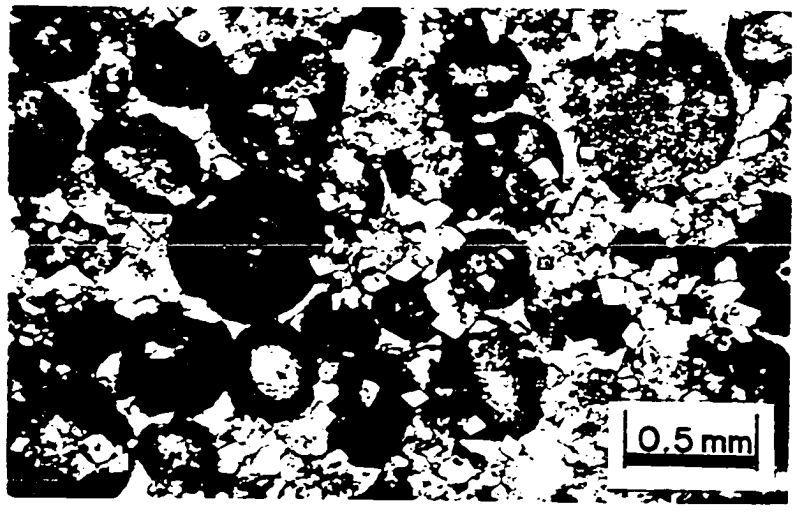
0.5 mm

Dolomite rhombs (1-2%) are scattered throughout and occur in both the sparry calcite and the peloids. Some of the peloids contain sparry calcite in their centers, others dolomite rhombs. A sparse amount (estimated at much less than 1%) of pyrite is irregularly disseminated throughout. Occasionally small tongues of replacement dolomite penetrate into the limestone beyond the major dolomite front along what appear to be minute factures or veinlets.

Transition zone

At the time this study was made the transition zone between the limestone and dolomite varied in width from 50 microns to several centimeters. Earlier observations of this zone at various stages of quarry development have shown it to form gradational zones as much as 1 meter or more in width. In hand specimens this zone appears as a light brown area texturally similar to the limestone between the dark brown dolomite and light gray limestone. Thin and polished section study of this zone show it to consist of calcite peloids in a matrix of sparry dolomite (Figures 6 and 7). The randomly oriented dolomite rhombs (average size approximately 0.1mm) are observed forming along the boundary between the sparry calcite and the peloids (Figure 8). As this transition zone progressively develops (Figure 7) the dolomite preferentially replaces the sparry calcite framework and results in a continuous dolomite framework about the peloids. A texture forms that is characterized by islands of peloids in a sea of dolomite rhombs. As the main dolomite zone is approached, this island-sea texture changes abruptly into an interlocking mosaic of dolomite where the peloids are replaced centripetally or by a transecting front of dolomitization.

Figure 7. Microphotograph of late stage transition zone and the final dolomite showing the relict outlines of former peloids in the dolomite. Transmitted plane polarized light

Figure 8. Microphotograph of dolomite rhombs forming in the boundary region between the peloids (dark) and sparry calcite matrix. Polished section, vertical incident light

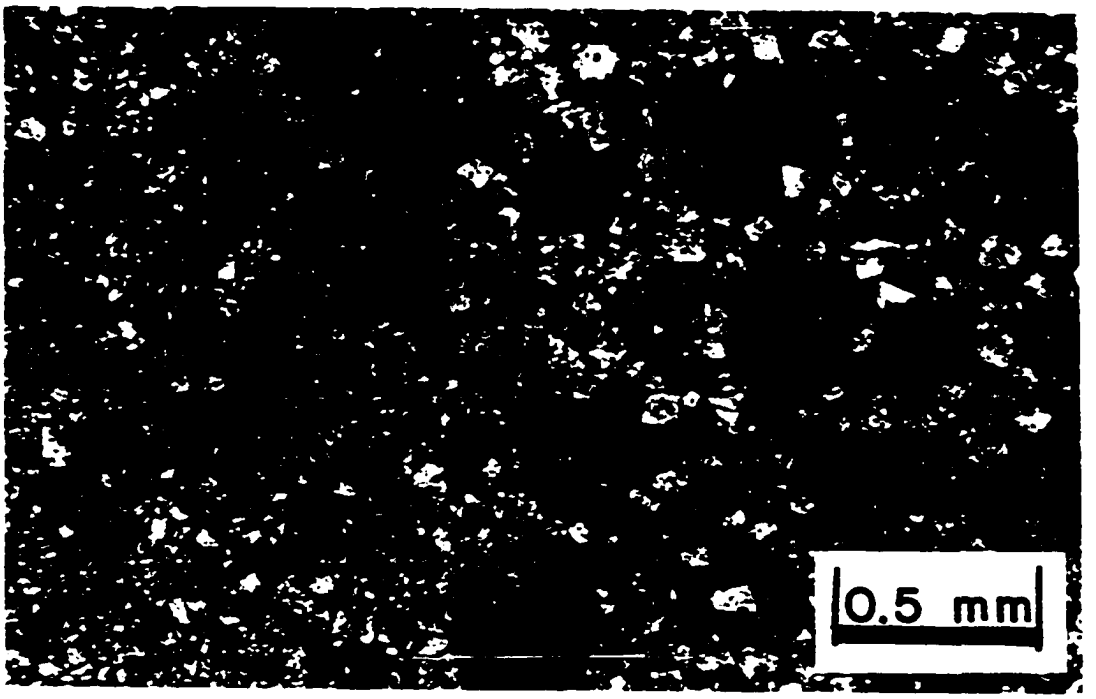
0.5 mm

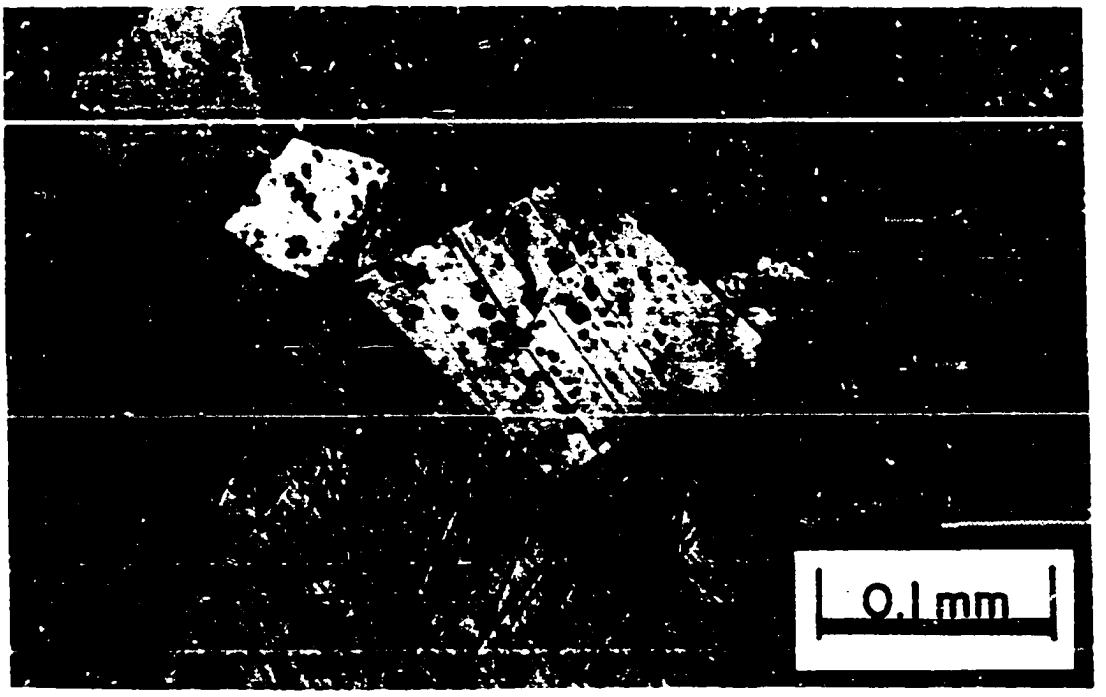
0.1 mm

Dolomite

The dolomite varieties observed in the samples are composed of a mosaic of fine to medium grained subhedral to euhedral randomly oriented dolomite rhombs usually obliterating all features characteristic of the associated peloid limestone. Occasionally there are vague indications of former peloids in the crystalline mosaic by a clustering of dusty inclusions surrounded by a clearer zone of rhombs (Figure 7). Dense peloids may persist as a microcrystalline calcite body in a sea of dolomite and are surrounded by euhedral dolomite rhombs. Occasionally sparry calcite was observed in the spaces between the dolomite rhombs. Disseminated opaques (estimated at less than 1%) are found throughout the dolomite both as anhedral pyrite masses and euhedral grains between rhombs. Occasional spherical to elliptical vugs (0.2-0.4mm) surrounded with inward projecting euhedral dolomite rhombs are observed.

Randall Quarry

The lithographic limestone and its dolomitized equivalent are exposed in the Randall Quarry located in Worth County, Iowa in Section 23, T99N, R20W. These flat lying carbonate rocks are part of the Rock Grove member of the Upper Devonian Shell Rock Formation. See Figure 8 for a general quarry section. The quarry face is predominantly composed of one foot thick beds of dense, dark brown banded medium to fine crystalline dolomite. Near the top of the face is a band of light gray lithographic limestone containing stromatoporoids. Within the dolomite there are lensatic zones of light gray hard lithographic limestone which change laterally into dolomite (Figure 9). Where these lensatic limestone zones occur, commonly

Figure 9. Generalized geologic section of carbonate rocks exposed in the Randall Quarry

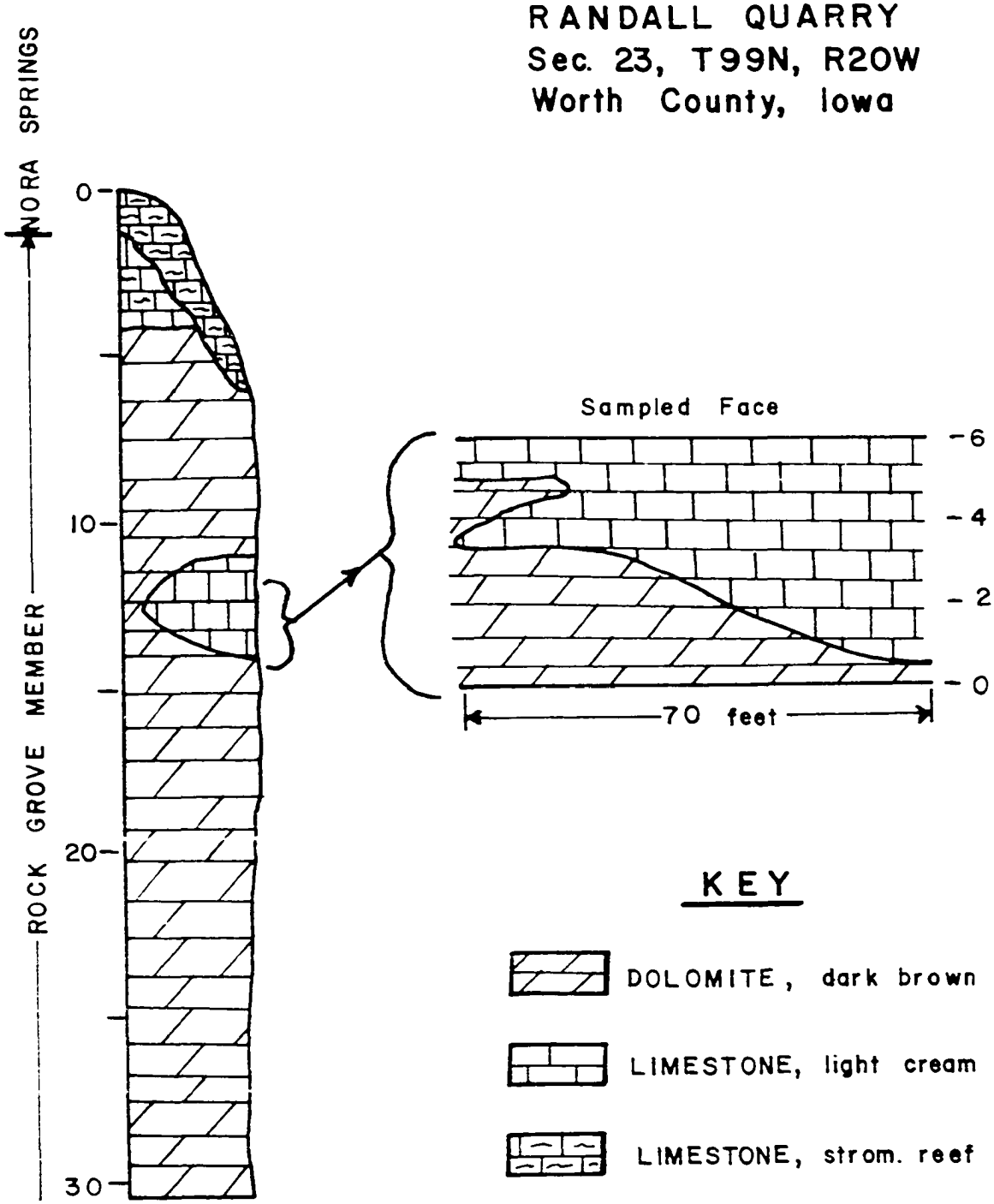
RANDALL QUARRY
Sec. 23, T99N, R20W
Worth County, Iowa
NORA SPRINGS
ROCK GROVE MEMBER
0
10
20
30
Sampled Face
6
4
2
0
70 feet
KEY
DOLOMITE, dark brown
LIMESTONE, light cream
LIMESTONE, strom. reef

a fracture surface is visible between the limestone and dolomite which did not allow sampling of a transition zone and only parent limestones and daughter dolomites were obtained. Where samples were obtained along the quarry face there was no apparent change in thickness of the unit as the rock changes from limestone to dolomite (Figure 1C).

Limestone

Macroscopically the limestone appears to be lithographic in texture containing occasional fossil fragments. Thin section study showed that the limestone is predominantly composed of microcrystalline calcite with varying amounts of fine grained (0.05mm) recrystallized sparry calcite and commonly termed a pelmicrite (Folk, 1959). The sections commonly exhibit a clotted or clustered appearance with diffuse boundaries between the microcrystalline and fine grained sparry calcite (Figure 11). Calcispheres are commonly observed and also occasional detrital silt-sized grains of quartz.

Dolomite

The dense dolomite shows a poorly developed color banding parallel to the bedding in the quarry and is composed of fine to medium grained dolomite. Microscopically the dolomite is an interlocking mosaic of medium grained (0.2mm average size) randomly oriented dolomite crystals. The dolomite crystals commonly show a zonal relationship with an interior of dusty inclusions surrounded by a clear rim zone (Figure 12). Relict features are occasionally observed and include calcisphere ghosts and dusty regions reminiscent of the clotted appearance of the limestone. (Compare Figures 11 and 12). Little to no porosity is observed and the sections

Figure 10. Sketch of the Randall Quarry face where samples were obtained for study of dolomitization

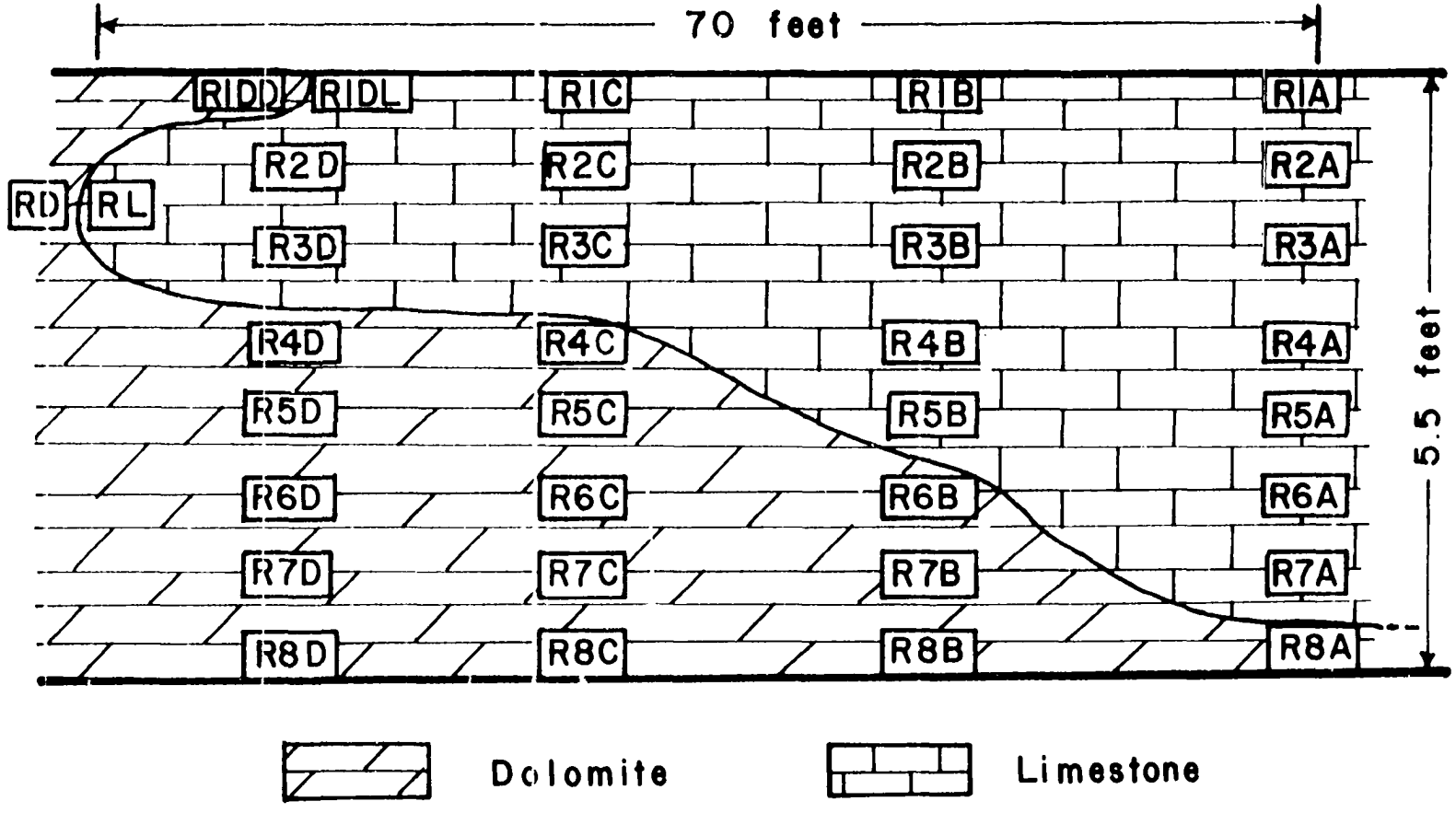
70 feet
R1D
R1DL
R1C
R1B
R1A
R2D
R2C
R2B
R2A
RD
RL
R3D
R3C
R3B
R3A
R4D
R4C
R4B
R4A
R5D
R5C
R5B
R5A
R6D
R6C
R6B
R6A
R7D
R7C
R7B
R7A
R8D
R8C
R8B
R8A
5.5 feet
Dolomite
Limestone

Figure 11. Microphotograph of lithographic limestone (pelmicrite) found at the Randall Quarry. Transmitted plane polarized light

Figure 12. Microphotograph of dolomite showing relict features and interlocking texture characteristic of dolomites found at the Randall Quarry. Transmitted plane polarized light

Figure 13. Late transition stage where a floating rhomb texture is being converted to a bridging framework. Transmitted plane polarized light


0.5mm


0.5mm

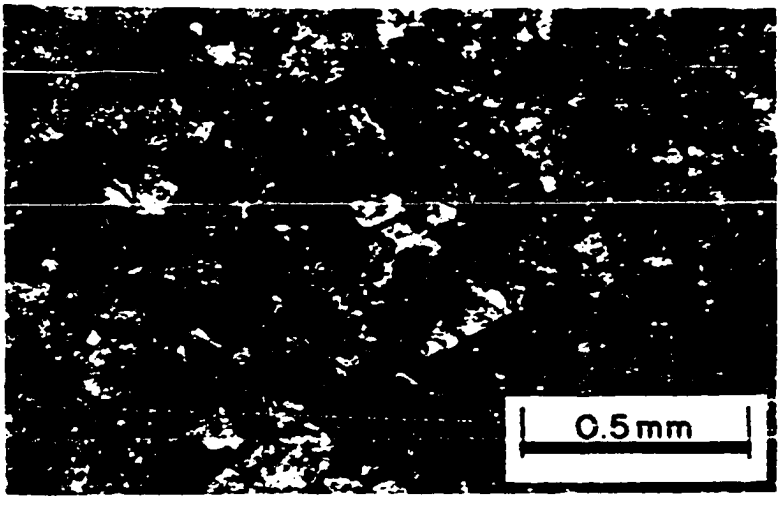
0.5mm

generally appear to be a completely interlocking mosaic of anhedral dolomite grains.

Because no transition zone was available, the exact paragenesis of how the limestone is dolomitized is not well documented. Samples collected on either side of the sharp contact between the limestone and dolomite were studied and indicate that there is a 1-5mm zone where a floating rhomb texture was developed (Figure 13). Dolomite rhombs in this zone are surrounded by microcrystalline calcite, zoned and stained with iron oxides.

## Summary of Petrography

Two types of limestone with contrasting textures being replaced by dolomite were obtained. The samples from the Ferguson Quarry are gradational from an peloid limestone through a transition zone into the dolomite. Study of these samples allows for a paragenesis to be determined in which the dolomite selectively replaces the sparry calcite material while maintaining the framework and finally the peloids. Commonly the dolomite obliterates all characteristics of its peloid limestone ancestry.

The Randall Quarry samples are representative of parent lithographic limestone and daughter dolomite. Study of these samples show that the limestone is predominately composed of microcrystalline calcite with various degrees of recrystallization and a clotted appearance. The dolomites are dense and exhibit dusty inclusions reminiscent of the clotted nature of the limestones.

## Paragenesis of Ferguson Quarry Samples

The petrographic study of the limestone, dolomite and transition zones show that the peloid limestone dolomitizes via a transition zone

where the sparry calcite matrix is selectively replaced by dolomite while maintaining the framework characteristic of the original limestone texture. As dolomitization proceeds by replacing the peloid bodies it usually destroys a vast majority of the original limestone texture. However, the dolomite phase does display a few recognizable relict features of the original limestone. These relict textures are inferred by an occasional unreplaced dense peloid remaining in the dolomite, a clumping of dusty inclusions surrounded by clear dolomite and occasional vugs in size range similar to the ovoids. Thus it is assumed that the dolomitization has maintained the original framework of the limestone and the unit container volume concept of replacement for computing gains and losses of material can be applied. Also no apparent volume changes as determined from variations in bed thicknesses were observed at the quarry during sample collection.

## Paragenesis of Randall Quarry Samples

The lack of good transition zones of adequate width suitable for study from this quarry hampers observation of the exact method by which the limestone is replaced by dolomite. Several samples studied along the sharp contact between the two phases indicated that the dolomitization may be via a floating rhomb type of transition (Figure 13). Because of inadequate petrographic evidence for the maintaining of a framework through a transition zone, use of the unit container volume model for gains and losses is based on field evidence of no apparent change in bedding thicknesses at the sampling site. In addition, there are occasional relict features, such as dusty and cloudy grains, preserved in the dolomites suggestive of the former pelmicrite texture of the lithographic limestone.

## Composition of the Carbonate Phases

During X-ray examination of the samples it was observed that the calcites and dolomite diffraction peaks were slightly shifted from the spacings described in the ASTM files. These lattice shifts are attributed to deviations from the ideal stoichiometry by the sample. The ordering peaks (10.1, 01.5 and 02.1) for the dolomites were observed in X-ray traces, though slightly diminished in height (Goldsmith and Graf, 1958b). Thus the dolomites are considered to be ordered structures. In order to estimate the departure of nonideality by the carbonate minerals, step-scaning at $0.01^{o}2\theta$ across the (00.6) peak was performed, in an effort to measure this spacing shift. From this value $C_o$ spacings were calculated and the machine error corrected against Reagent Grade $CaCO_3$ measurements. These values are tabulated in Table 2 along with the estimated mole% $MgCO_3$ in the carbonate structure as determined from values of $C_o$ versus $MgCO_3$ data given in Goldsmith and Graf (1958a) and Goldsmith et al. (1961).

### Ferguson Quarry samples

Measured $C_o$ spacings of the composite limestone samples from this quarry, composed of the peloids and sparry calcite phases, show two distinct compositions. These compositions are (1) 0.0-0.5 Mole % $MgCO_3$ and (2) 2.0-2.5 Mole % $MgCO_3$. Hand separation of the peloid bodies from the sparry calcite matrix, demonstrated that the 2.0-2.5 Mole % $MgCO_3$ phase was associated with them, and it is assumed that the sparry calcite is thus the 0.0-0.5% phase. Lattice spacing measurements of the dolomite phases indicate calcium-rich dolomites. The estimated $MgCO_3$ content from $C_o$ data for ordered dolomites show a range from 46-47 Mole % $MgCO_3$ for the

Table 2. X-ray lattice spacings and $MgCO_3$ mole fractions for selected samples from both quarries

| Sample | Limestone | | Dolomite | |
|---|---|---|---|---|
| | $C_o$ [a] | $MgCO_3$ [b] | $C_o$ [a] | $MgCO_3$ [b] |
| | | % | | % |
| Ferguson Quarry | | | | |
| 13-1 | 17.019<br>17.048 | 2.0<br>0.6 | 16.114 | 46.5 |
| 13-2 | 17.030<br>17.062 | 2.5<br>0.0 | 16.105 | 46.6 |
| 13-5 | 17.009<br>17.057 | 2.4<br>0.3 | 16.114 | 46.5 |
| 13-6 | 17.020<br>17.055 | 1.9<br>0.3 | 16.110 | 46.6 |
| 13-7 | 17.015<br>17.053 | 2.1<br>0.4 | 16.118 | 46.3 |
| 13-8 | 17.010<br>17.060 | 2.4<br>0.1 | 16.108 | 46.7 |
| Oolites | 17.020<br>17.009 | 2.0<br>2.4 | | |
| Randall Quarry | | | | |
| R4A | 17.036 | 1.2 | --- | --- |
| R4B | 17.035 | 1.2 | --- | --- |
| R5A | 17.042 | 0.9 | --- | --- |
| R5B | 17.050 | 0.05 | --- | --- |
| R4C | --- | --- | 16.110 | 46.6 |
| R4D | --- | --- | 16.086 | 47.4 |
| R5C | --- | --- | 16.112 | 46.5 |
| R5D | --- | --- | 16.108 | 46.7 |
| R1DL | 17.050 | 0.5 | --- | --- |
| R1DD | --- | --- | 16.115 | 46.4 |

[a] Machine error corrected against reagent grade calcite.

[b] From values for calcite and ordered dolomites (Goldsmith and Graf, 1958a).

dolomites (Goldsmith and Graf, 1958a).

The Ca, Mg, Fe, Mn chemical data for all samples from the quarry are fitted by a least squares method against both the calcite and dolomite contents, determined by quantitative X-ray diffraction. Extrapolation of the fits to 0.0 g/unit volume calcite and dolomite values are used as an estimate of the overall composition of dolomite and calcite, respectively. This data is tabulated in Table 3 along with the standard deviations for the y-axis intercept values. For the Ferguson Quarry the average compositions of the carbonates are:

$$\text{Limestone} - (Ca_{0.981}Mg_{0.017}Fe_{0.002}Mn_{0.0006})\ CO_3$$

$$\text{Dolomites} - (Ca_{0.541}Mg_{0.436}Fe_{0.021}Mn_{0.002})\ CO_3$$

These values are in good agreement with the nonideality of the carbonate structures indicated by X-ray diffraction measurements of $C_o$ shifts.

Randall Quarry samples

The limestone samples from this quarry show only a single $C_o$ lattice spacing corresponding to an 0.5-1.0 Mole % $MgCO_3$ solid solution. The dolomites are calcium-rich and have $C_o$ spacings corresponding to a $MgCO_3$ range of 46.5-47.5 Mole %. Extrapolated chemical data yielded the following average values of the molar compositions of the carbonate phases for the Randall Quarry:

$$\text{Limestone} - (Ca_{0.992}Mg_{0.006}Fe_{0.002}Mn_{0.0002})\ CO_3$$

$$\text{Dolomites} - (Ca_{0.539}Mg_{0.455}Fe_{0.005}Mn_{0.0003})\ CO_3$$

In this quarry the iron and manganese solid solution is insignificant for the samples studied.

Table 3. Regression extrapolations for average composition of calcite and dolomite from both quarries

| Element | mM ± 2 S.D. | Mole % ± 2 S.D. |
|---|---|---|
| Ferguson Quarry - Calcite | | |
| Ca | 25.100 ± 0.234 | 0.981 ± 0.0092 |
| Mg | 0.429 ± 0.118 | 0.017 ± 0.0046 |
| Fe | 0.052 ± 0.038 | 0.002 ± 0.0014 |
| Mn | 0.015 ± 0.004 | 0.0006 ± 0.0002 |
| Ferguson Quarry - Dolomite | | |
| Ca | 14.741 ± 0.172 | 0.541 ± 0.0060 |
| Mg | 11.892 ± 0.166 | 0.436 ± 0.0060 |
| Fe | 0.566 ± 0.042 | 0.021 ± 0.0016 |
| Mn | 0.053 ± 0.004 | 0.002 ± 0.0002 |
| Randall Quarry - Calcite | | |
| Ca | 24.957 ± 0.404 | 0.992 ± 0.0160 |
| Mg | 0.139 ± 0.094 | 0.006 ± 0.0038 |
| Fe | 0.042 ± 0.030 | 0.002 ± 0.0012 |
| Mn | 0.004 ± 0.006 | 0.0002 ± 0.0004 |
| Randall Quarry - Dolomite | | |
| Ca | 15.328 ± 0.154 | 0.539 ± 0.0108 |
| Mg | 12.924 ± 0.122 | 0.455 ± 0.0090 |
| Fe | 0.151 ± 0.017 | 0.005 ± 0.0012 |
| Mn | 0.009 ± 0.003 | 0.0003 ± 0.0002 |

Summary

The limestones of the Ferguson Quarry are composed of two distinct types of calcite; a 2-2.5% $M_2CO_3$ calcite characteristic of the peloids and a 0.0-0.5% $M_2CO_3$ calcite characteristic of the sparry calcite matrix. The dolomites are calcium-rich and show some solid solution of iron and manganese. Though these are considered nonstoichiometric carbonates they all show the order reflections indicative of ordered carbonate structures.

The limestones of the Randall Quarry are composed of one calcite type with 0.5-1.5% $MgCO_3$ in solid solution. Also, the dolomites are calcium-rich with only trace amounts of iron and manganese substitution. Again the carbonates studied show the order reflections indicative of ordered carbonate structures.

# PRESENTATION OF EXPERIMENTAL DATA

In order to have better control and internal consistency of the measured values for each core, as many measurements as possible were performed on each individual core. The experimental data obtained is considered characteristic of each core and not the whole block sample. Thus a variation of data exists from core to core and is considered to reflect the heterogeniety of the system caused by local environmental control. The relationship of mass and void partial volumes to the chemical data provide the evidence for the variations that exists between cores. This section will present the void volume data relationships for each quarry followed by the chemical data and computation of gains and losses of material within the unit container volume.

## Void Volume-Pore Radii Relationships

A critical aspect of this study is the necessity to account for mass and void volume changes associated with dolomitization of limestones. In this section partial volume data are presented because void volumes, mass volumes and the relationship of void volume to pore radii are important in interpretation of the replacement process.

### Ferguson Quarry samples

Because volume parameters were measured on core samples which are later used in chemical tests, volume-composition relationships are under much closer control and are representative of each core sample. Samples were obtained as part of gradational sequences of the limestone, transition and dolomite zones. (See Figure 14 for example of variation of physical

Figure 14. A plot of physical properties measured on selected cores for block sample Ferguson 13-5. The properties shown are porosity, grain density and bulk density

# FERGUSON 13-5

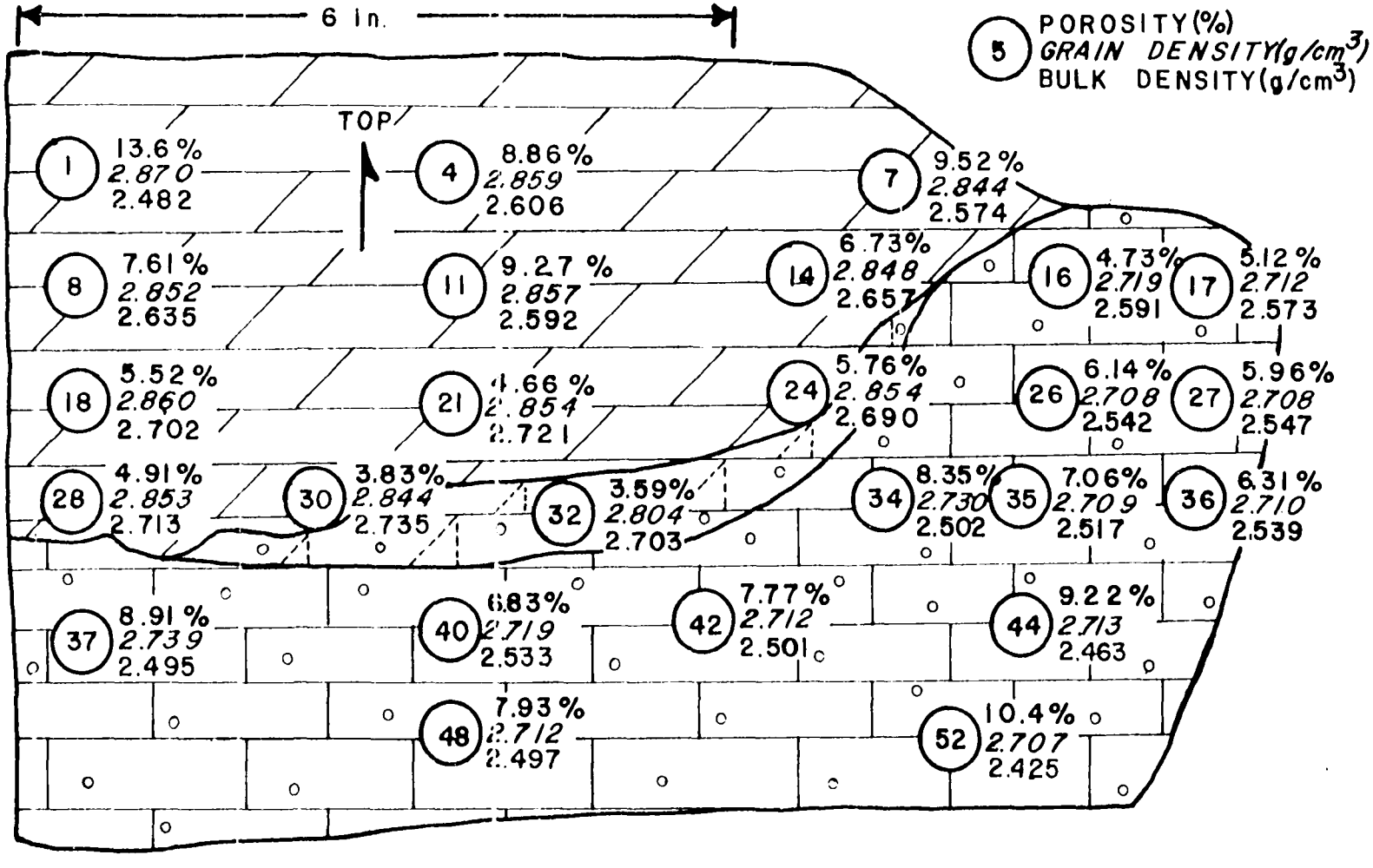

properties and core position in a given sample.) Figure 15 shows three frequency distributions of porosity for all samples representative of each zone along with a representative pore volume distribution curve. The data in this figure indicate a relationship between porosity, pore volume distribution and dolomitization. The peloid limestone averages 5.7 ± 1.5% porosity predominately in the pore radius range of 0.2 micron size and less. The transition zone averages 4.3 ± 1.1% porosity showing a decrease in pore volumes of the 0.2 micron size and less range and indicating development of secondary pores in the 1-10 micron size range at the expense of the smaller sized pores. In contrast the dolomites, averaging 8.9 ± 2.8% predominately in the 1 to 20 micron size range, show a higher porosity than either the limestone or transition zones. Only a small amount of fine pores remain in the dolomites indicating a marked increase in pore size at the expense of finer pores.

Randall Quarry samples

Block samples obtained from either side of the limestone-dolomite interface limited the study to parent-daughter samples with no available data for a transition zone. Figure 16 summarizes the void volume data for limestone and dolomite samples. Porosity values vary widely for lithographic limestones averaging 6.3 ± 3.4% with the voids predominately in the 0.3 microns size range and smaller. In contrast, dolomites are of lower porosity averaging 3.6 ± 1.2%. However, pore volume distributions indicate essentially none of the porosity is in the measurable size range and thus predominately in the less than 0.05 micron size range. This fact was also noted in petrographic studies where the dolomites are composed of

Figure 15. Void volume-pore radii relationships for samples from the Ferguson Quarry. Frequency distributions of porosity and a characteristic pore radii-volume distribution for the limestone, transition, and dolomite zones are shown

## LIMESTONE

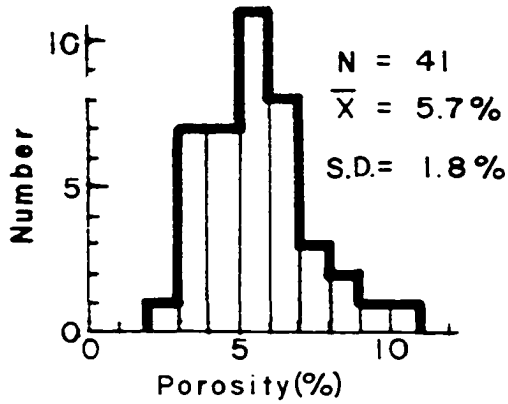


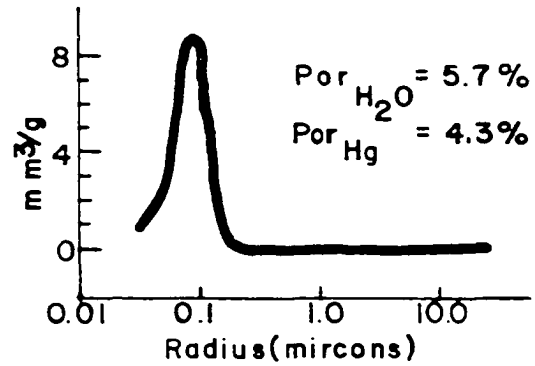


## TRANSITION

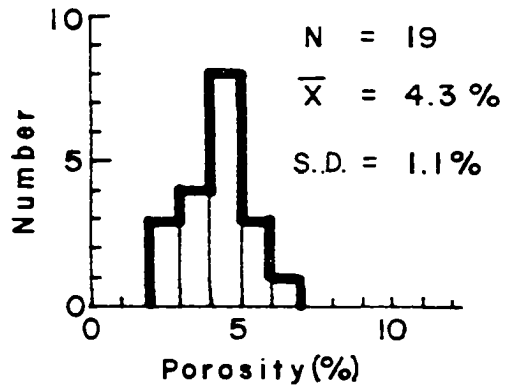


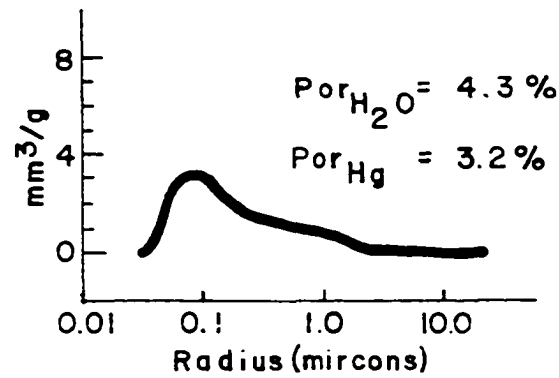


## DOLOMITE

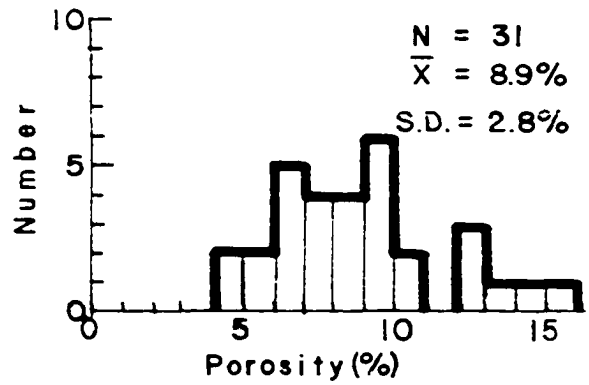


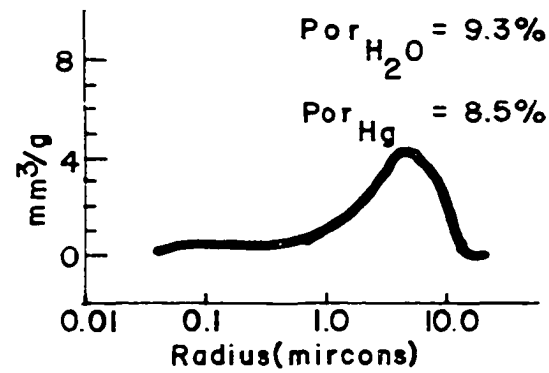

Figure 16. Void volume-pore radii relationships for samples from the Randall Quarry. Frequency distributions of porosity and a characteristic pore radii-volume distribution for the limestone and dolomite zones are shown

## LIMESTONE

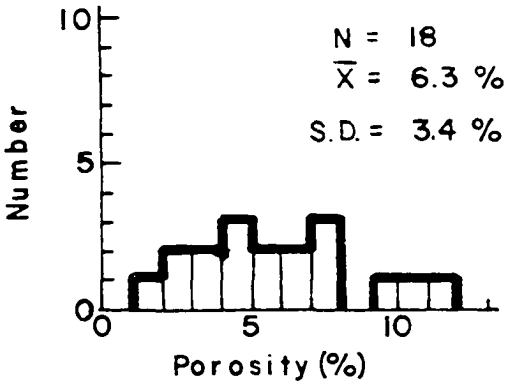


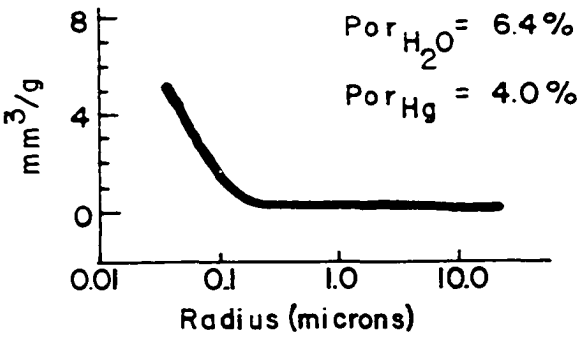


## DOLOMITE

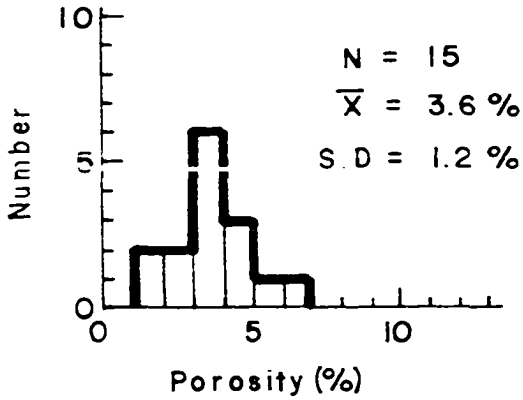


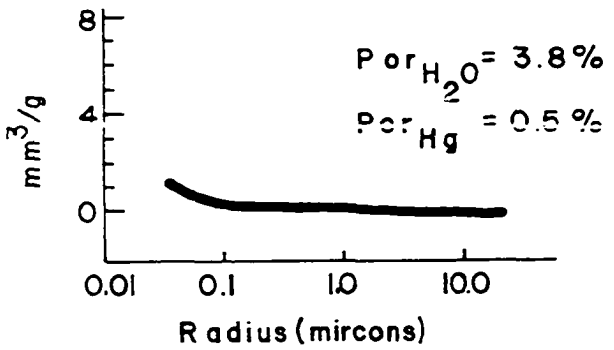

a dense interlocking mosaic of dolomite crystals lacking visible porosity. Due to lack of transition zone samples, the porosity-pore size relationships are not known for this portion of the system.

Summary

The overall void volume changes for the systems studied show two distinct types of volume changes during dolomitization. The Ferguson Quarry peloid limestone shows an average increase of porosity with dolomitization. Also, a definite relationship between pore volume and pore radius exists for dolomitization showing an obliteration of the small pore radii characteristic of the peloid limestones and formation of larger pores of the dolomite. Initial obliteration of small pores for larger pores is observed in transition zone samples.

The Randall Quarry samples demonstrate a different behavior of the void volume-void radii with dolomitization of a lithographic limestone. There is an overall decrease in porosity as well as a shift of pores sizes to very small radii (less than 0.1 microns). However, due to limitations of the equipment to measure pores below 0.05 microns radii, the exact pore volume-radius relationship is not known, but the majority of the radii are considered to be in the less than 0.05 micron size range. This extremely small pore radii characteristic of the dolomites is confirmed by petrographic study of the interlocking dolomite moxaic and its lack of visible porosity. Also the dolomite is extremely dense which would indicate presence of only small pores.

## Phase and Component Relationships

Evaluation of composition-volume relationships for a replacement process necessitates recomputation of the intensive weight percent data to thermodynamically extensive parameters, such that gains and losses may be computed. Application of the unit container volume concept to study of epigenetic dolomitization places the chemical data on an extensive basis allowing computation of gains and losses of phases and components related to dolomitization. Also, void or mass volume changes are accounted for and usable in explaining the mechanisms of the process. During replacement of limestone by dolomite the total volume is occupied by varying amounts of calcite, dolomite, pyrite, quartz and clay phases.

### Ferguson Quarry samples

The core sampling of the blocks obtained enables comparison of the parent-daughter compositional relationships for the dolomitization system. Figures 14, 17 and 18 are presented to show the variation of values for certain properties measured on cores extracted from block 13-5. Figure 14 presents the physical data, inspection of which shows a variability of the bulk density and porosity values on either side of the interface. Figure 17 gives the distribution of g/cc values for the phases calcite, dolomite and acid insoluble residue. Figure 18 gives the distribution of CaO, MgO, $Fe_2O_3$ components in g/cc for the samples. Inspection of the three diagrams shows that a positive relationship occurs between dolomite, iron, magnesium, calcium and acid insoluble residue values. Also it is apparent that a small variation of parameter values exists within the dolomite and limestone zones. Thus in the computation of gains and losses by random

Figure 17. Plot of calcite, dolomite and acid insoluble residue contents for Ferguson Block 13-5

# FERGUSON 13-5

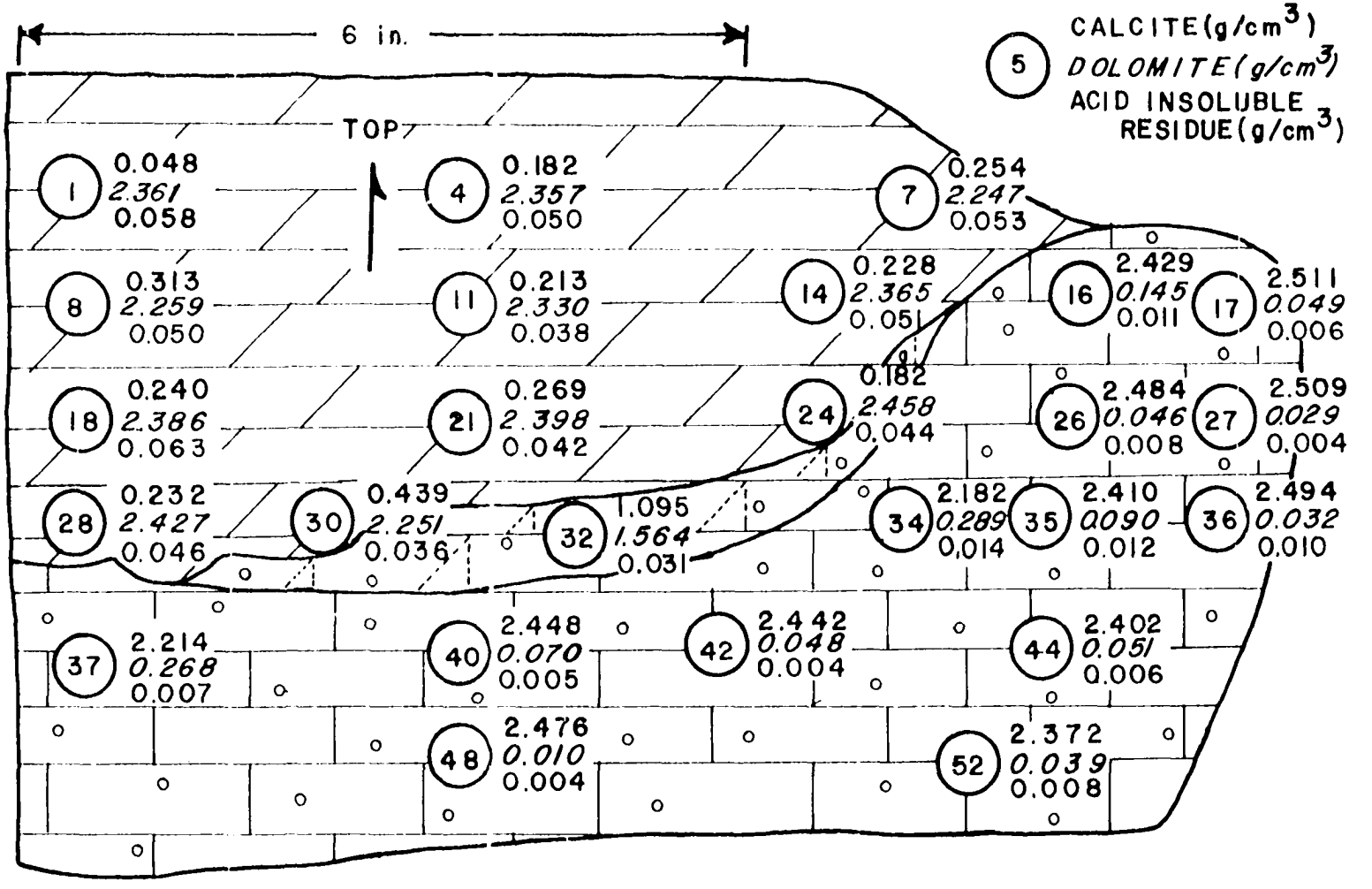

Figure 18. CaO, MgO and $Fe_2O_3$ contents for Ferguson Block 13-5

# FERGUSON 13-5

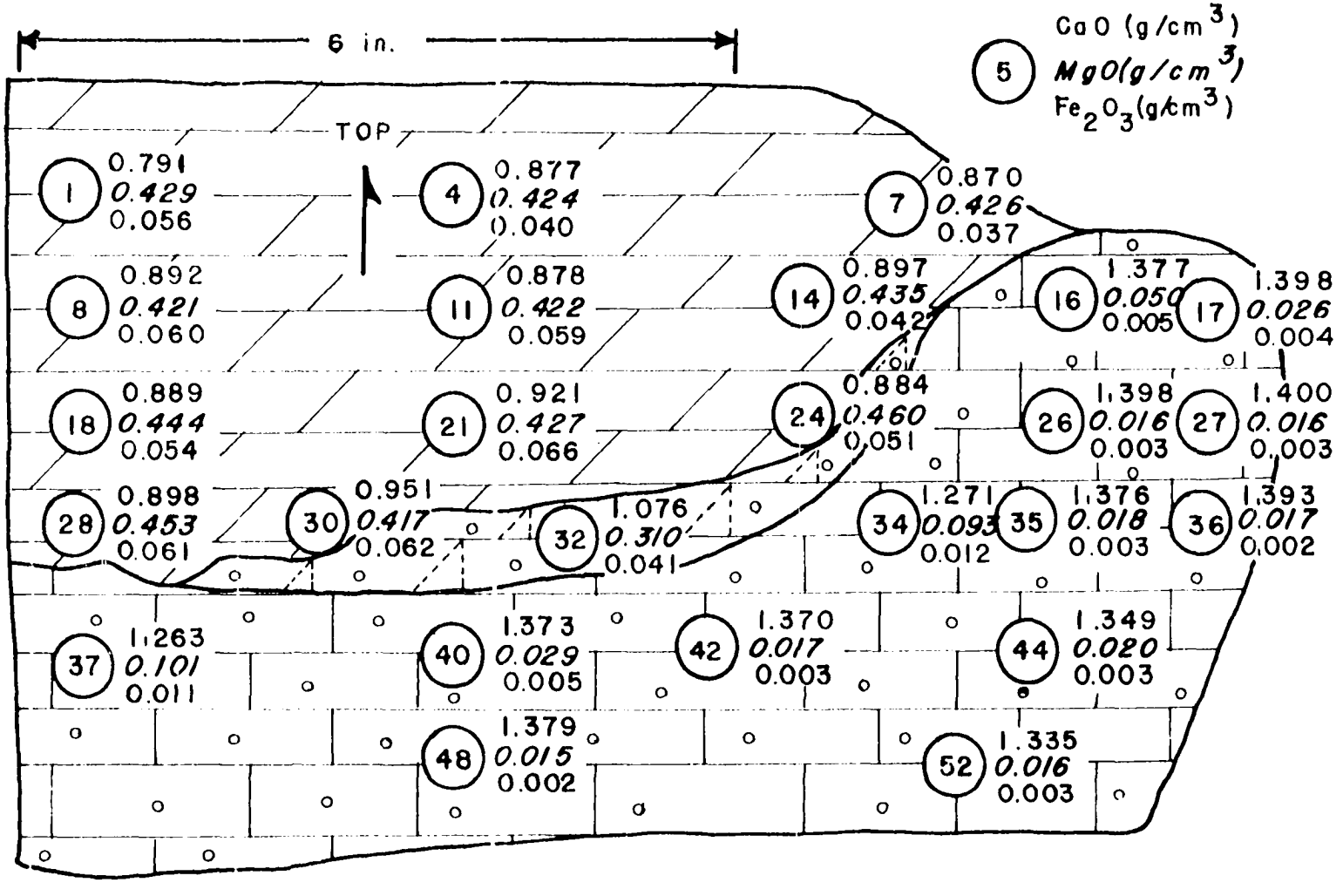

pairing of parent-daughter samples, a range of gains and losses will be observed within the block. Figure 19 is a plot of gains and losses of calcite and dolomite by random pairing for block 13-5. The comparison of random pairs yields a range of gains and losses dependent on the particular pair selected. A problem is raised as to which set of values is most representative. This leads to use of average values as a basis of comparisons to yield a better overall picture of the changes occurring during dolomitization. Table 4 is a summation of the gains and losses of phases and components for each block analyzed. There is a variation of changes within each block as well as between the block samples. In general, a definite pattern of changes is evident when considering the nature of the changes for the Ferguson Quarry. There is an increase of dolomite, pyrite, acid insoluble residue, iron, aluminum, manganese,magnesium, sodium, potassium, carbon dioxide, and sulfate. The only materials decreasing are calcite and calcium. Overall, there is a tendency for an increase of mass with a net gain of porosity.

Randall Quarry samples

Samples representative of dolomitization at the Randall Quarry were more limited than at the Ferguson Quarry because transition zones were not available. Therefore, the sampling was accomplished by four vertical sections taken across the limestone-dolomite interface (Figure 10). Eight samples were obtained at each vertical section, and the same unit traced laterally between the sections. Samples representative of the same unit within the dolomite and limestone were obtained to check the variability of chemical and physical properties within a single bedding unit. These

Figure 19. Frequency distribution diagram for gains and losses of dolomite and calcite contents obtained by random pairing of limestone and dolomite cores for Ferguson Block 13-5

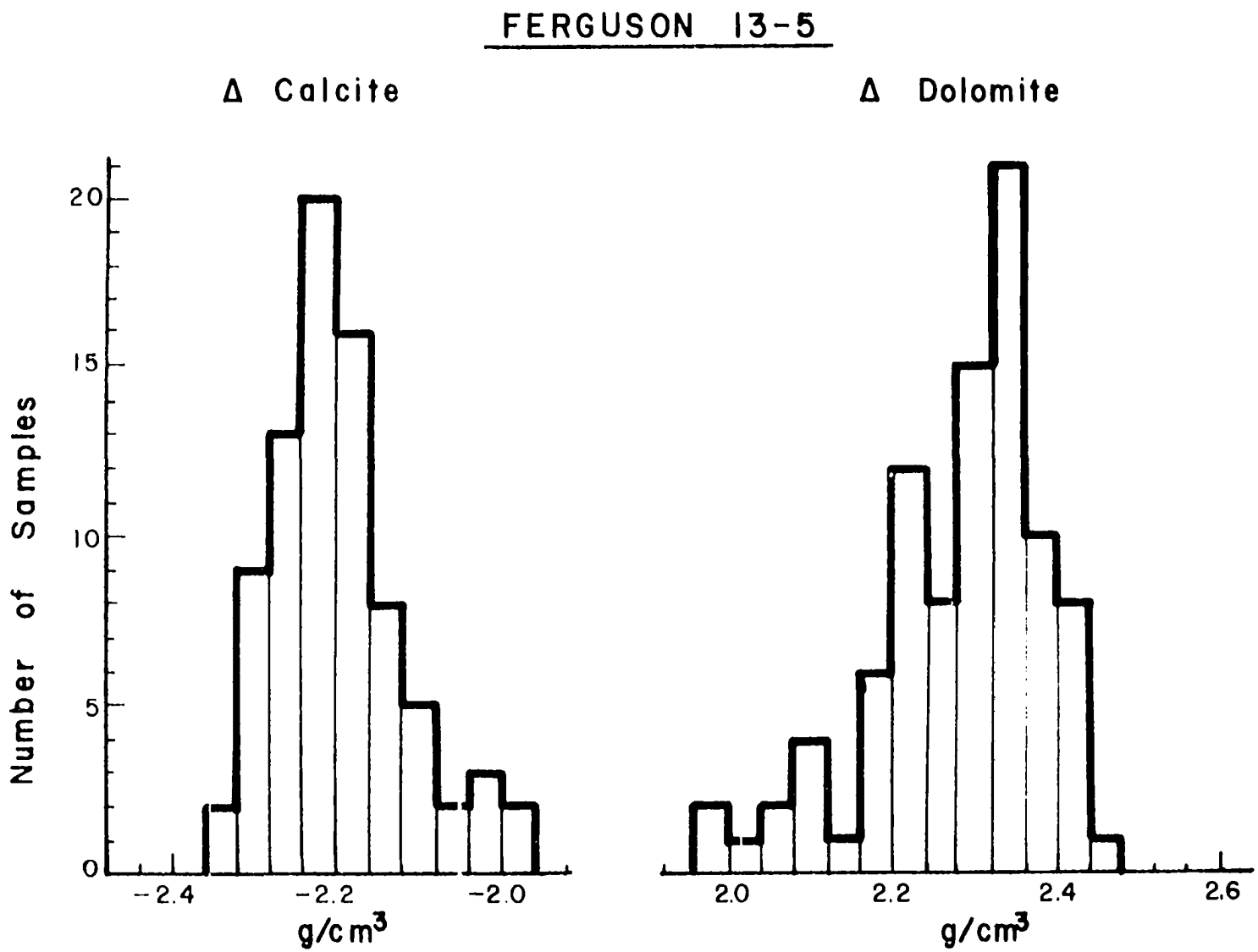
FERGUSON 13-5
Δ Calcite
Δ Dolomite
Number of Samples
0
5
10
15
20
-2.4
-2.2
-2.0
g/cm3
2.0
2.2
2.4
2.6
g/cm3

Table 4. Average gains and losses of material for selected sets of cores for Ferguson Quarry samples (values in grams per cc.)

| Constituent | 13-D | 13-1 | 13-2 | 13-3 | 13-4 | 13-5A | 13-5B | 13-6 | 13-7 | 13-8 |
|---|---|---|---|---|---|---|---|---|---|---|
| Dolomite | +2.3589 | +2.2892 | +2.3500 | +2.0517 | +2.1196 | +2.2212 | +2.3766 | +2.1630 | +2.2269 | +2.3859 |
| Calcite | -2.3936 | -2.4229 | -2.2728 | -2.0006 | -2.0301 | -2.2188 | -2.2662 | -2.3096 | -2.3447 | -2.4480 |
| Pyrite | +0.0041 | +0.0053 | +0.0024 | +0.0040 | +0.0036 | +0.0001 | +0.0019 | +0.0020 | +0.0004 | +0.0069 |
| AIR[a] | +0.0400 | +0.0321 | +0.0260 | +0.0479 | +0.0263 | +0.0381 | +0.0438 | +0.0389 | +0.0393 | +0.0466 |
| $Al_2O_3$ | +0.0017 | +0.0017 | +0.0011 | +0.0015 | +0.0009 | +0.0009 | +0.0019 | +0.0014 | +0.0014 | +0.0014 |
| $Fe_2O_3$ | +0.0373 | +0.0332 | +0.0496 | +0.0173 | +0.0208 | +0.0490 | +0.544 | +0.0255 | +0.0316 | +0.0263 |
| $Mn_2O_3$ | +0.0028 | +0.0024 | +0.0035 | +0.0014 | +0.0008 | +0.0038 | +0.0041 | +0.0005 | +0.0025 | +0.0019 |
| CaO | -0.5455 | -0.5831 | -0.4859 | -0.4154 | -0.4239 | -0.4988 | -0.5013 | -0.5711 | -0.5831 | -0.5761 |
| MgO | +0.4213 | +0.4043 | +0.4137 | +0.3631 | +0.3810 | +0.3885 | +0.4280 | +0.3905 | +0.4127 | +0.4360 |
| $Na_2O$ | +0.0013 | +0.0015 | +0.0012 | +0.0013 | +0.0012 | +0.0011 | +0.0007 | +0.0018 | +0.0013 | +0.0018 |
| $K_2O$ | +0.0011 | +0.0010 | +0.0008 | +0.0013 | +0.0006 | +0.0007 | +0.0004 | +0.0010 | +0.0010 | +0.0009 |
| $CO_2$ | +0.0509 | +0.0135 | +0.0984 | +0.0880 | +0.1120 | +0.0609 | +0.1258 | +0.0100 | +0.0158 | +0.0532 |
| $SO_3$ | +0.0023 | +0.0058 | +0.0031 | +0.0048 | +0.0020 | +0.0018 | +0.0009 | +0.0053 | +0.0040 | +0.0050 |
| Δ g/cc | -0.0367 | -0.1337 | +0.0872 | +0.0511 | +0.0895 | +0.0024 | +0.1104 | -0.1466 | -0.1178 | -0.0621 |
| Δ cc | +0.061 | +0.090 | +0.019 | +0.019 | +0.009 | +0.048 | +0.004 | +0.095 | +0.085 | +0.068 |
| Sr[b] | -33 | -42 | -65 | +63 | -1 | -55 | -99 | -12 | -4 | +12 |
| Cu[b] | -2.5 | +2.0 | +1.5 | +0.0 | -6.0 | -2.1 | -4.1 | -0.1 | -3.4 | +4.0 |
| Zn[b] | +71 | +2 | +14 | -21 | -6 | +29 | +48 | +27 | -46 | +4 |
| Pb[b] | -21 | -10 | -12 | -13 | -29 | -82 | -16 | -11 | -40 | +32 |

[a]Acid Insoluble Residue.

[b]Content in micrograms per cc.

properties are presented in Table 5 as average values and standard deviations. It is apparent that generally about 5% variation of properties, largely dependent on bulk density, exists for the samples and explains the variation observed by random pairing of sample sets for gains and losses of material.

Table 5. Average values and standard deviations for the samples collected at the Randall Quarry to test the lateral variation along a given bed

| Constituent | Limestone-g/cc | | Dolomite-g/cc | |
|---|---|---|---|---|
| | $\bar{X}$ | S.D. | $\bar{X}$ | S.D. |
| Dolomite | 0.0111 | 0.0048 | 2.5653 | 0.1066 |
| Calcite | 2.5638 | 0.0092 | 0.1371 | 0.0578 |
| Pyrite | 0.0002 | 0.0001 | 0.0004 | 0.0002 |
| AIR[a] | 0.0234 | 0.0129 | 0.0197 | 0.0020 |
| $Al_2O$ | 0.0004 | 0.0002 | 0.0006 | 0.0002 |
| $Fe_2O_3$ | 0.0043 | 0.0013 | 0.0066 | 0.0011 |
| $Mn_2O_3$ | 0.0003 | 0.0001 | 0.0006 | 0.0001 |
| CaO | 1.4300 | 0.0021 | 0.9263 | 0.0122 |
| MgO | 0.0068 | 0.0017 | 0.4929 | 0.0156 |
| $Na_2O$ | 0.0003 | 0.0001 | 0.0024 | 0.0001 |
| $K_2O$ | 0.0004 | 0.0001 | 0.0006 | 0.0001 |
| $CO_2$ | 1.1321 | 0.0059 | 1.2791 | 0.0259 |
| $SO_3$ | 0.0018 | 0.0010 | 0.0045 | 0.0007 |
| $Sr^b$ | 115 | 10 | 100 | 29 |
| $Cu^b$ | 3.2 | 0.8 | 2.4 | 1.0 |
| $Zn^b$ | 22 | 2.3 | 30 | 10 |
| $Pb^b$ | 13 | 4.6 | 7.7 | 2.6 |

[a]Acid Insoluble Residue.

[b]Content in micrograms per cc.

The parent-daughter average gains and losses of phases and oxides for four series of lateral comparisons from lower portion of sampled section are given Table 6. These data indicate increases in the amount of dolomite, acid insoluble residue, Mg, Fe, Al, Mn, Na, K, $CO_2$, and $SO_3$ with a decrease in calcite and Ca. There is no distinct trend of pyrite with dolomitization. Also, there is a decrease of pore space and addition of mass to the system. In contrast, two sample sets, RL and R1DL, obtained from the upper portion of the quarry display a pore creating phenomenon with an increase of porosity with dolomitization.

Table 6. Gains and losses of material for paired sets of data from Randall Quarry (grams per cc)

| Constituent | R4A | R5A | R6A | R7A | RL | R1DL |
|---|---|---|---|---|---|---|
| Dolomite | +2.5360 | +2.5587 | +2.6306 | +2.6318 | +1.9107 | +2.2515 |
| Calcite | -2.4457 | -2.3624 | -2.3401 | -2.4227 | -1.9682 | -2.3593 |
| Pyrite | 0.0000 | 0.0000 | -0.0001 | -0.0001 | -0.0025 | 0.0000 |
| AIR[a] | +0.0890 | +0.481 | -0.0060 | -0.0113 | +0.0347 | +0.0472 |
| $Al_2O_3$ | +0.0035 | +0.0018 | +0.0003 | +0.0004 | +0.0014 | +0.0017 |
| $Fe_2O_3$ | +0.231 | +0.0102 | +0.0070 | +0.0056 | +0.0065 | +0.0139 |
| $Mn_2O_3$ | +0.0004 | +0.0003 | +0.0003 | +0.0002 | +0.0001 | +0.0004 |
| CaO | -0.5231 | -0.5137 | -0.4580 | -0.4982 | -0.4811 | -0.5771 |
| MgO | +0.4821 | +0.5051 | +0.5121 | +0.5138 | +0.3811 | +0.4259 |
| $Na_2O$ | +0.0018 | +0.0012 | +0.0013 | +0.0017 | +0.0012 | +0.0017 |
| $K_2O$ | +0.0025 | +0.0012 | +0.0001 | +0.0003 | +0.0012 | +0.0012 |
| $CO_2$ | +0.1444 | +0.1872 | +0.2308 | +0.1896 | +0.0371 | +0.0312 |
| $SO_3$ | +0.0019 | +0.0020 | +0.0025 | +0.0028 | +0.0023 | +0.0030 |
| Δ g/cc | +0.0909 | +0.1963 | +0.2905 | +0.2091 | -0.0575 | -0.1078 |
| Δ cc | +0.013 | -0.026 | -0.060 | -0.029 | +0.055 | +0.082 |
| Sr[b] | -39 | -101 | -219 | -188 | -28 | -209 |
| Cu[b] | -3.5 | +6.1 | +3.1 | -0.1 | -1.5 | -2.1 |
| Zn[b] | -37 | +219 | +171 | -13 | 0.0 | -24 |
| Pb[b] | -9 | -5 | -4 | -1 | -14 | -3 |

[a]Acid Insoluble Residue.

[b]Content in micrograms per cc.

# DISCUSSION

Before discussing and interpreting the experimental results a few words concerning the system, model assumptions and pitfalls are required. It should be realized that the data obtained only provide net overall changes in a system undergoing a variety of changes through time in which dolomitization is considered the predominant change. In addition it must be understood that the system represents a continuum of changes ranging from unaltered limestone grading into dolomite. Unfortunately the methods used in sampling only provide data at a few points along this continuum. By analogy the sampling is equivalent to reading only a limited number of pages of a large text in a random but consecutive manner with the belief that this will provide some understanding of what the text is about.

One assumption that must be made if use of the unit container volume to describe quantitative changes for geologic processes is valid, is that negligible post-dolomitization changes have occurred. However, a possibility of secondary deposition of calcite in the pore spaces exists and probably occurs to a minor extent. Another problem is secondary leaching by groundwaters. Petrographic evidence of leaching was seldom observed in both quarries indicating a minimal effect on the system. By avoiding all visible styolitic seams during core sampling, this post-dolomitization phenomena is considered to be of minor effect. Thus careful selection of samples and petrographic study has hopefully minimized these secondary effects and the use of the unit container volume model represents a realistic estimate of the net changes for all processes occurring in the system.

Because a gram per unit volume basis for computations of gains and losses is used, no exact equation can be written to explain the process. This is due to differing amounts of mass on either side of the equation. As the pore fluids responsible for the process cannot be sampled, and only the solids were analyzed, the actual contribution of pore fluids cannot be uniquely ascertained. Ridge (1949, 1961) overcame this problem by introducing mobile components into both sides of the reaction, which while participating in the reaction, leave no solid evidence behind for us to measure. Also, the calculated gains and losses only represent the cumulative effect of all changes that may have occurred within the container. Analysis of physical, chemical and petrographic data indicates that epigenetic dolomitization is a complex process, and no simple equation of replacement can account for all the compositional and volume changes which have occurred. Considerable variation in the dolomitization process is evident not only between the two quarries, but also between individual blocks samples within a given quarry. Secondly, dolomitization is not the only process occurring because chemical evidence indicates that pyrite, quartz and clay minerals are concurrently introduced with dolomitization.

Analysis of the quantitative data based on the unit container volume concept of replacement will initially be compared to the currently accepted models used to explain replacement:

(1) Volume-for-volume

(2) Mole-for-mole.

The comparison to be used requires evaluation of mass changes occurring concurrently with volume changes for the carbonate phases. Following the analysis of volume-mass changes, petrogenic models for dolomitization

occurring in the Ferguson and Randall quarries, speculation on the type of fluids responsible, and complexities of the process are presented.

## Volume-Mass Changes of the Carbonate Phases

A method which allows interpretation of the experimental data with respect to mole-for-mole and volume-for-volume is to compare the changes in mass per unit volume with changes in volume of pore space for the carbonate minerals present when dolomitization occurs theoretically as a mole-for-mole and volume-for-volume process. Plotting of the experimental values obtained in this study along with the two theoretical values allows one to compare and contrast experimental data against accepted values for the theoretical processes by which dolomitization is generally assumed to occur. Several initial computations are presented for the expected mass per unit volume and pore volume changes for mole-for-mole and volume-for-volume modes of replacement. If it is assumed that dolomitization occurs as an interaction of solid $CaCO_3$ with pore fluids containing $Mg^{2+}$ and $CO_3^{2-}$ ions, the following assumptions are used:

a) Reaction proceeds stepwise by leaching of the $CaCO_3$ and deposition of the dolomite.

b) Only $Ca^{2+}$, $Mg^{2+}$, and $CO_3^{2-}$ ions are added or removed by the pore fluids to the solids.

c) All the pre-existing $CaCO_3$ is removed or converted to dolomite or a 100 percent replacement.

d) The total volume of space before and after is considered that occupied by the pre-existing $CaCO_3$.

The stepwise reactions can be characterized by

a) $CaCO_3 + H_2O \rightarrow Ca^{2+} + HCO^-_{3aq} + OH^-$

b) $Ca^{2+}_{aq} + Mg^{2+}_{aq} + 2HCO^-_3 + 2OH^- \rightarrow CaMg(CO_3)_2 + 2H_2O$

with the overall reaction represented as

$$2CaCO_3 + (1+X)Mg^{2+}_{aq} + (X)HCO^-_{3aq} + (X)OH^- \rightarrow$$

$$(1+X)CaMg(CO_3)_2 + (1-X)Ca^{2+}_{aq} + (X)H_2O$$

where X is that molar quantity of dolomite needed to balance the equation for a given pore or mass volume constraint.

Case I - Mole-for-Mole (assuming no additional $CO^{2-}_3$ is added to the system)

Molar Basis - $2CaCO_3 + Mg^{2+}_{aq} \rightarrow CaMg(CO_3)_2 + Ca^{2+}_{aq}$

Volume Basis - 2(36.93 cc/mole) → 1(64.76 cc/mole) + 9.1 cc voids

Mass Basis - 2(100.09 g/mole → 184.43 g/mole

g/cc - 2.710 g/cc → 2.497 g/c

Therefore: Δ g/cc = -0.213 g/cc

Δ pores = +0.123 cc

Case II - Volume-for-Volume (assuming all of the final volume is occupied by dolomite, hence X = 0.14)

Molar Basis - $2CaCO_3 + 1.14\ Mg^{2+}_{aq} + 0.14\ HCO^-_3 \rightarrow$

$$1.14\ CaMg(CO_3)_2 + 0.86\ Ca^{2+} + 0.14\ H_2O$$

Volume Basis - 2(36.93 cc/mole) → 1.14 (64.76 cc/moles) + 0.00 voids

Mass Basis - 2(100.09 g/mole) → 1.14 (184.43 cc/moles)

g/cc - 2.710 g/cc → 2.848 g/cc

Therefore: Δ g/cc = +0.138 g/cc

Δ pores = +0.000 cc

Plotting these unique solutions obtained in Case I and Case II for

carbonate replacement in terms of Δ g/cc versus Δ cc pore space is shown in Figure 20. If the process of dolomitization is actually operative by Case I or Case II, experimental values obtained for this study should group about that theoretical value representative of the replacement method by which dolomitization occurs. Also plotted on Figure 20 are experimental values obtained by use of paired averages of before and after comparisons for both quarries. It is immediately apparent that the experimental values do not cluster about the mole-for-mole or volume-for-volume points, but scatter all along or below the line considered representative of 100% conversion of calcite to dolomite which passes through the theoretical points. For the examples studied the conclusion is reached that dolomitization has occurred in a variety of ways. Samples from the lower portion of the Randall Quarry paired sets all fall near or beyond the volume-for-volume value, indicating the process is pore filling where more dolomite mass volume has been added to the system than calcite mass volume removed. The two data sets from the upper portion of the Randall Quarry show a net gain in pore space for the process falling between the mole-for-mole and volume-for-volume values. However, the paired sets of Ferguson Quarry samples generally fall somewhere between the mole-for-mole and volume-for-volume values, indicating an increase in net pore volume.

Also plotted on Figure 20 are 50% replacement values for Cases I and II for calcite replacement by dolomite. All of the experimental values plot below the 100% dolomite replacement by varying amounts. Those points below the theoretical 100% line are considered representative of incomplete dolomite replacement and a measure of the degree of completeness of the replacement reaction within the total volume. In addition, it was assumed

Figure 20. Plot of $\Sigma$ pores versus $\Delta$ g/cm$^3$ for the carbonate phases in systems studied and for theoretical Cases I and II

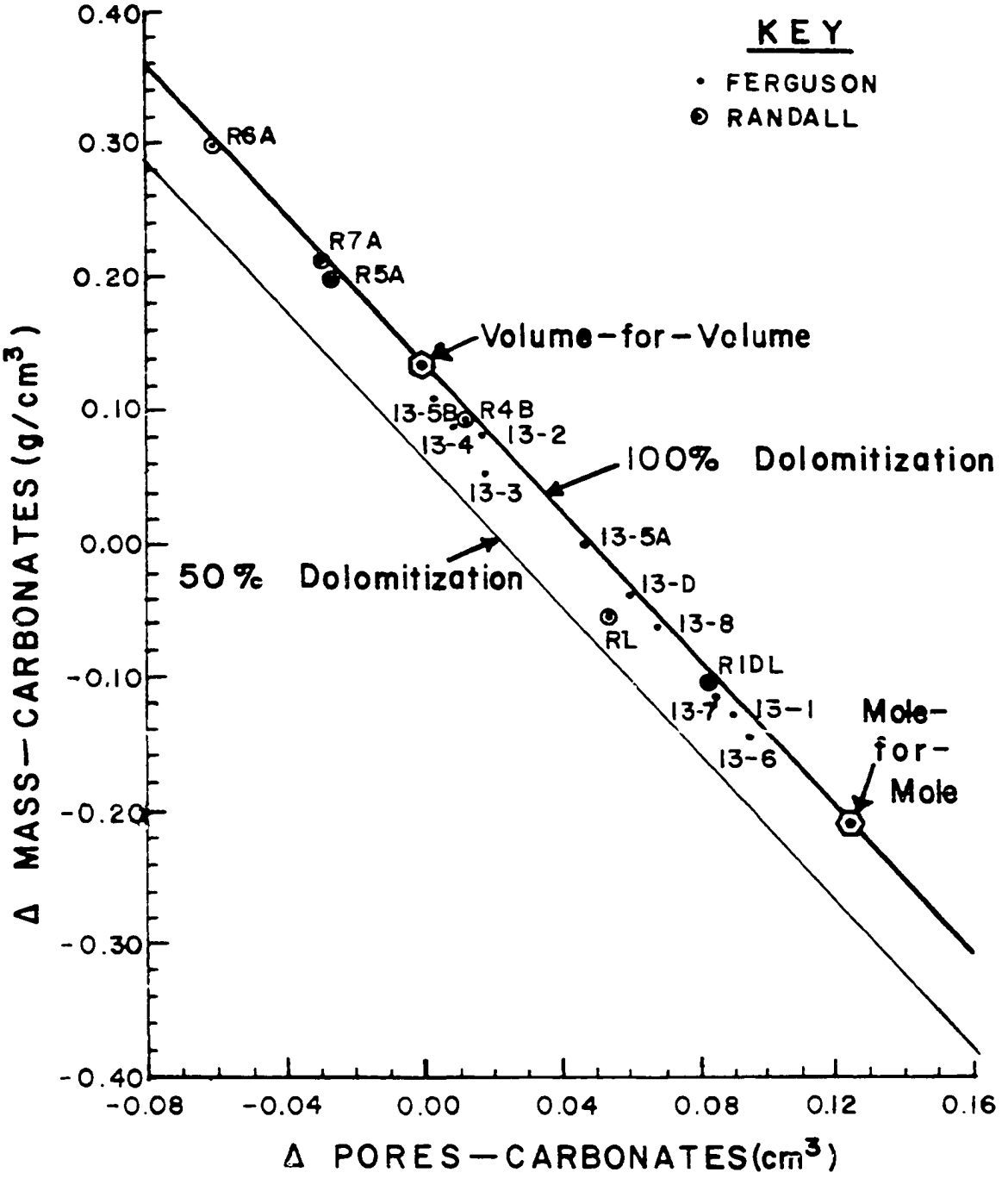
KEY
• FERGUSON
⊙ RANDALL
R6A
R7A
R5A
Volume-for-Volume
13-5B
R4B
13-4
13-2
100% Dolomitization
13-3
13-5A
50% Dolomitization
13-D
RL
13-8
RIDL
13-7
13-1
13-6
Mole-for-Mole
0.40
0.30
0.20
0.10
0.00
-0.10
-0.20
-0.30
-0.40
-0.08
-0.04
0.00
0.04
0.08
0.12
0.16
Δ MASS—CARBONATES (g/cm³)
Δ PORES—CARBONATES(cm³)

for the theoretical points that the total container volume was occupied by either carbonate minerals or pores, and it should be noted that the experimental points have other material such as quartz, pyrite and clays competing for the available space. Therefore, the 100% line is considered a boundary condition for the theoretical system concerned only with carbonate mineral replacement reactions, and the experimental values could fall below the 100% line by varying degrees depending on the completeness of the reaction.

Another important feature of Figure 20 is the wide variation of changes observed for the dolomite replacement for each quarry system, as well as, within the individual blocks from the quarry. The conclusion drawn from this variation is that epigenetic dolomitization must be a replacement process operative in a unique way for each local microenvironment. This can most readily be explained by viewing dolomitization as occurring as a two step process: initial leaching of the calcite and subsequent deposition of the dolomite (Landes, 1946; Hewett, 1928; Hanshaw et al., 1971). The leaching process probably occurs along a thin fluid film between grains by dissolution of the calcite at its boundaries and subsequent deposition of dolomite in the formed void space. However, it is possible for the subsequent dolomite to fill: (1) only a portion of the leached voids, (2) exactly all of the leached voids or (3) all of the leached voids plus some of the pre-existing voids. Therefore, in view of net changes which can occur, differing rates of leaching and deposition for replacement best explains the variable experimental composition-volume relationships observed.

If the process is assumed to be a sequential leaching and deposition

operation, this implies that the pre-existing calcite structure is destroyed and carbonate ions are momentarily released into the pore fluids. Thus the possibility of isotopic exchange of oxygen and carbon atoms can occur during this interlude between leaching and deposition. Degens and Epstein (1964), Pinckney and Rye (1972), Lovering et al. (1963), and Friedman and Sanders (1967) have shown that with epigenetic and hydrothermal dolomites there is commonly an enrichment of heavier isotopes in dolomite phases with respect to calcite. Table 7 is a summary of average carbon and oxygen isotope ratio values measured on selected samples from both quarries relative to a modern marine carbonate. Though the variation of values was larger than desired, the average values tabulated indicate enrichment of the heavier isotopes during dolomitization. Friedman and Sanders (1967) concluded that this heavier isotope enrichment is due to brines in which at least partial isotopic equilibration of the released carbonate ions with the pore fluids has occurred.

Table 7. Average oxygen and carbon isotope ratios for selected limestone and dolomite samples. Values given are relative to a modern marine carbonate

| Sample | $O^{18}/O^{16}$ | $C^{13}/C^{12}$ |
|---|---|---|
| Randall | | |
| Limestone | -9.3 | -5.5 |
| Dolomite | -4.6 | +0.5 |
| Ferguson | | |
| Limestone | -3.7 | -5.5 |
| Dolomite | +3.8 | -5.0 |

Also, another factor that could influence oxygen and carbon isotope ratios is the additional $CO_3^{2-}$ added from pore fluids to the system during replacement. This addition further substantiates that leaching and redeposition has occurred because the mole-for-mole replacement assumes only the $CO_3^{2-}$ from pre-existing calcite is incorporated into the dolomite.

Therefore, the changes occurring within the system during dolomitization are complex and wide ranging. These changes represent a continuum from mole-to-mole to volume-to-volume and beyond to net pore filling. Secondly, the easiest method to explain this phenomena is that dolomitization occurs as a two step process: initial calcite leaching and subsequent dolomite deposition by the pore fluids. The idea of differing rates of leaching and deposition to explain the changes of mass and volume was advanced by Landes (1946) to explain differences in porosity among certain dolomites. This study gives the evidence needed for substantiating these earlier ideas. Also, by leaching and redeposition, carbon and oxygen isotopic exchange between the leached $CO_3$ and the pore fluids can occur generally with an enrichment of the heavier isotypes.

## Petrogenic Models of Dolomitization

By combining all available evidence from this study it is possible to propose a petrogenetic model for the dolomitization process. It is assumed that dolomitization of lithified limestones occurs by flowing pore fluids, not in equilibrium with the limestone, altering the material as it flows. The path taken by the fluids will be along that of least resistance, or the interconnected pores available in the rock. Therefore, one of the principal factors influencing the dolomitization process is the

interconnected pores space as related to the size of the pores and their location in the carbonate rock.

Ferguson Quarry

Inspection of the data presented in Figure 21 indicates a relationship between dolomitization and the pore volume-pore radii exists. The significance of this relationship is that it shows the control of dolomitization by the availability of interconnected pores to the fluids. In the peloid limestone the predominant pore space is in the 0.2 micron and less size range. This size range is located both in the peloids and the boundary region between the peloids and the sparry calcite matrix. Visual observations of bleeding of mercury from specimens after high pressure impregnation tests indicated that most of the bleeding occurred from the boundary region. Thus it is postulated that the fluid flow will be predominately through this boundary region and formation of dolomite is observed to begin here on the basis of paragenetic evidence (Figure 8). The continued formation of dolomite rhombs in this zone creates and extends locally a region with larger pore radii due to the random packing of the rhombs thereby selectively channeling pore fluids along this new zone. Physical evidence for grain boundary control of the fluids is indicated by formation of a larger radii shoulder on the curve showing the pore volume-pore radii relationship in the initial transition region (Figure 21). Progressive alteration produces a slightly bimodel distribution of the pore volume-pore radii as the sparry calcite is selectively replaced. This secondary peak for the larger radius pores is interpreted as an increase in pore size which can be attributed to the packing of

Figure 21. Variation of physical and chemical parameters as to position from interface between the zones for the Ferguson Quarry samples

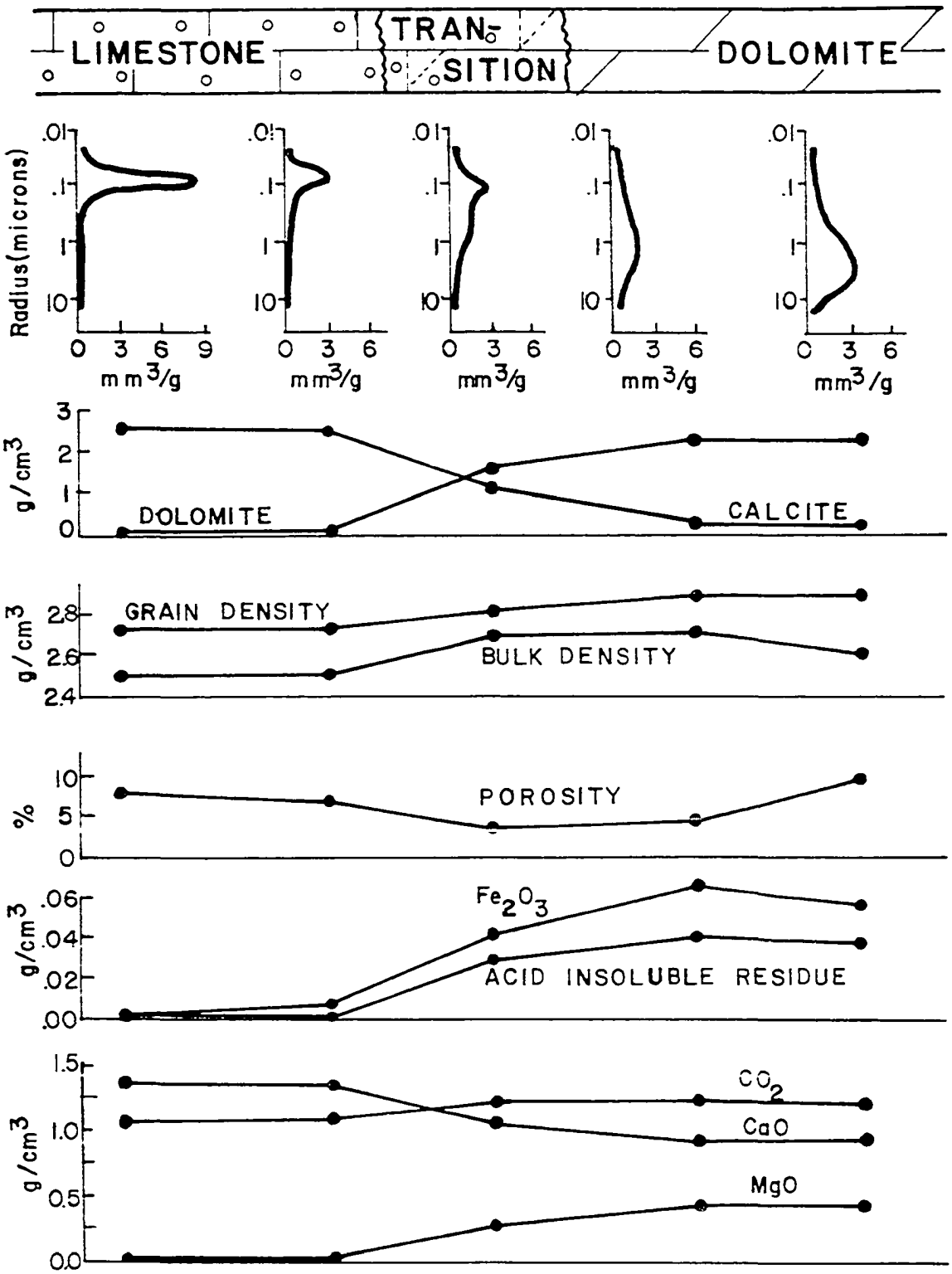
LIMESTONE
TRANSITION
DOLOMITE
Radius(microns)
.01
.1
1
10
0 3 6 9
mm3/g
0 3 6
g/cm3
DOLOMITE
CALCITE
GRAIN DENSITY
BULK DENSITY
2.8
2.6
2.4
%
POROSITY
Fe2O3
ACID INSOLUBLE RESIDUE
.06
.04
.02
.00
CO2
CaO
MgO
1.5
1.0
0.5
0.0

dolomite rhombs being more open than the interlocking sparry calcite matrix. The small radius peak is considered that portion of the void space remaining in the unreplaced peloids of the transition zone samples. Following complete replacement of sparry calcite, the peloids are replaced in a variety of ways ranging from centripetal replacement to transecting fronts across the ovoids. The final result of the replacement is a mosaic of randomly oriented dolomite rhombs with varying degrees of pore space predominately in the pore size range of 1-20 microns. In this petrogenic model flow of the fluids responsible for dolomitization has been controlled by interconnectedness of the pores as related to grain boundaries.

Additional evidence for selective replacement of sparry calcite first is considered to be related to twinning of the sparry calcite as observed in thin sections (Figure 5) as twinned crystals are more reactive relative to untwinned crystals. Other evidence for this selectivity was observed during carbonate phase studies when the peloid and sparry calcite were separated by crushing of Ferguson Quarry samples. It was noted that after crushing the peloids generally remained as discrete entities whereas the sparry calcite was reduced to a shattered mass of cleavage fragments. This indicates that the peloids consisting of microcrystalline calcite were better indurated and probably less permeable. The selectivity of dolomite replacement for the sparry calcite matrix was also noted by Beales(1965) in his study of pelleted limestone diagenesis. However, Beales did not pursue the cause of this selectivity. In this study the selectivity of sparry calcite to dolomitization is inferred to be the influence of texture, structural control and fluid flow. The pore radii variability with dolomitization demonstrated in Figure 21 shows the local

micro-pore-environment exerts substantial control of the calcite - dolomite exchange during the replacement process.

Randall Quarry

The dolomitization system sampled here differs from that at Ferguson. The limestone is of a lithographic texture in contrast to the peloid limestone of Ferguson. Also, the dolomites here consist of a dense, interlocking, randomly oriented, anhedral mosaic of dolomite grains (Figure 22). However, lack of transition zone samples does not yield enough paragenetic, physical and chemical evidence of the transition to present a thorough discussion of how the dolomitization occurs. However, by analogy the process would be controlled by the available interconnected pore space for fluid flow.

The lithographic limestone has about one-half of its pore space in the 0.2-0.05 micron size range and the remainder in the less than 0.05 micron sizes. This implies that a low permeability exists and thus a need for greater fluid pressure differentials or longer time intervals for fluid flow. Though grain boundary control is present, the lack of two distinct calcite grain morphologies typical of a peloid limestone as contrasted to the lithographic limestone implies the process probably controlled more by diffusion of the pore fluids throughout the rock rather than restriction of fluid flow to certain zones. In contrast to the limestones, the dolomites have virtually all of the void space in the less than 0.05 micron size range. Thus before and after evidence from chemical and void volume study indicates pore filling to have occurred for the lower portion of the Randall samples. The upper Randall Quarry samples

Figure 22. Variation of physical and chemical parameters as to position from interface between the zones for Randall Quarry samples

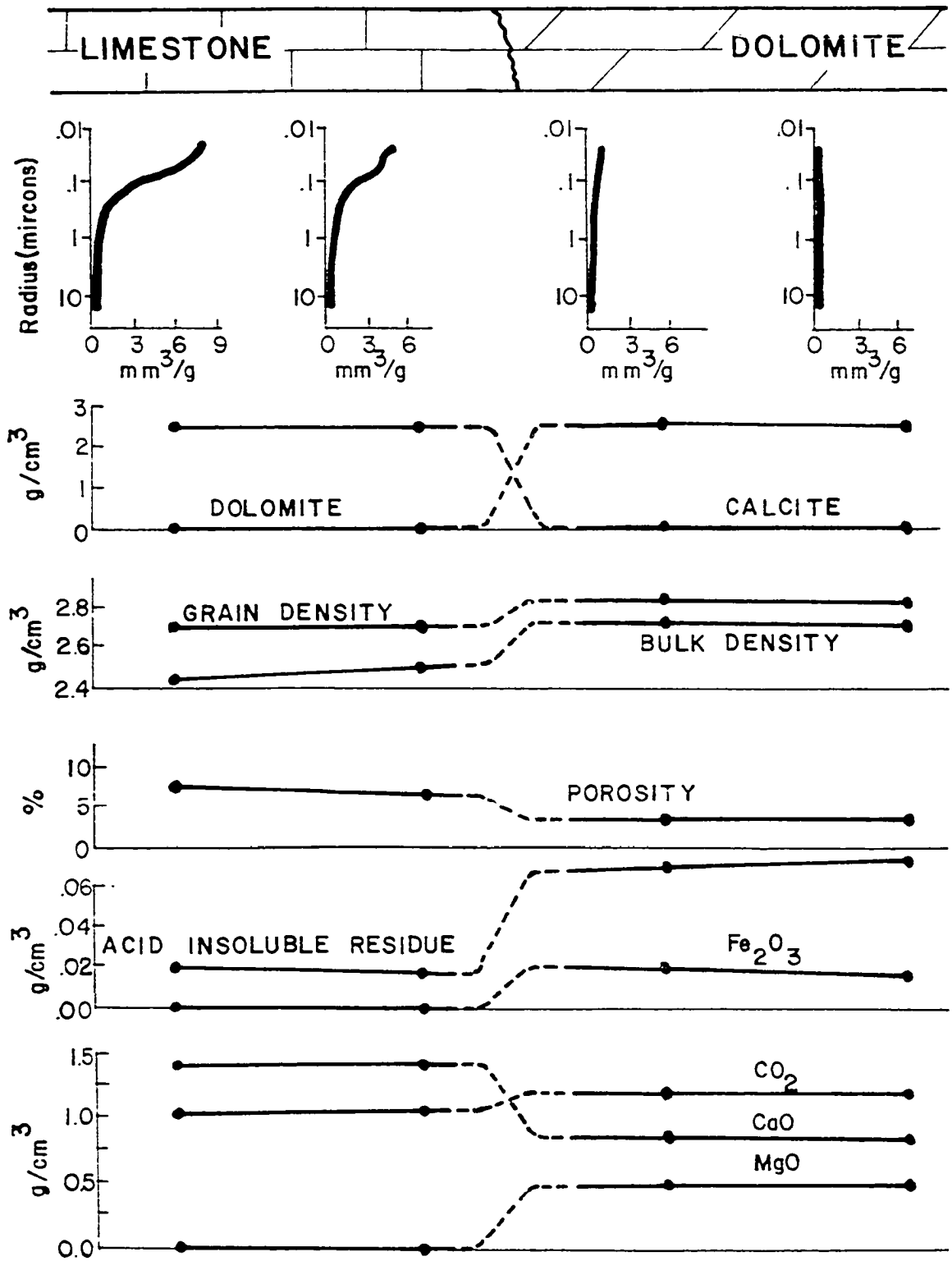
LIMESTONE
DOLOMITE
Radius (mircons)
.01
.1
1
10
0 3 6 9
mm3/g
g/cm3
DOLOMITE
CALCITE
GRAIN DENSITY
BULK DENSITY
%
POROSITY
ACID INSOLUBLE RESIDUE
Fe2O3
CO2
CaO
MgO

sets demonstrate an increase in pore volume similar to the Ferguson Quarry.

Dolomitization as sampled at Randall demonstrates a different type of process in that it appears to be more of a diffusional nature along minute pore spaces throughout the limestone where the pore fluids are not restricted to certain zones within the rock as is the case at Ferguson. Such a process would imply less selectivity during dolomitization. Again the replacement is considered to be via leaching and deposition along grain boundary films.

## Competing Reactions and Complexity of the Process

The process of dolomitization studied is not limited to just an exchange of magnesium for calcium in the carbonate structure, but also introduction of additional ions of iron and manganese in solid solution. The solid solution of iron in the dolomites at Ferguson has also been noted by Isenberger (1966). The increase of iron and manganese in the carbonate phases is quite common in epigenetic dolomites (Hewett, 1928).

Other reactions are also occurring simultaneously with dolomitization, compete for the available space and include introduction of pyrite, quartz and clay phases (Tables 5 and 6; Figures 21 and 22). Also, these phases are 3 to 10 times greater in abundance than the limestones. Thus dolomitization commonly includes introduction of other noncarbonate material.

Because a variety of ions are involved in dolomitization it is necessary to speculate on the type of fluid responsible for the dolomitization. Other minor elements being introduced include iron, manganese, sodium, potassium and sulfate. Inspection of Eh-pH diagrams (Garrels

and Christ, 1965; Krumbein and Garrels, 1952) for iron and manganese in presence of sulfur and carbon dioxide indicate that these ions would form carbonates under reducing conditions, in a pH range of 7-10 and that pyrite is stable in this environment. The presence of a minor amount of iron substitution in the carbonates perhaps indicates presence of a high $CO_2$ content in the fluids due to leaching of the $CaCO_3$. This situation would be possible as a leaching and redeposition process of replacement with incorporation of $Fe^{2+}$ at this time. The increase of $K^+$, $Na^+$, $CO_3^{2-}$ and $SO_4^{2-}$ in the dolomites tends to confirm that the pore fluids are saline in nature and the principal anions are $CO_3^{2-}$ and $SO_4^{2-}$. Because of a lack of dolomite zonation of the Ferguson Quarry the pore fluids responsible are considered to have been rather uniform in composition throughout the process.

Semi-quantitative tests for total chloride content (Table 8) of selected limestones and dolomites by nitric acid dissolution and using mercuric and silver nitrate titrations indicates the chlorides are higher in the limestones. This is an inverse relationship to $SO_4^{2-}$ content and presumed to be a result of the leaching of the calcite in which trapped chloride salts in grain boundaries and fluid inclusions are released and flushed out by the pore fluids. The increase of $SO_4^{2-}$ is considered indicative that dolomitization was due to a sulfate-rich pore fluid reacting to form dolomite.

The trace elements Sr, Cu, Pb, and Zn analyzed do not indicate any degree of relationship with dolomitization. The trace elements Cu, Pb and Zn analyzed were selected on the basis of several occurrences of sphalerite in the Ferguson Quarry. There is a general decrease of Sr

Table 8. Chloride content of selected samples

| Sample | | Chloride - ppm | Lithology |
|---|---|---|---|
| Ferguson | 13-1-2 | 5 | Dolomite |
| | 1-8 | 186 | Limestone |
| Ferguson | 13-5-14 | 11 | Dolomite |
| | 5-17 | 170 | Limestone |
| Randall | R4C | 37 | Dolomite |
| | R4B | 205 | Limestone |

and Pb with dolomitization; whereas zinc and cooper tend to be less definitive in their changes and a pattern is not discernible. The Sr and Pb changes are expected because they are large radius cations and would be preferentially excluded from the dolomite structure which prefers smaller cations relative to the calcite structure. It is apparent that Sr and Pb ions behave as expected for the carbonate structures present. The other two trace elements Cu and Zn do not show any definitive relationship with dolomitization. At the present time further study of these and other trace elements for the samples could be pursued but probably would not contribute much new insight into the conclusions already drawn for the process.

Earlier it was postulated that the pore volume-pore radii relationship influenced the flow, location and selectivity of dolomitization by constraining the pore fluids to certain paths in the rock. However, several problems still need to be answered. If one assumes the limestone

is initially saturated with pore fluids; what happens to this fluid, how does it affect dolomitization? Generally, this fluid has been ignored as the investigator assumes the process occurs as a chemical front passes through, altering the rock as it advances. Lovering (1969) and Usdowski (1968) circumvented this problem by assuming the existing pore solutions were heated which put the solutions into the dolomite stability field with the resultant replacement.

The phenomenon that dolomitization could occur in the zone of mixing between two different pore fluids was advanced by Hanshaw et al. (1971). They postulated that when two separate solutions both in equilibrium with calcite and dolomite are mixed, the resulting solution may become under saturated with respect to calcite causing solution of the calcite and precipitation of the dolomite. The mixing of two saturated solutions and obtaining under saturations with respect to the mineral was demonstrated by Runnells(1969) and Holland (1964). Also, how is the increase of silica related to the dolomitization as observed in the samples? If dolomitization does occur in the zone of mixing, do possible changes in pH influence silica saturation with the dolomitization?

If one assumes that dolomitization occurs as a sequential leaching and deposition in a zone of mixing between two pore fluids; a limestone pore fluid, and a saline dolomite pore fluid both separately in equilibrium with the phases calcite and dolomite. The saline pore fluid probably contains $Fe^{2+}$, $Mn^{+}$, $Na^{+}$, $K^{+}$, $Ca^{2+}$, $Mg^{2+}$, $SO_4^{2-}$, and $HCO_3^{-}$ ions. If this pore solution is of high pH>8.5-9.0 there can be a much larger amount of dissolved silica present in this solution than normally present in most pore waters. Krauskopf (1967) summarized that the silica solubility

limit as being approximately 10 ppm below 8.5 pH but increases rapidly with increasing pH above 8.5. When mixing occurs, causing undersaturation with respect to calcite, leaching of the calcite occurs. This causes a temporary local high concentration of $HCO_3^-$, $OH^-$ and $Ca^{2+}$, as well as raising the pH. Subsequent precipitation of dolomite will cause a reduction of the $HCO_3^-$ and $OH^-$ content lowering the pH. When this reduction of pH occurs, supersaturation of the solution with respect to silica may occur and precipitation of silica after the dolomite. This pH control and carbonate deposition was noted as a possible reaction couple for chert formation by Krauskopf (1967). A possible local source of silica at Ferguson is the overlying green dolomite band, which contains 5-10 percent silica in the form of microcrystalline quartz. Silica could have been mobilized from this zone by the fluids and precipitated during deposition of the dolomite in the sampled dolomites. At the Randall Quarry an increase of silica is also noted and again assumed to be brought about by dolomitization.

Therefore it is possible that mixing of two fluids could be responsible for dolomitization of limestones. Also, pH control of the leaching and deposition process can be used to explain the silica increase associated with dolomitization. The control of dolomitization by alkalinity and salinity has been advanced by Lipperman (1968), Skinner (1963), Barnes and O'Neil (1971).

## Relation of Model to Nature

In summary it is proper to ask whether the petrogenic models for dolomitization postulated above are valid when compared to dolomitization

as observed in nature. Two possibilities can be postulated for comparison of the proposed model to dolomitization actually observed:

(1) If the reaction occurs in a mole-for-mole basis, two possibilities exist.

(a) If the reaction occurred throughout the entire rock as a completely homogeneous process, no porosity would result because collapse of the open space due to overburden pressure (assuming that adequate static pressure exists).

(b) If the reaction is localized in one area only, then a cavity representing 12.3% of its former mass volume would result in this place.

(2) If dolomitization varies from mole-to-mole to volume-for-volume and occurs hetereogeneously throughout the rock wherever local microenvironments exert the necessary physical control for the appropriate process, the net result would demonstrate local porosity variations scattered throughout the rock.

Of these two possibilities, the latter or a heterogeneous process relates better to the actual results of dolomitization observed. The implication is that the overall result will be a summation of each microenvironment controlled process giving a general trend of the system. If enough supporting framework is retained, there should be no thickening or thinning of the beds indicative of no volume change for the rock during the dolomitization. However, locally a wide range of partial volume changes can occur within as long as a framework is maintained. Also, much of what other investigators have said depends on their scale of observation used for discussing trends of dolomitization:

(1) Outcrop and regional scale: no overall volume changes.

(2) Block sample scale: no overall volume changes.

(3) Core samples: partial volumes differ from sample to sample.

In other words, it is perhaps closer to nature to have variations exist for the dolomitization process for each local environment than to consider one method of dolomite replacement as uniformly occurring throughout the rock.

# CONCLUSIONS

A model of alteration or replacement is proposed by which changes can occur within a unit container volume. This unit container volume is partitioned between the mass and void volumes; each of which may change during the replacement process. Replacement of rocks occurs by interaction of moving pore fluids with the mineral phases present, usually by leaching and deposition. Thus there can occur (1) complete leaching of the mass within the container, (2) complete deposition of material to fill the available void space, or (3) both leaching and deposition at the same time. However, the important aspect is that leaching and deposition rates can be independent of each other, with a wide range of interchange of mass and void volume possible. Thus X amount of mass can be removed, and Y amount of mass can be deposited; where Y can be greater than, less than or equal to X. Application of the unit container volume model to study of replacement allows one to account for composition - volume changes occurring in a system undergoing a replacement process. When this unit container volume is used in study of epigenetic dolomitization and compared to the modes of dolomitization generally used to explain the process, it is shown that dolomite replacement occurs with a variety of composition volume relationships that do not cluster about either mole-for-mole or volume-for-volume. Therefore, application of the unit container volume to replacement studies appears to explain better the actual field observation of epigenetic dolomitization than does the commonly invoked mole-for-mole or volume-for-volume.

In dolomitization of a peloid limestone, there occurs a variety of

mass and volume changes within the system. However, through combination of pore volume-pore radius relationships, pore volume changes, petrographic evidence, chemical and phase studies it is postulated that the dolomitization is controlled by localization of the pore fluid flow to certain channels or pathways. Initially, these pathways are predominately along the boundary region between the peloids and the sparry calcite matrix commonly localizing the initial dolomite formation to this region. The pore fluids are now even more localized to this region as packing of the dolomite rhombs creates fewer but larger pores and selectively replaces the sparry calcite first. The intermediate result is a maze of peloids in a sparry dolomite matrix which maintains the framework of the system. The reactive pore fluids continue to react with the remaining peloids by both centripetally and transecting front replacements of the peloids resulting in a mosaic of subhedral to euhedral dolomite grains. Thus in peloid limestones it is considered that the dolomitization is controlled by location of interconnected pore spaces.

Analogous to the peloid limestone, dolomitization of a lithographic limestone composed of microcrystalline calcite, is again controlled by the interconnected pore space. Apparently, the lack of grain size differences does not localize flow of the fluids to certain zones in the rock. Thus the fluids should permeate throughout the limestone and show little preference to location or type of calcite being replaced. The intermediate result of this dolomitization is considered a floating rhomb texture. The dolomitization process continues and results in a dense anhedral mosaic of dolomite grains and a net loss of pore space for the Randall quarry.

Generally the Ferguson Quarry samples tend to be between mole-for-mole and volume-for-volume with an average porosity increase of 3 percent. In contrast the lower portion of the Randall Quarry samples show a 2 percent decrease in porosity with dolomitization or pore filling. The upper sets from Randall show a similar behavior to that at Ferguson. In order to better explain these changes it is assumed that dolomitization occurs by a two step sequential leaching and deposition process, where the rates of leaching and deposition can differ. Thus this study provides the evidence needed to substantiate the earlier postulates that dolomitization occurs as a leaching and deposition process, with a wide range of porosity changes allowable depending on the relative rates (Landes, 1946; Hewett, 1928).

However, dolomitization is not the only change in mass occurring, other material being added includes pyrite, silica, and clays. Thus these other processes are also competing for space along with dolomitization and complicate evaluation of the processes. Another feature of dolomitization is the incorporation of iron and manganese into the dolomite structure. Also there is additional carbonate ions introduced from the fluids during dolomitization.

Speculation of the type of fluids responsible for the dolomitization indicates that the fluids were probably saline and of high pH. Not only has $Mg^{2+}$ been added to the dolomite but also Na, K, Al, Fe, Mn, $SO_3$, and $CO_3$ indicating that probably sulfate-rich solutions are responsible for the dolomitization. The silica increase may be due to the localized control of pH and supersaturation as a result of the precipitation of the dolomite. Another aspect of the dolomitization fluids is the idea of the

replacement occurring as a result of mixing of two pore fluids. This mixing would be between the fluids in the dolomite pervading the limestone and its pore fluids. This aspect has been largely ignored by most investigators but may be an explanation of regional dolomitization in the past.

Finally, in evaluation of the experimental data it was observed that local microenvironments in the samples tended to spread the values about a general average value for the whole sample. Thus the model can better explain the heterogeniety of nature on a small observational scale, which on a large observational scale would appear to be homogeneous changes. Though the model of replacement proposed is a simplified view of the complexities of nature it gives a better insight into the overall changes that have occurred in the system. Careful selection of samples and petrographic evidence of maintaining of the framework allows use of the unit container model to ascertain the composition-volume relationships in the parent-daughter system.

# REFERENCES CITED

Ames, L. L. 1961. The metasomatic replacement of limestone by alkaline fluoride bearing solution. Econ. Geology 59: 730-739.

Bathurst, R. G. C. 1971. Carbonate sediments and their diagenesis. Amsterdam, Elsevier Publishing Co.

Barnes, Ivan and O'Neil, J. R. 1971. Calcium-magnesium carbonate solid solutions from Holocene conglomerate cements and travertines in the Coast Range of California. Geochim. et Cosmochim. Acta 35: 699-718.

Barth, T. F. W. 1948. Oxygen in rocks: A basis for petrographic calculations. Jour. Geology 56: 50-60.

Beales, F. W. 1965. Diagenesis in pelletted limestones. Soc. Econ. Paleontologists and Mineralogists Spec. Pub. 13: 49-70.

Boglepov, V. G. 1963. The recomputation of the chemical analyses of rocks in studying metasomatic processes. International Geol. Rev. 5: 1585-1592.

Degens, E. T. and Epstein, Samuel. 1964. Oxygen and carbon isotope ratios in coexisting calcites and dolomites from recent and ancient sediments. Geochim. et Cosmochim. Acta 28: 23-44.

Diehl, Harvey. 1964. Calcein, calmagite, and o,o'- dehydroxyazobenzene titrimetric, colorimetric and fluorimetric reagents for calcium and magnesium. Columbus, Ohio, G. Frederick Smith Chemical Co.

Elwell, J. H., Simon, D. E., and Lemish, John. 1968. Approach to evaluation of geochemical change (Abstract). Geol. Soc. America Spec. Paper 121: 654-655.

Fairbridge, R. W. 1957. The dolomite question. Soc. Econ. Paleontologists and Mineralogists Spec. Pub. 5: 125-178.

Folk, R. L. 1959. Practical petrographic classification of limestones. Amer. Assoc. Petroleum Geologists Bull. 43: 1-38.

Friedman, G. N. and Sanders, J. E. 1967. Origin and occurrence of dolostones. In Chilingar, G. V., Bissel, H. H. and Fairbridge, R. W., eds. Carbonate Rocks. Vol. 9A. Pp. 267-348. Amsterdam, Elsevier Publishing Co.

Galle, O. K. and Runnells, R. T. 1960. Determination of $CO_2$ in carbonate rocks by controlled loss on ignition. Jour. Sed. Petrology 30: 613-618.

Garrels, R. M. and Christ, C. L. 1965. Solutions, minerals and equiliberia. New York, New York, Harper and Row Pub. Co.

Garrels, R. M. and Dreyer, R. M. 1952. The mechanism of limestone replacement at low temperatures and pressures. Geol. Soc. America Bull. 63: 352-274.

Garrels, R. M. and Mackenzie, F. T. 1971. Evolution of sedimentary rocks. New York, New York, W. W. Norton and Co.

Goldich, S. S. 1938. A study in rock weathering. Jour. Geology 46: 17-58.

Goldsmith, J. R. and Graf, D. L. 1958a. Relation between lattice constants and composition of the Ca-Mg carbonates. Am. Mineralogist 43: 84-101.

Goldsmith, J. R. and Graf, D. L. 1958b. Structural and compositional variations in some natural dolomites. Jour. Geology 66: 678-693.

Goldsmith, J. R., Graf, D. L. and Heard, H. C. 1961. Lattice constants of the Ca-Mg carbonates. Am. Mineralogist 46: 453-459.

Gresens, R. L. 1967. Composition-volume relationships of metasomatism. Chem. Geol. 2: 47-65.

Hanshaw, B. B., Bask, W., and Deike, R. G. 1971. A geochemical hypothesis for dolomitization by groundwater. Econ. Geology 66: 710-724.

Hemley, J. J. and Jones, W. R. 1964. Chemical aspects of hydrothermal alteration with emphasis on hydrogen metasomatism. Econ. Geology 59: 538-569.

Hewett, D. F. 1928. Dolomitization and ore deposition. Econ. Geology 23: 821-863.

Hillebrand, W. F. 1919. The analysis of silicate and carbonate rocks. U.S. Geol. Sur. Bull. 700.

Hiltrop, C. L. and Lemish, John. 1959. The relationship of pore-size distributions and other rock properties to the service ability of some carbonate rocks. Highway Research Board Bull. 239: 1-23.

Hohlt, R. H. 1958. The nature and origin of limestone porosity. Colorado School Mines Quart. 43: 1-49.

Holland, H. D. 1964. Solubility of calcite in NaCl solutions between 50° and 200°C (Abstract). Geol. Soc. America Spec. Paper 82: 94-95.

Isenberger, K. J. 1966. Properties of some selected Iowa carbonate aggregates. Unpublished M.S. thesis. Ames, Iowa, Library, Iowa State University of Science and Technology.

Krauskopf, K. B. 1967. Introduction to geochemistry. New York, New York, McGraw-Hill Book Co.

Krumbein, W. C. and Garrels, R. M. 1952. Origin and classification of chemical sediments in terms of pH and oxidation-reduction potentials. Jour. Geology 60: 1-33.

Landes, K. K. 1946. Porosity through dolomitization. Am. Assoc. Petroleum Geologists Bull. 30: 305-318.

Lindgren, Waldemar. 1912. The nature of replacement. Econ. Geology 7: 521-535.

Lindgren, Waldemar. 1918. Volume changes in metamorphism. Jour. Geology 26: 542-554.

Lindgren, Waldemar. 1933. Mineral deposits. 4th ed. New York, New York, McGraw-Hill Book Co.

Lipperman, Friedrich. 1968. Synthesis of $BaMg(CO_3)_2$ (norsethite) at 20°C and the formation of dolomite in sediments. In Müller, German and Friedman, G. M., eds. Recent developments in carbonate sedimentology in Central Europe. Pp. 33-37. Heidelberg, Springer-Verlag.

Lisitsyna, N. A. 1966. A method of geochemical study of the weathered crust. Lithology and Mineral Resources 1: 1-14.

Lovering, T. S. 1949. Rock alteration as a guide to ore, East Tintic District, Utah. Econ. Geology Mono. 1.

Lovering, T. S. 1969. The origin of hydrothermal and low temperature dolomite. Econ. Geology 64: 743-754.

Lovering, T. S., McCarthy, J. H. and Friedman, Irving. 1963. Significance of $O^{18}/O^{16}$ ratios in hydrothermally dolomitized limestones and manganese carbonate replacement ores of the Drum Mountains, Juab County, Utah. U.S. Geol. Survey Prof. Paper 475B: B1-B9.

Meyers, Charles and Hemley, J. J. 1967. Wall rock alteration. In Barnes, H. L., ed. Geochemistry of hydrothermal ore deposits. Pp. 166-235. New York, New York, Holt, Rhinehart and Winston.

Michels, D. E. 1966. Processes in mineral replacement. Unpublished Ph.D. thesis. Golden, Colorado, Library, Colorado School of Mines.

Murray, R. C. 1960. Origin of porosity in carbonate rocks. Jour. Sed. Petrology 30: 59-84.

Pinckney, D. M. and Rye, R. D. 1972. Variation of $O^{18}/O^{16}$, $C^{13}/C^{12}$, texture, and mineralogy in altered limestone in the Hill Mine, Cave-in District, Illinois. Econ. Geology 67: 1-18.

Poldervaart, Arie. 1953. Petrological calculations in metasomatic processes. Am. Jour. Sci. 251: 481-504.

Ridge, J. D. 1949. Replacement and equating of volume and weight. Jour. Geology 57: 522-550.

Ridge, J. D. 1961. Gain and loss of material in a series of replacements (Abstract). Geol. Soc. Am. Spec. Paper 68: 252-253.

Runnells, D. D. 1969. Diagenesis, chemical sediments and the mixing of natural waters. Jour. Sed. Petrology 39: 1188-1201.

Schneider, R. C. 1954. Petrography of some carbonate rocks at Ferguson and Legrand, Iowa. Unpublished M.S. thesis. Ames, Iowa, Library, Iowa State University of Science and Technology.

Simon, D. E., Elwell, J. H., Sendlein, L. V. A. and Lemish, John. 1969. Measurement of physical and chemical changes induced during weathering of a carbonate rock unit. Iowa Acad. Sci. Proc. 76: 320-329.

Skinner, H. C. W. 1963. Precipitation of calcian dolomites and magnesium calcites in the southeast of South Australia. Amer. Jour. Sci. 261: 449-472.

Steidlmann, E. 1917. Origin of dolomite. Geol. Soc. America Bull. 28: 431-450.

Taylor, V. A. 1965. An experimental study of some replacement processes. Unpublished Ph.D. thesis. Tallahassee, Florida, Library, Florida State University.

Tickell, F. G. 1965. The techniques of sedimentary mineralogy. Amsterdam, Elsevier Publishing Co.

Turner, F. J. and Verhoogen, John. 1960. Igneous and metamorphic petrology. New York, New York, McGraw-Hill Pub. Co.

Twenhofel, W. H. 1932. Treatise on sedimentation. 2nd ed. Baltimore, Md., New York, New York, Williams and Wilkins.

Usdowski, H. E. 1968. The formation of dolomite in sediments. In Müller, German and Friedman, G. M., eds. Recent developments in carbonate sedimentology in Central Europe. Pp. 21-32. Heidelberg, Springer-Verlag.

Van Hise, C. R. 1904. A treatise on metamorphism. U.S. Geol. Survey Monograph 47.

Van Tuyl, F. M. 1916. The origin of dolomite. Iowa Geol. Surv. Ann. Rept. 25: 251-422.

Wallace, C. M. 1962. Relationship of pore size to texture in some carbonate rocks. Unpublished M.S. thesis. Ames, Iowa, Library, Iowa State University of Science and Technology.

Weyl, P. K. 1960. Porosity through dolomitization, conservation of mass requirements. Jour. Sed. Petrology 30: 85-90.

Zenger, D. H. 1972. Dolomitization and uniformatiarianism. Jour. Geological Education 20: 107-124.

# ACKNOWLEDGEMENTS

This opportunity is taken to express thanks to Dr. John Lemish for his encouragement, guidance and continuous efforts in making this study possible.

Special thanks goes to my wife, Kathy, for her constant encouragement and devotion throughout the past few years. Without her constant encouragement throughout this study much of the progress would not have been possible.

Thanks is expressed to all the faculty members of the Earth Science Department for their time and availability for discussions on various aspects of this study whenever necessary. Also, support for use of depa mental equipment and supplies is acknowledged.

A debt of gratitude is due to the Geology Division of the Iowa State Highway Commission Materials Department for their discussions and availability for sample collection of the carbonate rock exposures that were applicable for this study.

# APPENDIX A

## Analysis of Limestones and Dolomites

Rapid chemical analyses of limestones and dolomites were performed on a Perkin Elmer Model 305A Atomic Absorption Spectrophotometer. Therefore, the following dissolution technique was adapted for element determinations using this equipment.

Two grams of thoroughly mixed sample is placed in a 250 ml beaker and 40 ml 1:4 HCl cautiously added to dissolve the sample, covered with a watch glass, evaporated to dryness and redissolved in 10 ml HCl and 10 ml $H_2O$. This solution is filtered and the filtrate diluted to 250 ml. The insoluble residue is now leached with 5 ml $HNO_3$, filtered and the filtrate diluted to 100 ml. The filter paper is burned off in a pre-weighed platinum crucible, cooled and weighed. This material is reported as acid insoluble residue.

The majority of elements can be analyzed directly without dilution of the solutions using standards balanced for the Ca and Mg content of the samples. See Table 9 for instrument settings and other necessary information. In all cases the upper concentration standard is expanded out to a full scale value and all readings taken on a chart recorder.

Ca and Mg are analyzed by 40X dilutions with the addition of 2500 ppm Sr as a molecular suppressant in both samples and standards. For magnesium determinations in dolomites, a 20 ppm standard is zero suppressed and a 35 ppm standard expanded to full scale. The samples readings are then bracketed by standards above and below. Similarly a 0.0 ppm Mg stand and a 4 ppm Mg standard are used for limestone samples. The calcium determination is done likewise except that 30 ppm Ca is zero suppressed and 60 ppm scale expanded when analyzing dolomites and 60 ppm Ca zero suppressed and

90 ppm scale expanded for limestone samples. The reproducibility of this technique has a ±0.5% or less coefficient of variation for duplicate dilutions.

Table 9. Instrument parameters used for carbonate rock analyses

| Element | Line Å | Burner | Fuel | Dil. | Range stds. ppm | Other[a] |
|---|---|---|---|---|---|---|
| Ca | 4227 | ⊥ | Air-$C_2H_2$ | 40X | 30-90 | 2500 ppm Sr |
| Mg | 2852 | ⊥ | Air-$C_2H_2$ | 40X | 0-35 | 2500 ppm Sr |
| Fe | 2483 | ⊥ | Air-$C_2H_2$ | 1X, 5X | 0-40 | Ca, Mg matched |
| Al | 3093 | ∥ | $N_2O$-$C_2H_2$ | 1X | 0-20 | Ca, Mg matched |
| Mn | 2800 | ∥ | Air-$C_2H_2$ | 1X | 0-10 | Ca, Mg matched |
| Na | 5890 | ⊥ | Air-$C_2H_2$ | 1X | 0-10 | Ca, Mg matched |
| K | 7665 | ⊥ | Air-$C_2H_2$ | 1X | 0-10 | Ca, Mg matched |
| Pb | 2833 | ∥ | Air-$C_2H_2$ | 1X | 0-2 | Ca, Mg, & back correction |
| Cu | 3247 | ∥ | Air-$C_2H_2$ | 1X | 0-2 | Ca, Mg, & back correction |
| Zn | 2193 | ∥ | Air-$C_2H_2$ | 1X | 0-2 | Ca, Mg, & back correction |
| Sr | 4607 | ∥ | $N_2O$-$C_2H_2$ | 1X | 0-10 | Emission |

[a]All readings are on chart recorder output with bracketing of samples by standards.

Commonly for trace elements in low concentrations, a background correction is necessary as an apparent absorption due to light scatter gives higher than true readings. This technique was used for Cu, Pb, and

Zn determinations, by using a nearby nonabsorbing wavelength for the element to measure the sample contribution to the apparent absorbance by the sample.

The phases calcite and dolomite were quantitatively determined by stepwise fixed count integration of the principal diffraction peak $d_{10.4}$ for each mineral phase using X-ray diffraction (Simon, in preparation). The integrated values for the two phases were compared against a standard curve prepared in a similar manner to ascertain the percent dolomite and is corrected for pyrite and acid insoluble residue content. The reproducibility of this technique is ±1.1% for a single determination. The pyrite content is estimated from the iron content of the nitric acid leach and the silica plus clay content from the acid insoluble residue.

# APPENDIX B

Table 10. Physical and chemical data for Ferguson Quarry samples

| | D-1 | D-2 | D-3 | D-4 | D-5 | D-6 | D-7 |
|---|---|---|---|---|---|---|---|
| Calcite[a] | 2.4680 | 0.1665 | 0.0508 | 0.0207 | 0.0838 | 0.1012 | 2.4883 |
| Dolomite[a] | 0.1340 | 2.3681 | 2.5038 | 2.4690 | 2.5506 | 2.4670 | 0.0709 |
| Pyrite[a] | 0.0034 | 0.0082 | 0.0062 | 0.0078 | 0.0062 | 0.0064 | 0.0024 |
| AIR[a,b] | 0.0101 | 0.0590 | 0.0359 | 0.0450 | 0.0398 | 0.0666 | 0.0085 |
| $Al_2O_3$[a] | 0.0003 | 0.0027 | 0.0012 | 0.0018 | 0.0017 | 0.0026 | 0.0003 |
| $Fe_2O_3$[a] | 0.0062 | 0.0301 | 0.0312 | 0.0280 | 0.0598 | 0.0649 | 0.0048 |
| $Mn_2O_3$[a] | 0.0012 | 0.0034 | 0.0036 | 0.0024 | 0.0051 | 0.0052 | 0.0011 |
| CaO[a] | 1.3890 | 0.8638 | 0.8485 | 0.8086 | 0.8684 | 0.8460 | 1.3961 |
| MgO[a] | 0.0535 | 0.4544 | 0.4671 | 0.4567 | 0.4729 | 0.4585 | 0.0277 |
| $Na_2O$[a] | 0.0006 | 0.0021 | 0.0019 | 0.0021 | 0.0016 | 0.0014 | 0.0004 |
| $K_2O$[a] | 0.0002 | 0.0019 | 0.0008 | 0.0012 | 0.0009 | 0.0016 | 0.0001 |
| $CO_2$[a] | 1.1529 | 1.1868 | 1.2055 | 1.1452 | 1.2298 | 1.1951 | 1.1303 |
| $SO_3$[a] | 0.0010 | 0.0056 | 0.0017 | 0.0047 | 0.0023 | 0.0021 | 0.0009 |
| Sr(HCl)[c] | 124 | 128 | 100 | 126 | 102 | 76 | 116 |
| Cu(HCl)[c] | 2.4 | 2.0 | 0.1 | 0.6 | 1.3 | 1.8 | 2.6 |
| Zn(HCl)[c] | 43 | 105 | 27 | 22 | 39 | 62 | 20 |
| Pb(HCl)[c] | 8.9 | 4.3 | 1.8 | 2.5 | 4.3 | 3.5 | 10.0 |
| $Cu(HNO_3)$[c] | 3.4 | 2.6 | 2.4 | 3.3 | 2.1 | 2.5 | 1.1 |
| $Zn(HNO_3)$[c] | 83 | 150 | 41 | 60 | 53 | 22 | 34 |
| $Pb(HNO_3)$[c] | 9.2 | 6.4 | 4.1 | 3.8 | 2.2 | 5.7 | 3.7 |
| Porosity[d] | 3.69% | 7.25% | 8.83% | 12.39% | 6.20% | 7.27% | 5.22% |
| Bulk density[a] | 2.619 | 2.619 | 2.604 | 2.504 | 2.689 | 2.651 | 2.573 |
| Grain density[a] | 2.719 | 2.824 | 2.856 | 2.859 | 2.866 | 2.859 | 2.715 |

[a]Grams per cubic centimeter.

[b]Acid Insoluble Residue.

[c]Parts per million.

[d]Volume percent.

Table 10. (Continued)

| | 1-2 | 1-4 | 1-6 | 1-8 | 1-10 | 1-12 | 1-14 |
|---|---|---|---|---|---|---|---|
| Calcite[a] | 0.0242 | 0.0685 | 2.5329 | 2.5797 | 0.1888 | 2.4951 | 2.4461 |
| Dolomite[a] | 2.3461 | 2.4483 | 0.0714 | 0.0374 | 2.2958 | 0.1010 | 0.1011 |
| Pyrite[a] | 0.0069 | 0.0088 | 0.0027 | 0.0024 | 0.0084 | 0.0039 | 0.0027 |
| AIR[a,b] | 0.0284 | 0.0396 | 0.0057 | 0.0035 | 0.0440 | 0.0057 | 0.0086 |
| $Al_2O_3$[a] | 0.0014 | 0.0019 | 0.0002 | 0.0002 | 0.0023 | 0.0002 | 0.0002 |
| $Fe_2O_3$[a] | 0.0356 | 0.0323 | 0.0047 | 0.0029 | 0.0465 | 0.0061 | 0.0060 |
| $Mn_2O_3$[a] | 0.0030 | 0.0035 | 0.0010 | 0.0012 | 0.0043 | 0.0011 | 0.0012 |
| CaO[a] | 0.7821 | 0.8377 | 1.4985 | 1.4295 | 0.8393 | 1.3930 | 1.3636 |
| MgO[a] | 0.4381 | 0.4659 | 0.0339 | 0.0229 | 0.4973 | 0.0432 | 0.0402 |
| $Na_2O$[a] | 0.0019 | 0.0021 | 0.0005 | 0.0004 | 0.0016 | 0.0005 | 0.0004 |
| $K_2O$[a] | 0.0009 | 0.0013 | 0.0002 | 0.0002 | 0.0015 | 0.0002 | 0.0002 |
| $CO_2$[a] | 1.1143 | 1.1816 | 1.1566 | 1.1610 | 1.1935 | 1.1526 | 1.1368 |
| $SO_3$[a] | 0.0039 | 0.0060 | 0.0007 | 0.0004 | 0.0089 | 0.0000 | 0.0008 |
| Sr(HCl)[c] | 115 | 101 | 110 | 129 | 89 | 104 | 92 |
| Cu(HCl)[c] | 1.6 | 2.2 | 2.0 | 2.8 | 2.3 | 2.1 | 1.5 |
| Zn(HCl)[c] | 25 | 17 | 12 | 16 | 19 | 13 | 13 |
| Pb(HCl)[c] | 6.6 | 4.1 | 8.8 | 10.9 | 2.0 | 6.6 | 5.2 |
| $Cu(HNO_3)$[c] | 2.2 | 2.4 | 1.2 | 1.1 | 1.3 | 1.4 | 1.2 |
| $Zn(HNO_3)$[c] | 7.7 | 3.9 | 8.0 | 10.3 | 14.9 | 9.1 | 16.3 |
| $Pb(HNO_3)$[c] | 3.2 | 4.5 | 4.9 | 4.4 | 3.6 | 3.3 | 1.3 |
| Porosity[d] | 15.56% | 9.51% | 3.60% | 3.22% | 10.05% | 4.16% | 6.00% |
| Bulk density[a] | 2.417 | 2.581 | 2.615 | 2.625 | 2.558 | 2.607 | 2.561 |
| Grain density[a] | 2.862 | 2.852 | 2.713 | 2.712 | 2.844 | 2.720 | 2.724 |

Table 10. (Continued)

| | 1-16 | 1-20 | 2-1 | 2-4 | 2-7 | 2-10 | 3-2 |
|---|---|---|---|---|---|---|---|
| Calcite[a] | 2.5295 | 2.5134 | 0.2336 | 0.1732 | 0.1005 | 2.4419 | 0.6509 |
| Dolomite[a] | 0.0601 | 0.0414 | 2.3995 | 2.4554 | 2.4765 | 0.0938 | 1.9278 |
| Pyrite[a] | 0.0018 | 0.0018 | 0.0023 | 0.0024 | 0.0065 | 0.0013 | 0.0034 |
| AIR[a,b] | 0.0027 | 0.0049 | 0.0280 | 0.0197 | 0.0387 | 0.0028 | 0.0537 |
| $Al_2O_3$[a] | 0.0001 | 0.0001 | 0.0014 | 0.0010 | 0.0016 | 0.0002 | 0.0022 |
| $Fe_2O_3$[a] | 0.0049 | 0.0044 | 0.0517 | 0.0501 | 0.0612 | 0.0047 | 0.0171 |
| $Mn_2O_3$[a] | 0.0015 | 0.0012 | 0.0050 | 0.0047 | 0.0047 | 0.0013 | 0.0021 |
| CaO[a] | 1.4192 | 1.4032 | 0.9097 | 0.9005 | 0.8605 | 1.3761 | 0.9787 |
| MgO[a] | 0.0236 | 0.0200 | 0.4404 | 0.4419 | 0.4475 | 0.0296 | 0.3784 |
| $Na_2O$[a] | 0.0004 | 0.0004 | 0.0016 | 0.0017 | 0.0014 | 0.0004 | 0.0018 |
| $K_2O$[a] | 0.0001 | 0.0001 | 0.0010 | 0.0007 | 0.0010 | 0.0001 | 0.0016 |
| $CO_2$[a] | 1.1408 | 1.1262 | 1.2289 | 1.2336 | 1.2049 | 1.1241 | 1.2074 |
| $SO_3$[a] | 0.0005 | 0.0003 | 0.0037 | 0.0033 | 0.0027 | 0.0001 | 0.0072 |
| Sr(HCl)[c] | 135 | 106 | 79 | 89 | 66 | 107 | 115 |
| Cu(HCl)[c] | 2.3 | 2.6 | 2.4 | 1.7 | 1.4 | 1.8 | 0.7 |
| Zn(HCl)[c] | 24 | 11 | 17 | 16 | 17 | 11 | 15 |
| Pb(HCl)[c] | 11.1 | 10.3 | 0.9 | 4.2 | 2.5 | 7.0 | 0.0 |
| $Cu(HNO_3)$[c] | 0.9 | 1.0 | 1.4 | 0.8 | 2.1 | 1.0 | 1.4 |
| $Zn(HNO_3)$[c] | 18 | 16 | 7.6 | 6.5 | 9.7 | 8.7 | 13 |
| $Pb(HNO_3)$[c] | 1.3 | 2.2 | 3.0 | 2.0 | 3.1 | 3.3 | 2.9 |
| Porosity[d] | 4.34% | 5.65% | 6.27% | 6.70% | 7.68% | 6.35% | 5.75% |
| Bulk density[a] | 2.596 | 2.563 | 2.674 | 2.660 | 2.631 | 2.541 | 2.654 |
| Grain density[a] | 2.713 | 2.712 | 2.853 | 2.852 | 2.849 | 2.714 | 2.816 |

Table 10. (Continued)

| | 3-5 | 3-7 | 3-9 | 3-12 | 3-14 | 3-16 | 3-18 |
|---|---|---|---|---|---|---|---|
| Calcite[a] | 0.2072 | 0.5690 | 2.4912 | 0.9246 | 0.5796 | 0.3904 | 2.4688 |
| Dolomite[a] | 2.3446 | 2.0423 | 0.0938 | 1.7687 | 2.1061 | 2.2401 | 0.0672 |
| Pyrite[a] | 0.0034 | 0.0100 | 0.0015 | 0.0024 | 0.0031 | 0.0077 | 0.0012 |
| AIR[a,b] | 0.0800 | 0.0429 | 0.0077 | 0.0379 | 0.0424 | 0.0565 | 0.0067 |
| $Al_2O_3$[a] | 0.0038 | 0.0018 | 0.0002 | 0.0016 | 0.0020 | 0.0015 | 0.0015 |
| $Fe_2O_3$[a] | 0.0169 | 0.0236 | 0.0077 | 0.0387 | 0.0363 | 0.0241 | 0.0049 |
| $Mn_2O_3$[a] | 0.0021 | 0.0023 | 0.0013 | 0.0042 | 0.0038 | 0.0028 | 0.0011 |
| CaO[a] | 0.9002 | 0.9918 | 1.4005 | 1.0383 | 1.0368 | 0.9569 | 1.3761 |
| MgO[a] | 0.4321 | 0.3862 | 0.0389 | 0.3669 | 0.3705 | 0.4228 | 0.0309 |
| $Na_2O$[a] | 0.0020 | 0.0018 | 0.0005 | 0.0015 | 0.0016 | 0.0019 | 0.0004 |
| $K_2O$[a] | 0.0024 | 0.0012 | 0.0002 | 0.0012 | 0.0012 | 0.0011 | 0.0002 |
| $CO_2$[a] | 1.2039 | 1.2110 | 1.1368 | 1.2467 | 1.2410 | 1.2271 | 1.1233 |
| $SO_3$[a] | 0.0049 | 0.0050 | 0.0003 | 0.0022 | 0.0039 | 0.0045 | 0.0004 |
| Sr(HCl)[c] | 111 | 103 | 103 | 108 | 103 | 156 | 95 |
| Cu(HCl)[c] | 0.9 | 1.2 | 2.3 | 0.2 | 1.0 | 1.0 | 0.6 |
| Zn(HCl)[c] | 15 | 15 | 10 | 11 | 13 | 29 | 17 |
| Pb(HCl)[c] | 0.3 | 1.2 | 6.3 | 0.9 | 0.3 | 0.0 | 2.3 |
| $Cu(HNO_3)$[a] | 0.8 | 1.7 | 1.3 | 1.3 | 1.9 | 61 | 0.8 |
| $Zn(HNO_3)$[c] | 7.8 | 27 | 26 | 21 | 18 | 23 | 40 |
| $Pb(HNO_3)$[c] | 2.8 | 3.2 | 1.6 | 1.8 | 3.8 | 3.8 | 7.6 |
| Porosity[d] | 6.46% | 5.26% | 4.48% | 2.75% | 2.79% | 4.50% | 6.20% |
| Bulk density[a] | 2.652 | 2.678 | 2.596 | 2.742 | 2.743 | 2.707 | 2.547 |
| Grain density[a] | 2.835 | 2.826 | 2.717 | 2.820 | 2.822 | 2.834 | 2.715 |

Table 10. (Continued)

| | 3-20 | 3-23 | 3-25 | 4-3 | 4-7 | 4-9 | 4-11 |
|---|---|---|---|---|---|---|---|
| Calcite[a] | 2.0800 | 1.2755 | 1.2382 | 0.8642 | 0.3725 | 2.4926 | 0.4579 |
| Dolomite[a] | 0.4917 | 1.4485 | 1.4327 | 1.7642 | 2.2806 | 0.0936 | 2.1826 |
| Pyrite[a] | 0.0017 | 0.0030 | 0.0041 | 0.0041 | 0.0050 | 0.0007 | 0.0049 |
| AIR[a,b] | 0.0111 | 0.0461 | 0.0375 | 0.0338 | 0.0298 | 0.0091 | 0.0447 |
| $Al_2O_3$[a] | 0.0017 | 0.0012 | 0.0010 | 0.0012 | 0.0010 | 0.0004 | 0.0012 |
| $Fe_2O_3$[a] | 0.0161 | 0.0427 | 0.0428 | 0.0215 | 0.0251 | 0.0052 | 0.0277 |
| $Mn_2O_3$[a] | 0.0020 | 0.0051 | 0.0043 | 0.0023 | 0.0025 | 0.0010 | 0.0028 |
| CaO[a] | 1.2728 | 1.1149 | 1.1129 | 1.0522 | 0.9573 | 1.4023 | 0.9579 |
| MgO[a] | 0.1350 | 0.2991 | 0.2919 | 0.3422 | 0.4235 | 0.0326 | 0.4164 |
| $Na_2O$[a] | 0.0005 | 0.0007 | 0.0008 | 0.0016 | 0.0020 | 0.0007 | 0.0016 |
| $K_2O$[a] | 0.0002 | 0.0008 | 0.0007 | 0.0009 | 0.0007 | 0.0001 | 0.0008 |
| $CO_2$[a] | 1.1460 | 1.2311 | 1.2193 | 1.2121 | 1.2477 | 1.1452 | 1.3469 |
| $SO_3$[a] | 0.0004 | 0.0008 | 0.0005 | 0.0028 | 0.0042 | 0.0003 | 0.0018 |
| Sr(HCl)[c] | 93 | 88 | 81 | 123 | 106 | 111 | 99 |
| Cu(HCl)[c] | 0.3 | 0.7 | 0.6 | 0.3 | 0.4 | 1.6 | 0.0 |
| Zn(HCl)[c] | 45 | 20 | 8.5 | 13 | 26 | 10 | 11 |
| Pb(HCl)[c] | 5.2 | 0.3 | 0.3 | 1.7 | 0.3 | 5.3 | 0.0 |
| $Cu(HNO_3)$[c] | 0.7 | 0.8 | 0.7 | 0.8 | 1.2 | 0.6 | 1.1 |
| $Zn(HNO_3)$[c] | 14 | 10 | 6.0 | 22 | 9.1 | 9.0 | 10.0 |
| $Pb(HNO_3)$[c] | 3.6 | 2.7 | 2.9 | 2.5 | 2.9 | 2.6 | 3.0 |
| Porosity[d] | 5.86% | 2.03% | 3.07% | 4.75% | 4.73% | 4.27% | 4.83% |
| Bulk density[a] | 2.588 | 2.746 | 2.716 | 2.675 | 2.699 | 2.598 | 2.697 |
| Grain density[a] | 2.749 | 2.802 | 2.802 | 2.808 | 2.833 | 2.714 | 2.834 |

Table 10. (Continued)

| | 4-13 | 4-15 | 4-17 | 4-19 | 4-22 | 4-24 | 4-28 |
|---|---|---|---|---|---|---|---|
| Calcite[a] | 0.4987 | 2.5091 | 2.4330 | 0.7690 | 2.4685 | 2.4623 | 0.9527 |
| Dolomite[a] | 2.1553 | 0.0591 | 0.1345 | 1.8609 | 0.0664 | 0.0796 | 1.7190 |
| Pyrite[a] | 0.0036 | 0.0007 | 0.0011 | 0.0038 | 0.0008 | 0.0010 | 0.0025 |
| AIR[a,b] | 0.0328 | 0.0075 | 0.0107 | 0.0500 | 0.0101 | 0.0103 | 0.0185 |
| $Al_2O_3$[a] | 0.0012 | 0.0002 | 0.0002 | 0.0018 | 0.0002 | 0.0002 | 0.0005 |
| $Fe_2O_3$[a] | 0.0253 | 0.0046 | 0.0060 | 0.0274 | 0.0047 | 0.0053 | 0.0383 |
| $Mn_2O_3$[a] | 0.0027 | 0.0010 | 0.0014 | 0.0034 | 0.0046 | 0.0009 | 0.0038 |
| CaO[a] | 0.9719 | 1.4030 | 1.3642 | 1.0289 | 1.3822 | 1.3799 | 1.0606 |
| MgO[a] | 0.4117 | 0.0276 | 0.0549 | 0.3587 | 0.0303 | 0.0355 | 0.3421 |
| $Na_2O$[a] | 0.0017 | 0.0003 | 0.0009 | 0.0014 | 0.0005 | 0.0006 | 0.0016 |
| $K_2O$[a] | 0.0007 | 0.0001 | 0.0001 | 0.0012 | 0.0002 | 0.0002 | 0.0005 |
| $CO_2$[a] | 1.2447 | 1.1330 | 1.1415 | 1.2137 | 1.1148 | 1.1208 | 1.2288 |
| $SO_3$[a] | 0.0033 | 0.0015 | 0.0007 | 0.0034 | 0.0023 | 0.0009 | 0.0025 |
| Sr(HCl)[c] | 94 | 120 | 108 | 100 | 88 | 99 | 96 |
| Cu(HCl)[c] | 0.0 | 1.2 | 1.4 | 0.4 | 7.4 | 2.4 | 1.4 |
| Zn(HCl)[c] | 18 | 13 | 11 | 14 | 71 | 24 | 22 |
| Pb(HCl)[c] | 0.0 | 6.5 | 1.7 | 2.2 | 8.4 | 7.2 | 5.3 |
| $Cu(HNO_3)$[c] | 1.3 | 0.4 | 0.5 | 0.8 | 1.2 | 0.9 | 1.2 |
| $Zn(HNO_3)$[c] | 22 | 13 | 12 | 7.5 | 4.7 | 13 | 8.9 |
| $Pb(HNO_3)$[c] | 2.4 | 3.1 | 1.6 | 1.3 | 3.5 | 1.3 | 2.1 |
| Porosity[d] | 4.65% | 4.97% | 5.14% | 4.86% | 5.99% | 5.89% | 4.22% |
| Bulk density[a] | 2.700 | 2.580 | 2.582 | 2.694 | 2.551 | 2.556 | 2.700 |
| Grain density[a] | 2.832 | 2.715 | 2.722 | 2.832 | 2.714 | 2.716 | 2.819 |

Table 10. (Continued)

| | 4-29 | 4-31 | 5-1 | 5-4 | 5-7 | 5-8 | 5-11 |
|---|---|---|---|---|---|---|---|
| Calcite[a] | 2.3931 | 2.4106 | 0.0477 | 0.1815 | 0.2541 | 0.3130 | 0.2126 |
| Dolomite[a] | 0.1236 | 0.1094 | 2.3609 | 2.3574 | 2.2469 | 2.2588 | 2.3302 |
| Pyrite[a] | 0.0011 | 0.0012 | 0.0047 | 0.0082 | 0.0064 | 0.0037 | 0.0056 |
| AIR[a,b] | 0.0077 | 0.0085 | 0.0578 | 0.0495 | 0.0534 | 0.0501 | 0.0381 |
| $Al_2O_3$[a] | 0.0001 | 0.0001 | 0.0021 | 0.0018 | 0.0018 | 0.0014 | 0.0009 |
| $Fe_2O_3$[a] | 0.0049 | 0.0074 | 0.0556 | 0.0397 | 0.0374 | 0.0596 | 0.0588 |
| $Mn_2O_3$[a] | 0.0008 | 0.0010 | 0.0056 | 0.0057 | 0.0031 | 0.0048 | 0.0051 |
| CaO[a] | 1.3774 | 1.3507 | 0.7912 | 0.8772 | 0.8706 | 0.8918 | 0.8775 |
| MgO[a] | 0.0294 | 0.0488 | 0.4292 | 0.4236 | 0.4265 | 0.4214 | 0.4223 |
| $Na_2O$[a] | 0.0004 | 0.0004 | 0.0017 | 0.0020 | 0.0019 | 0.0015 | 0.0015 |
| $K_2O$[a] | 0.0001 | 0.0002 | 0.0015 | 0.0012 | 0.0013 | 0.0010 | 0.0006 |
| $CO_2$[a] | 1.1044 | 1.1123 | 1.1291 | 1.1943 | 1.1664 | 1.1963 | 1.1799 |
| $SO_3$[a] | 0.0003 | 0.0005 | 0.0031 | 0.0024 | 0.0045 | 0.0031 | 0.0013 |
| Sr(HCl)[c] | 96 | 282 | 74 | 63 | 78 | 77 | 74 |
| Cu(HCl)[c] | 1.5 | 1.7 | 3.4 | 3.6 | 5.9 | 0.9 | 0.6 |
| Zn(HCl)[c] | 13 | 15 | 40 | 43 | 62 | 16 | 18 |
| Pb(HCl)[c] | 0.0 | 0.6 | 5.7 | 0.6 | 0.0 | 3.4 | 3.4 |
| $Cu(HNO_3)$[c] | 1.1 | 1.2 | 2.6 | 3.3 | 3.9 | 1.8 | 1.8 |
| $Zn(HNO_3)$[c] | 7.2 | 7.5 | 39 | 23 | 26 | 12 | 9.2 |
| $Pb(HNO_3)$[c] | 5.7 | 5.0 | 5.5 | 6.5 | 6.3 | 5.5 | 4.7 |
| Porosity[d] | 6.83% | 6.89% | 13.55% | 8.86% | 9.52% | 7.61% | 9.27% |
| Bulk density[a] | 2.527 | 2.532 | 2.482 | 2.606 | 2.574 | 2.635 | 2.592 |
| Grain density[a] | 2.712 | 2.720 | 2.870 | 2.859 | 2.844 | 2.852 | 2.857 |

Table 10. (Continued)

| | 5-14 | 5-16 | 5-17 | 5-18 | 5-21 | 5-24 | 5-26 |
|---|---|---|---|---|---|---|---|
| Calcite[a] | 0.2279 | 2.4294 | 2.5106 | 0.2400 | 0.2694 | 0.1816 | 2.4837 |
| Dolomite[a] | 2.3649 | 0.1447 | 0.0489 | 2.3863 | 2.3981 | 2.4577 | 0.0458 |
| Pyrite[a] | 0.0047 | 0.0049 | 0.0044 | 0.0056 | 0.0062 | 0.0025 | 0.0030 |
| AIR[a,b] | 0.0514 | 0.0105 | 0.0064 | 0.0625 | 0.0423 | 0.0443 | 0.0078 |
| $Al_2O_3$[a] | 0.0010 | 0.0002 | 0.0003 | 0.0020 | 0.0011 | 0.0009 | 0.0001 |
| $Fe_2O_3$[a] | 0.0418 | 0.0051 | 0.0036 | 0.0540 | 0.0660 | 0.0514 | 0.0026 |
| $Mn_2O_3$[a] | 0.0044 | 0.0010 | 0.0009 | 0.0052 | 0.0057 | 0.0044 | 0.0010 |
| CaO[a] | 0.8968 | 1.3768 | 1.3982 | 0.8891 | 0.9206 | 0.8841 | 1.3982 |
| MgO[a] | 0.4350 | 0.0497 | 0.0257 | 0.4440 | 0.4272 | 0.4600 | 0.0156 |
| $Na_2O$[a] | 0.0016 | 0.0004 | 0.0005 | 0.0013 | 0.0013 | 0.0012 | 0.0007 |
| $K_2O$[a] | 0.0007 | 0.0001 | 0.0001 | 0.0012 | 0.0005 | 0.0006 | 0.0004 |
| $CO_2$[a] | 1.2166 | 1.1417 | 1.1317 | 1.2351 | 1.2486 | 1.2398 | 1.1121 |
| $SO_3$[a] | 0.0025 | 0.0003 | 0.0008 | 0.0016 | 0.0010 | 0.0006 | 0.0001 |
| Sr(HCl)[c] | 80 | 99 | 100 | 65 | 69 | 61 | 115 |
| Cu(HCl)[c] | 0.6 | 2.2 | 2.7 | 0.4 | 0.9 | 0.4 | 4.5 |
| Zn(HCl)[c] | 19 | 14 | 15 | 37 | 16 | 14 | 17 |
| Pb(HCl)[c] | 3.4 | 3.4 | 62 | 0.0 | 2.0 | 0.0 | 7.9 |
| $Cu(HNO_3)$[c] | 2.7 | 1.5 | 1.0 | 2.2 | 2.9 | 1.7 | 1.2 |
| $Zn(HNO_3)$[c] | 18 | 6.6 | 5.2 | 9.8 | 30 | 8.2 | 4.7 |
| $Pb(HNO_3)$[c] | 5.5 | 4.7 | 8.2 | 4.2 | 3.8 | 3.3 | 3.0 |
| Porosity[d] | 6.73% | 4.73% | 5.12% | 5.52% | 4.66% | 5.76% | 6.14% |
| Bulk density[a] | 2.657 | 2.591 | 2.573 | 2.702 | 2.721 | 2.690 | 2.542 |
| Grain density[a] | 2.848 | 2.719 | 2.712 | 2.860 | 2.854 | 2.854 | 2.708 |

Table 10. (Continued)

| | 5-27 | 5-28 | 5-30 | 5-32 | 5-34 | 5-35 | 5-36 |
|---|---|---|---|---|---|---|---|
| Calcite[a] | 2.5092 | 0.2319 | 0.4390 | 1.0945 | 2.1815 | 2.4101 | 2.4935 |
| Dolomite[a] | 0.0289 | 2.4271 | 2.2510 | 1.5640 | 0.2891 | 0.0900 | 0.0316 |
| Pyrite[a] | 0.0029 | 0.0009 | 0.0021 | 0.0042 | 0.0116 | 0.0039 | 0.0029 |
| AIR[a,b] | 0.0040 | 0.0455 | 0.0362 | 0.0306 | 0.0139 | 0.0115 | 0.0096 |
| $Al_2O_3$[a] | 0.0002 | 0.0012 | 0.0010 | 0.0012 | 0.0004 | 0.0000 | 0.0001 |
| $Fe_2O_3$[a] | 0.0027 | 0.0609 | 0.0669 | 0.0412 | 0.0120 | 0.0027 | 0.0024 |
| $Mn_2O_3$[a] | 0.0011 | 0.0051 | 0.0059 | 0.0045 | 0.0014 | 0.0010 | 0.0011 |
| CaO[a] | 1.4001 | 0.8984 | 0.9507 | 1.0756 | 1.2711 | 1.3763 | 1.3930 |
| MgO[a] | 0.0158 | 0.4529 | 0.4165 | 0.3096 | 0.0933 | 0.0184 | 0.0167 |
| $Na_2O$[a] | 0.0006 | 0.0013 | 0.0014 | 0.0010 | 0.0005 | 0.0003 | 0.0003 |
| $K_2O$[a] | 0.0003 | 0.0013 | 0.0010 | 0.0005 | 0.0002 | 0.0001 | 0.0001 |
| $CO_2$[a] | 1.1186 | 1.2431 | 1.2512 | 1.2304 | 1.0947 | 1.1020 | 1.1122 |
| $SO_3$[a] | 0.0003 | 0.0020 | 0.0017 | 0.0038 | 0.0026 | 0.0004 | 0.0004 |
| Sr(HCl)[c] | 101 | 59 | 70 | 62 | 75 | 100 | 94 |
| Cu(HCl)[c] | 2.3 | 1.7 | 1.8 | 6.1 | 5.6 | 1.4 | 1.6 |
| Zn(HCl)[c] | 13 | 35 | 28 | 28 | 19 | 15 | 11 |
| Pb(HCl)[c] | 7.9 | 0.0 | 0.0 | 2.8 | 6.7 | 5.7 | 3.2 |
| $Cu(HNO_3)$[c] | 1.2 | 1.8 | 1.9 | 3.0 | 3.4 | 1.3 | 1.0 |
| $Zn(HNO_3)$[c] | 8.9 | 13 | 12 | 52 | 13 | 11 | 6.3 |
| $Pb(HNO_3)$[c] | 2.9 | 3.3 | 1.8 | 4.6 | 6.4 | 3.1 | 1.7 |
| Porosity[d] | 5.96% | 4.91% | 3.83% | 3.59% | 8.35% | 7.06% | 6.31% |
| Bulk density[a] | 2.547 | 2.713 | 2.735 | 2.703 | 2.502 | 2.517 | 2.539 |
| Grain density[a] | 2.708 | 2.853 | 2.844 | 2.804 | 2.730 | 2.709 | 2.710 |

Table 10. (Continued)

| | 5-37 | 5-40 | 5-42 | 5-44 | 5-48 | 5-52 | 6-2 |
|---|---|---|---|---|---|---|---|
| Calcite[a] | 2.2138 | 2.4481 | 2.4424 | 2.4022 | 2.4761 | 2.3718 | 0.1030 |
| Dolomite[a] | 0.2683 | 0.0697 | 0.0478 | 0.0508 | 0.0104 | 0.0391 | 2.3308 |
| Pyrite[a] | 0.0038 | 0.0052 | 0.0050 | 0.0025 | 0.0033 | 0.0030 | 0.0055 |
| AIR[a,b] | 0.0069 | 0.0053 | 0.0044 | 0.0058 | 0.0043 | 0.0080 | 0.0275 |
| $Al_2O_3$[a] | 0.0003 | 0.0002 | 0.0002 | 0.0002 | 0.0003 | 0.0002 | 0.0012 |
| $Fe_2O_3$[a] | 0.0113 | 0.0051 | 0.0028 | 0.0030 | 0.0021 | 0.0026 | 0.0401 |
| $Mn_2O_3$[a] | 0.0018 | 0.0014 | 0.0012 | 0.0008 | 0.0012 | 0.0008 | 0.0034 |
| CaO[a] | 1.2626 | 1.3730 | 1.3699 | 1.3490 | 1.3789 | 1.3350 | 0.8139 |
| MgO[a] | 0.1008 | 0.0291 | 0.0172 | 0.0199 | 0.0149 | 0.0158 | 0.4263 |
| $Na_2O$[a] | 0.0004 | 0.0003 | 0.0003 | 0.0003 | 0.0003 | 0.0003 | 0.0021 |
| $K_2O$[a] | 0.0001 | 0.0009 | 0.0001 | 0.0001 | 0.0001 | 0.0001 | 0.0008 |
| $CO_2$[a] | 1.1061 | 1.1103 | 1.0993 | 1.0806 | 1.0901 | 1.0576 | 1.1533 |
| $SO_3$[a] | 0.0006 | 0.0017 | 0.0003 | 0.0005 | 0.0011 | 0.0013 | 0.0045 |
| Sr(HCl)[c] | 78 | 84 | 86 | 80 | 81 | 77 | 100 |
| Cu(HCl)[c] | 4.5 | 3.4 | 3.9 | 3.8 | 4.2 | 4.3 | 0.8 |
| Zn(HCl)[c] | 13 | 13 | 12 | 12 | 13 | 9.8 | 23 |
| Pb(HCl)[c] | 5.6 | 6.8 | 5.3 | 3.7 | 11 | 6.6 | 0.3 |
| $Cu(HNO_3)$[c] | 2.1 | 2.6 | 1.8 | 1.6 | 1.6 | 2.0 | 1.3 |
| $Zn(HNO_3)$[c] | 17 | 44 | 15 | 15 | 11 | 21 | 11 |
| $Pb(HNO_3)$[c] | 3.0 | 4.8 | 2.8 | 6.1 | 4.6 | 3.5 | 3.9 |
| Porosity[d] | 8.91% | 6.83% | 7.77% | 9.22% | 7.93% | 10.41% | 12.94% |
| Bulk density[a] | 2.495 | 2.533 | 2.501 | 2.463 | 2.497 | 2.425 | 2.479 |
| Grain density[a] | 2.739 | 2.719 | 2.712 | 2.713 | 2.712 | 2.707 | 2.847 |

Table 10. (Continued)

| | 6-5 | 6-7 | 6-8 | 7-1 | 7-2 | 7-4 | 7-6 |
|---|---|---|---|---|---|---|---|
| Calcite[a] | 0.0186 | 2.2156 | 2.5253 | 2.4495 | 0.1648 | 2.0360 | 2.4837 |
| Dolomite[a] | 2.4934 | 0.4101 | 0.0894 | 0.1720 | 2.3958 | 0.5179 | 0.1195 |
| Pyrite[a] | 0.0055 | 0.0019 | 0.0051 | 0.0022 | 0.0010 | 0.0029 | 0.0040 |
| AIR[a,b] | 0.0581 | 0.0066 | 0.0028 | 0.0053 | 0.0648 | 0.0095 | 0.0097 |
| $Al_2O_3$[a] | 0.0020 | 0.0002 | 0.0002 | 0.0003 | 0.0020 | 0.0003 | 0.0001 |
| $Fe_2O_3$[a] | 0.0309 | 0.0124 | 0.0077 | 0.0047 | 0.0307 | 0.0197 | 0.0059 |
| $Mn_2O_3$[a] | 0.0030 | 0.0017 | 0.0017 | 0.0011 | 0.0029 | 0.0023 | 0.0011 |
| CaO[a] | 0.8325 | 1.3750 | 1.4136 | 1.4247 | 0.8427 | 1.3093 | 1.4041 |
| MgO[a] | 0.4690 | 0.0779 | 0.0365 | 0.0350 | 0.4728 | 0.0829 | 0.0389 |
| $Na_2O$[a] | 0.0024 | 0.0006 | 0.0004 | 0.0015 | 0.0022 | 0.0005 | 0.0008 |
| $K_2O$[a] | 0.0015 | 0.0002 | 0.0002 | 0.0003 | 0.0016 | 0.0002 | 0.0003 |
| $CO_2$[a] | 1.1816 | 1.1593 | 1.1554 | 1.1566 | 1.1912 | 1.1400 | 1.1536 |
| $SO_3$[a] | 0.0071 | 0.0008 | 0.0002 | 0.0009 | 0.0038 | 0.0003 | 0.0006 |
| Sr(HCl)[c] | 104 | 109 | 100 | 103 | 101 | 82 | 97 |
| Cu(HCl)[c] | 1.6 | 1.0 | 1.3 | 3.8 | 3.3 | 1.5 | 6.0 |
| Zn(HCl)[c] | 23 | 12 | 9.5 | 16 | 16 | 14 | 91 |
| Pb(HCl)[c] | 0.3 | 1.2 | 6.7 | 3.6 | 3.4 | 2.4 | 37 |
| $Cu(HNO_3)$[c] | 1.7 | 1.1 | 1.9 | 2.0 | 1.2 | 1.3 | 1.8 |
| $Zn(HNO_3)$[c] | 9.1 | 12 | 11 | 18 | 15 | 12 | 85 |
| $Pb(HNO_3)$[c] | 2.1 | 2.3 | 2.4 | 2.0 | 2.9 | 3.4 | 2.8 |
| Porosity[d] | 9.02% | 3.75% | 3.40% | 2.48% | 8.46% | 6.12% | 3.44% |
| Bulk density[a] | 2.594 | 2.637 | 2.624 | 2.633 | 2.616 | 2.568 | 2.620 |
| Grain density[a] | 2.852 | 2.740 | 2.716 | 2.699 | 2.857 | 2.736 | 2.714 |

Table 10. (Continued)

| | 7-7 | 7-9 | 7-10 | 7-13 | 7-14 | 7-16 | 7-18 |
|---|---|---|---|---|---|---|---|
| Calcite[a] | 0.1175 | 0.0145 | 2.4230 | 2.4695 | 0.1500 | 2.3728 | 2.5173 |
| Dolomite[a] | 2.3694 | 2.3952 | 0.1278 | 0.1423 | 2.3089 | 0.1866 | 0.0550 |
| Pyrite[a] | 0.0071 | 0.0032 | 0.0023 | 0.0046 | 0.0035 | 0.0017 | 0.0019 |
| AIR[a,b] | 0.0504 | 0.0310 | 0.0060 | 0.0123 | 0.0444 | 0.0008 | 0.0061 |
| $Al_2O_3$[a] | 0.0018 | 0.0009 | 0.0000 | 0.0000 | 0.0012 | 0.0000 | 0.0000 |
| $Fe_2O_3$[a] | 0.0336 | 0.0369 | 0.0065 | 0.0070 | 0.0492 | 0.0058 | 0.0058 |
| $Mn_2O_3$[a] | 0.0037 | 0.0033 | 0.0014 | 0.0014 | 0.0043 | 0.0016 | 0.0016 |
| CaO[a] | 0.8363 | 0.7932 | 1.3991 | 1.3975 | 0.8211 | 1.3976 | 1.4148 |
| MgO[a] | 0.4478 | 0.4422 | 0.0246 | 0.0524 | 0.4387 | 0.0219 | 0.0248 |
| $Na_2O$[a] | 0.0021 | 0.0022 | 0.0004 | 0.0006 | 0.0018 | 0.0005 | 0.0004 |
| $K_2O$[a] | 0.0013 | 0.0008 | 0.0002 | 0.0002 | 0.0010 | 0.0002 | 0.0002 |
| $CO_2$[a] | 1.1691 | 1.1369 | 1.1200 | 1.1542 | 1.1504 | 1.1325 | 1.1256 |
| $SO_3$[a] | 0.0052 | 0.0040 | 0.0012 | 0.0012 | 0.0069 | 0.0000 | 0.0003 |
| Sr(HCl)[c] | 98 | 102 | 102 | 98 | 98 | 111 | 112 |
| Cu(HCl)[c] | 2.4 | 2.4 | 2.7 | 3.0 | 3.0 | 2.8 | 2.5 |
| Zn(HCl)[c] | 37 | 40 | 22 | 20 | 25 | 23 | 10 |
| Pb(HCl)[c] | 2.8 | 0.8 | 2.9 | 29 | 4.4 | 5.6 | 10 |
| $Cu(HNO_3)$[c] | 3.1 | 1.8 | 1.9 | 2.0 | 1.1 | 1.7 | 1.7 |
| $Zn(HNO_3)$[c] | 38 | 22 | 20 | 23 | 39 | 13 | 19 |
| $Pb(HNO_3)$[c] | 6.8 | 3.5 | 3.2 | 3.2 | 2.8 | 1.2 | 1.8 |
| Porosity[d] | 10.54% | 14.18% | 5.66% | 3.22% | 12.16% | 5.62% | 4.89% |
| Bulk density[a] | 2.559 | 2.455 | 2.562 | 2.632 | 2.523 | 2.563 | 2.582 |
| Grain density[a] | 2.860 | 2.860 | 2.715 | 2.722 | 2.872 | 2.715 | 2.715 |

Table 10. (Continued)

| | 8-2 | 8-5 | 8-7 | 8-9 | 8-11 | 8-14 | 8-16 |
|---|---|---|---|---|---|---|---|
| Calcite[a] | 0.0778 | 0.0267 | 2.0745 | 2.5358 | 0.0137 | 2.4443 | 2.4820 |
| Dolomite[a] | 2.4650 | 2.4963 | 0.5435 | 0.0682 | 2.4373 | 0.1125 | 0.0603 |
| Pyrite[a] | 0.0047 | 0.0030 | 0.0030 | 0.0019 | 0.0202 | 0.0030 | 0.0023 |
| AIR[a,b] | 0.0398 | 0.0302 | 0.0027 | 0.0049 | 0.0868 | 0.0085 | 0.0036 |
| $Al_2O_3$[a] | 0.0010 | 0.0013 | 0.0002 | 0.0000 | 0.0021 | 0.0002 | 0.0001 |
| $Fe_2O_3$[a] | 0.0331 | 0.0355 | 0.0139 | 0.0039 | 0.0270 | 0.0084 | 0.0045 |
| $Mn_2O_3$[a] | 0.0031 | 0.0032 | 0.0018 | 0.0015 | 0.0034 | 0.0012 | 0.0011 |
| CaO[a] | 0.8432 | 0.8327 | 1.3275 | 1.4282 | 0.7946 | 1.3793 | 1.3912 |
| MgO[a] | 0.4764 | 0.4721 | 0.1043 | 0.0245 | 0.4465 | 0.0407 | 0.0220 |
| $Na_2O$[a] | 0.0023 | 0.0022 | 0.0007 | 0.0004 | 0.0034 | 0.0007 | 0.0004 |
| $K_2O$[a] | 0.0009 | 0.0008 | 0.0003 | 0.0001 | 0.0017 | 0.0002 | 0.0002 |
| $CO_2$[a] | 1.1920 | 1.1833 | 1.1715 | 1.1461 | 1.1818 | 1.1272 | 1.1241 |
| $SO_3$[a] | 0.0070 | 0.0053 | 0.0016 | 0.0002 | 0.0031 | 0.0000 | 0.0011 |
| Sr(HCl)[c] | 108 | 104 | 103 | 115 | 100 | 93 | 92 |
| Cu(HCl)[c] | 2.2 | 1.9 | 1.0 | 1.3 | 2.8 | 1.9 | 1.3 |
| Zn(HCl)[c] | 22 | 20 | 11 | 9.4 | 21 | 20 | 12 |
| Pb(HCl)[c] | 3.7 | 44 | 2.9 | 9.9 | 8.9 | 6.9 | 4.1 |
| $Cu(HNO_3)$[c] | 1.7 | 0.9 | 1.5 | 1.4 | 3.3 | 1.4 | 0.9 |
| $Zn(HNO_3)$[c] | 14 | 16 | 21 | 16 | 26 | 46 | 14 |
| $Pb(HNO_3)$[c] | 1.6 | 1.5 | 4.1 | 5.5 | 12 | 4.6 | 3.9 |
| Porosity[d] | 8.81% | 9.97% | 4.09% | 3.74% | 9.98% | 5.10% | 5.85% |
| Bulk density[a] | 2.604 | 2.570 | 2.628 | 2.612 | 2.570 | 2.570 | 2.551 |
| Grain density[a] | 2.856 | 2.855 | 2.740 | 2.714 | 2.855 | 2.708 | 2.710 |

# APPENDIX C

Table 11. Physical and chemical data for Randall Quarry samples

| | R1A | R2A | R3A | R4A | R5A | R6A | R7A |
|---|---|---|---|---|---|---|---|
| Calcite[a] | 2.5597 | 2.5546 | 2.3743 | 2.4782 | 2.4071 | 2.4233 | 2.4686 |
| Dolomite[a] | 0.0144 | 0.0255 | 0.0062 | 0.0077 | 0.0046 | 0.0066 | 0.0049 |
| Pyrite[a] | 0.0003 | 0.0005 | 0.0002 | 0.0002 | 0.0001 | 0.0002 | 0.0003 |
| AIR[a,b] | 0.0304 | 0.0186 | 0.0148 | 0.0202 | 0.0100 | 0.0267 | 0.0412 |
| $Al_2O_3$[a] | 0.0006 | 0.0005 | 0.0002 | 0.0003 | 0.0001 | 0.0004 | 0.0007 |
| $Fe_2O_3$[a] | 0.0046 | 0.0063 | 0.0021 | 0.0046 | 0.0018 | 0.0025 | 0.0036 |
| $Mn_2O_3$[a] | 0.0003 | 0.0002 | 0.0002 | 0.0003 | 0.0003 | 0.0004 | 0.0004 |
| CaO[a] | 1.4299 | 1.4341 | 1.3232 | 1.3838 | 1.3461 | 1.3467 | 1.3737 |
| MgO[a] | 0.0070 | 0.0057 | 0.0061 | 0.0065 | 0.0057 | 0.0090 | 0.0081 |
| $Na_2O$[a] | 0.0004 | 0.0003 | 0.0004 | 0.0004 | 0.0002 | 0.0004 | 0.0003 |
| $K_2O$[a] | 0.0006 | 0.0004 | 0.0002 | 0.0004 | 0.0002 | 0.0005 | 0.0006 |
| $CO_2$[a] | 1.1324 | 1.1347 | 1.0489 | 1.0909 | 1.0579 | 1.0713 | 1.0881 |
| $SO_3$[a] | 0.0001 | 0.0013 | 0.0001 | 0.0001 | 0.0001 | 0.0000 | 0.0005 |
| Sr(HCl)[c] | 123 | 117 | 172 | 142 | 133 | 168 | 156 |
| Cu(HCl)[c] | 1.8 | 1.1 | 2.2 | 2.7 | 2.2 | 2.0 | 1.7 |
| Zn(HCl)[c] | 15 | 9.6 | 11 | 7.1 | 11 | 15 | 9.6 |
| Pb(HCl)[c] | 8.2 | 9.5 | 9.7 | 11 | 8.1 | 9.2 | 8.7 |
| $Cu(HNO_3)$[c] | 1.2 | 0.9 | 1.4 | 3.4 | 0.9 | 0.8 | 1.5 |
| $Zn(HNO_3)$[c] | 19 | 15 | 15 | 20 | 10 | 9.8 | 17 |
| $Pb(HNO_3)$[c] | 2.8 | 3.9 | 3.6 | 2.8 | 2.6 | 1.8 | 2.5 |
| Porosity[d] | 3.73% | 3.95% | 11.26% | 7.46% | 10.43% | 9.10% | 6.97% |
| Bulk density[a] | 2.607 | 2.603 | 2.397 | 2.508 | 2.423 | 2.458 | 2.518 |
| Grain density[a] | 2.708 | 2.710 | 2.702 | 2.710 | 2.705 | 2.705 | 2.708 |

[a]Grams per cubic centimeter.

[b]Acid Insoluble Residue.

[c]Parts per million.

[d]Volume percent.

Table 11. (Continued)

| | R8A | R1B | R2B | R3B | R4B | R5B | R6B |
|---|---|---|---|---|---|---|---|
| Calcite[a] | 0.1332 | 2.5532 | 2.5551 | 2.2707 | 2.5364 | 2.5023 | 0.0672 |
| Dolomite[a] | 2.5906 | 0.0100 | 0.0074 | 0.0048 | 0.0028 | 0.0053 | 2.6635 |
| Pyrite[a] | 0.0006 | 0.0001 | 0.0001 | 0.0002 | 0.0003 | 0.0002 | 0.0002 |
| AIR[a,b] | 0.0197 | 0.0259 | 0.0076 | 0.0152 | 0.0172 | 0.0049 | 0.0147 |
| $Al_2O_3$[a] | 0.0004 | 0.0008 | 0.0005 | 0.0003 | 0.0003 | 0.0002 | 0.0006 |
| $Fe_2O_3$[a] | 0.0060 | 0.0033 | 0.0028 | 0.0026 | 0.0028 | 0.0027 | 0.0114 |
| $Mn_2O_3$[a] | 0.0007 | 0.0002 | 0.0002 | 0.0002 | 0.0003 | 0.0004 | 0.0008 |
| CaO[a] | 0.9278 | 1.4234 | 1.4325 | 1.2618 | 1.4129 | 1.3957 | 0.8563 |
| MgO[a] | 0.5006 | 0.0078 | 0.0056 | 0.0067 | 0.0067 | 0.0076 | 0.5349 |
| $Na_2O$[a] | 0.0026 | 0.0005 | 0.0003 | 0.0003 | 0.0002 | 0.0003 | 0.0012 |
| $K_2O$[a] | 0.0006 | 0.0006 | 0.0004 | 010003 | 0.0003 | 0.0002 | 0.0004 |
| $CO_2$[a] | 1.2915 | 1.1286 | 1.1223 | 1.0041 | 1.1184 | 1.1016 | 1.3292 |
| $SO_3$[a] | 0.0041 | 0.0002 | 0.0013 | 0.0008 | 0.0024 | 0.0007 | 0.0029 |
| Sr(HCl)[c] | 136 | 123 | 106 | 182 | 128 | 130 | 56 |
| Cu(HCl)[c] | 0.4 | 2.4 | 1.6 | 1.6 | 4.0 | 2.4 | 2.2 |
| Zn(HCl)[c] | 13 | 24 | 11 | 15 | 16 | 13 | 9.2 |
| Pb(HCl)[c] | 3.8 | 8.7 | 6.0 | 11 | 8.1 | 9.0 | 4.0 |
| $Cu(HNO_3)$[c] | 1.5 | 0.8 | 1.1 | 0.8 | 1.3 | 2.1 | 1.1 |
| $Zn(HNO_3)$[c] | 11 | 16 | 12 | 31 | 9.7 | 12 | 9.9 |
| $Pb(HNO_3)$[c] | 4.1 | 2.7 | 0.5 | 2.3 | 1.4 | 1.6 | 0.7 |
| Porosity[d] | 2.46% | 4.31% | 4.94% | 15.29% | 5.38% | 7.15% | 3.16% |
| Bulk density[a] | 2.755 | 2.592 | 2.574 | 2.293 | 2.562 | 2.515 | 2.753 |
| Grain density[a] | 2.825 | 2.705 | 2.708 | 2.706 | 2.707 | 2.709 | 2.842 |

Table 11. (Continued)

| | R7B | R8B | R1C | R2C | R3C | R4C | R5C |
|---|---|---|---|---|---|---|---|
| Calcite[a] | 0.0424 | 0.0834 | 2.4894 | 2.5693 | 2.4961 | 0.0928 | 0.0825 |
| Dolomite[a] | 2.6587 | 2.6603 | 0.0072 | 0.0095 | 0.0156 | 2.5599 | 2.5793 |
| Pyrite[a] | 0.0002 | 0.0006 | 0.0002 | 0.0002 | 0.0004 | 0.0002 | 0.0002 |
| AIR[a,b] | 0.0373 | 0.0171 | 0.0303 | 0.0191 | 0.0213 | 0.0726 | 0.0349 |
| $Al_2O_3$[a] | 0.0011 | 0.0007 | 0.0008 | 0.0001 | 0.0003 | 0.0018 | 0.0019 |
| $Fe_2O_3$[a] | 0.0130 | 0.0069 | 0.0053 | 0.0040 | 0.0042 | 0.0377 | 0.0164 |
| $Mn_2O_3$[a] | 0.0007 | 0.0007 | 0.0003 | 0.0003 | 0.0003 | 0.0009 | 0.0007 |
| CaO[a] | 0.8595 | 0.9239 | 1.3834 | 1.4344 | 1.4000 | 0.8741 | 0.8257 |
| MgO[a] | 0.5403 | 0.5113 | 0.0078 | 0.0064 | 0.0003 | 0.4854 | 0.5277 |
| $Na_2O$[a] | 0.0016 | 0.0023 | 0.0003 | 0.0002 | 0.0003 | 0.0018 | 0.0014 |
| $K_2O$[a] | 0.0009 | 0.0006 | 0.0008 | 0.0002 | 0.0003 | 0.0010 | 0.0017 |
| $CO_2$[a] | 1.2891 | 1.3050 | 1.1106 | 1.1335 | 1.1075 | 1.2555 | 1.2923 |
| $SO_3$[a] | 0.0021 | 0.0057 | 0.0010 | 0.0011 | 0.0009 | 0.0014 | 0.0016 |
| Sr(HCl)[c] | 56 | 439 | 109 | 108 | 109 | 115 | 42 |
| Cu(HCl)[c] | 0.6 | 0.3 | 2.7 | 2.2 | 8.5 | 0.5 | 5.2 |
| Zn(HCl)[c] | 5.9 | 7.1 | 8.8 | 12 | 5.6 | 7.6 | 25 |
| Pb(HCl)[c] | 1.9 | 2.8 | 9.4 | 11 | 6.7 | 0.3 | 0.3 |
| $Cu(HNO_3)$[c] | 1.2 | 0.9 | 0.9 | 1.3 | 0.7 | 1.1 | 1.2 |
| $Zn(HNO_3)$[c] | 6.1 | 6.6 | 7.2 | 6.9 | 4.3 | 4.4 | 53 |
| $Pb(HNO_3)$[c] | 2.2 | 2.4 | 1.6 | 1.6 | 0.6 | 3.3 | 4.2 |
| Porosity[d] | 3.38% | 1.80% | 6.55% | 4.02% | 6.42% | 3.82% | 4.77% |
| Bulk density[a] | 2.746 | 2.776 | 2.531 | 2.600 | 2.536 | 2.733 | 2.705 |
| Grain density[a] | 2.842 | 2.827 | 2.708 | 2.709 | 2.710 | 2.841 | 2.841 |

Table 11. (Continued)

| | R6C | R7C | R8C | R1DL | R1DD | R2D | R3D |
|---|---|---|---|---|---|---|---|
| Calcite[a] | 0.1321 | 0.0501 | 0.2322 | 2.4923 | 0.1330 | 2.5760 | 2.6119 |
| Dolomite[a] | 2.6020 | 2.6412 | 2.3857 | 0.0118 | 2.2633 | 0.0031 | 0.0047 |
| Pyrite[a] | 0.0001 | 0.0001 | 0.0002 | 0.0001 | 0.0001 | 0.0002 | 0.0002 |
| AIR[a,b] | 0.0335 | 0.0182 | 0.0192 | 0.0523 | 0.0995 | 0.0482 | 0.0172 |
| $Al_2O_3$[a] | 0.0009 | 0.0008 | 0.0006 | 0.0012 | 0.0029 | 0.0005 | 0.0004 |
| $Fe_2O_3$[a] | 0.0108 | 0.0073 | 0.0054 | 0.0034 | 0.0173 | 0.0042 | 0.0029 |
| $Mn_2O_3$[a] | 0.0007 | 0.0006 | 0.0006 | 0.0002 | 0.0006 | 0.0004 | 0.0003 |
| CaO[a] | 0.9122 | 0.8816 | 0.9095 | 1.3880 | 0.8109 | 1.4292 | 1.4541 |
| MgO[a] | 0.5157 | 0.5178 | 0.4688 | 0.0104 | 0.4363 | 0.0097 | 0.0084 |
| $Na_2O$[a] | 0.0015 | 0.0021 | 0.0023 | 0.0006 | 0.0023 | 0.0003 | 0.0004 |
| $K_2O$[a] | 0.0008 | 0.0007 | 0.0006 | 0.0011 | 0.0023 | 0.0004 | 0.0005 |
| $CO_2$[a] | 1.2952 | 1.2867 | 1.2363 | 1.1033 | 1.1345 | 1.1380 | 1.1521 |
| $SO_3$[a] | 0.0008 | 0.0039 | 0.0040 | 0.0018 | 0.0048 | 0.0035 | 0.0018 |
| Sr(HCl)[c] | 57 | 80 | 100 | 181 | 101 | 130 | 126 |
| Cu(HCl)[c] | 2.1 | 1.4 | 1.2 | 2.8 | 1.4 | 2.9 | 4.8 |
| Zn(HCl)[c] | 52 | 41 | 26 | 35 | 28 | 13 | 16 |
| Pb(HCl)[c] | 6.8 | 5.0 | 2.9 | 13 | 6.8 | 11 | 25 |
| $Cu(HNO_3)$[c] | 2.0 | 1.9 | 1.6 | 0.8 | 1.4 | 1.7 | 1.7 |
| $Zn(HNO_3)$[c] | 157 | 33 | 12 | 15 | 12 | 9.1 | 18 |
| $Pb(HNO_3)$[c] | 5.0 | 6.2 | 3.1 | 2.6 | 7.5 | 8.9 | 3.2 |
| Porosity[d] | 1.79% | 3.93% | 6.18% | 5.26% | 10.99% | 2.71% | 2.56% |
| Bulk density[a] | 2.773 | 2.720 | 2.648 | 2.563 | 2.512 | 2.635 | 2.639 |
| Grain density[a] | 2.823 | 2.831 | 2.822 | 2.706 | 2.822 | 2.709 | 2.708 |

Table 11. (Continued)

| | R4D | R5D | R6D | R7D | R8D | RL | RD |
|---|---|---|---|---|---|---|---|
| Calcite[a] | 0.0304 | 0.1020 | 0.0504 | 0.0451 | 0.0994 | 2.6404 | 0.6710 |
| Dolomite[a] | 2.5225 | 2.5479 | 2.6462 | 2.6101 | 2.6247 | 0.0085 | 1.9192 |
| Pyrite[a] | 0.0002 | 0.0002 | 0.0001 | 0.0001 | 0.0003 | 0.0027 | 0.0002 |
| AIR[a,b] | 0.1428 | 0.0764 | 0.0122 | 0.0341 | 0.0227 | 0.0190 | 0.0537 |
| $Al_2O_3$[a] | 0.0058 | 0.0020 | 0.0005 | 0.0013 | 0.0009 | 0.0003 | 0.0017 |
| $Fe_2O_3$[a] | 0.0158 | 0.0083 | 0.0062 | 0.0073 | 0.0083 | 0.0019 | 0.0084 |
| $Mn_2O_3$[a] | 0.0005 | 0.0007 | 0.0006 | 0.0006 | 0.0006 | 0.0005 | 0.0006 |
| CaO[a] | 0.8388 | 0.8693 | 0.8977 | 0.8854 | 0.9438 | 1.4706 | 0.9895 |
| MgO[a] | 0.4912 | 0.4990 | 0.5127 | 0.5075 | 0.4909 | 0.0075 | 0.3886 |
| $Na_2O$[a] | 0.0023 | 0.0019 | 0.0025 | 0.0022 | 0.0024 | 0.0002 | 0.0020 |
| $K_2O$[a] | 0.0044 | 0.0016 | 0.0006 | 0.0011 | 0.0008 | 0.0004 | 0.0014 |
| $CO_2$[a] | 1.2098 | 1.2549 | 1.2819 | 1.2572 | 1.2836 | 1.1689 | 1.2060 |
| $SO_3$[a] | 0.0048 | 0.0031 | 0.0035 | 0.0039 | 0.0043 | 0.0006 | 0.0029 |
| Sr(HCl)[c] | 105 | 121 | 109 | 90 | 107 | 91 | 82 |
| Cu(HCl)[c] | 3.7 | 2.8 | 1.4 | 2.4 | 1.8 | 1.6 | 1.7 |
| Zn(HCl)[c] | 28 | 51 | 15 | 26 | 17 | 8.2 | 17 |
| Pb(HCl)[c] | 4.9 | 5.4 | 3.2 | 9.4 | 5.1 | 11 | 4.2 |
| $Cu(HNO_3)$[c] | 2.8 | 2.2 | 2.0 | 1.4 | 2.0 | 1.1 | 1.4 |
| $Zn(HNO_3)$[c] | 36 | 72 | 32 | 16 | 22 | 15 | 77 |
| $Pb(HNO_3)$[c] | 7.2 | 5.2 | 5.4 | 6.3 | 7.0 | 1.7 | 3.0 |
| Porosity[d] | 3.89% | 3.09% | 4.03% | 4.42% | 2.32% | 1.46% | 5.08% |
| Bulk density[a] | 2.717 | 2.738 | 2.719 | 2.701 | 2.759 | 2.673 | 2.655 |
| Grain density[a] | 2.827 | 2.824 | 2.833 | 2.826 | 2.824 | 2.713 | 2.798 |